2010

Earthquake Engineering Simulation with Flexible Cladding System

Jun Jie Li
University of Massachusetts Amherst, jjli@student.umass.edu

EARTHQUAKE ENGINEERING SIMULATION

WITH FLEXIBLE CLADDING SYSTEM

A Thesis Presented

by

JUN JIE LI

Submitted to the Graduate School of the
University of Massachusetts Amherst in fulfillment
of the requirements for the degree of

MASTER OF SCIENCE IN CIVIL ENGINEERING

September 2010

Civil and Environmental Engineering

EARTHQUAKE ENGINGEERING SIMULATION

WITH FLEXIBLE CLADDING SYSTEM

A Thesis Presented

by

JUN JIE LI

Approved as to style and content by:

_____

Scott A. Civjan, Chair

_____

Sergio F. Brena, Member

_____

Richard N. Palmer, Department Head

Civil and Environmental Engineering

ABSTRACT

EARTHQUAKE ENGINEERING SIMULATION WITH FLEXIBLE CLADDING SYSTEM

SEPTEMBER 2010

JUN JIE LI, B.S., UNIVERSTIY OF MASSACHUSETTS AMHERST

M.A., UNIVERSTIY OF MASSACHUSETTS AMHERST

M.S.C.E., UNIVERSTIY OF MASSACHUSETTS AMHERST

Directed by: Professor Scott A. Civjan

This research investigates the interaction between heavy precast cladding units attached to steel framed buildings. Cladding systems are designed as non-structural components and are not expected to contribute to the energy absorption of the primary structure. However, research has indicated that the cladding system may be designed to reduce the response of the primary structure under seismic excitations. The use of flexible connections between the cladding and primary structural frames may be able to provide beneficial effects to the entire structural response. In this study, a series of earthquake engineering simulations were conducted in OPENSEES to analyze the effects of the flexible connections of the cladding on both a 3 story and 9 story prototype structures. The research focus is on the 3 story structure. The results from 3 story and 9 story structures indicate that the flexible cladding connections have the ability to transfer hysteretic energy from the primary structure to the flexible cladding connections.

TABLE OF CONTENTS

Page

LIST OF TABLES

Table Page

LIST OF FIGURES

Figure Page

CHAPTER I

INTRODUCTION

1.1 Cladding Systems

Precast concrete cladding systems are commonly used throughout the building industry. Among precast concrete claddings, non-load bearing precast concrete cladding is the most common. Generally, in this system cladding panels are used to transfer lateral load to other structure components. They are usually used in the façades of the buildings to enclose space; however, they also resist wind, seismic forces. The shapes and sizes of the cladding panels can be varied depending on design requirements and specifications. Typical heights of the cladding components do not exceed floor-to-floor height, and widths of the wall are typically less than or equal to the bay width of the building. Typical cladding units can be separated as solid wall panels (Figure 1.1), window wall units (Figure 1.2), spandrels (Figure 1.3), mullions, and column covers (Precast/Prestressed, 2007).

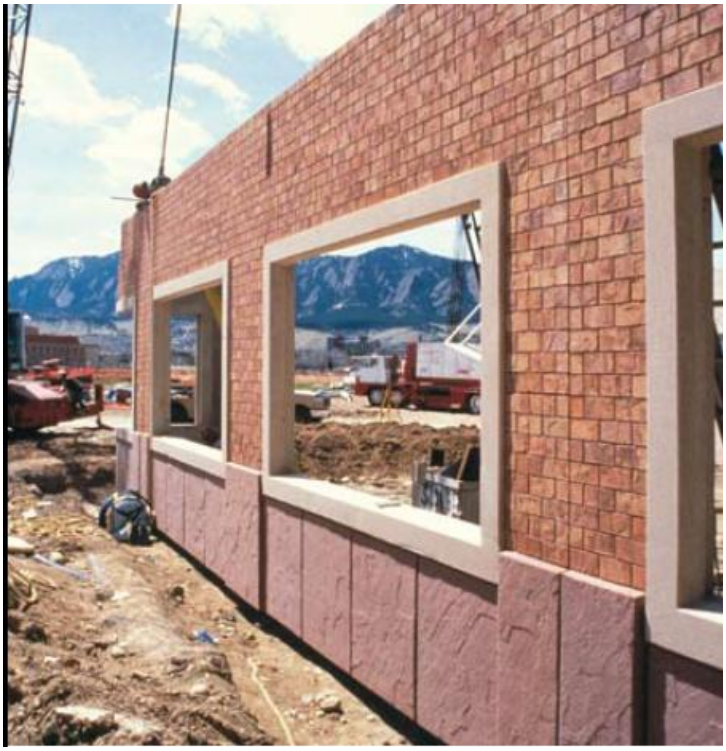

Figure 1.1 Solid wall panels (from Precast/Prestressed 2007, by permission)

Figure 1.2 Window wall panels (from Precast/Prestressed 2007, by permission)

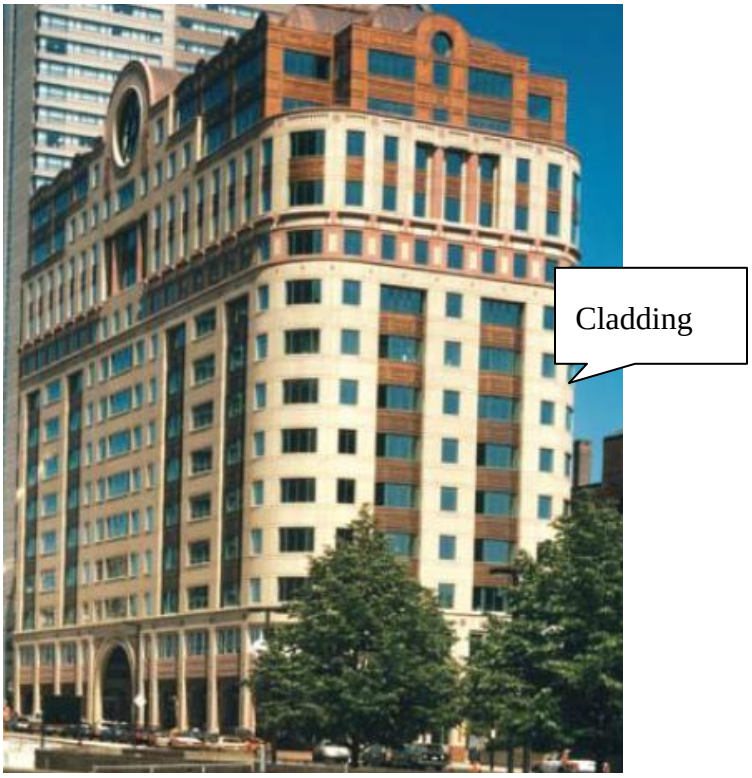

Figure 1.3 Spandrel panels (from Precast/Prestressed 2007, by permission)

Typical cross-sections of the cladding walls consist of the concrete façade layer which contribute most of the cladding weights and layers of insulation, air space and an inner layer of gypsum wallboard. Typical cross sections are shown in Figure 1.4.

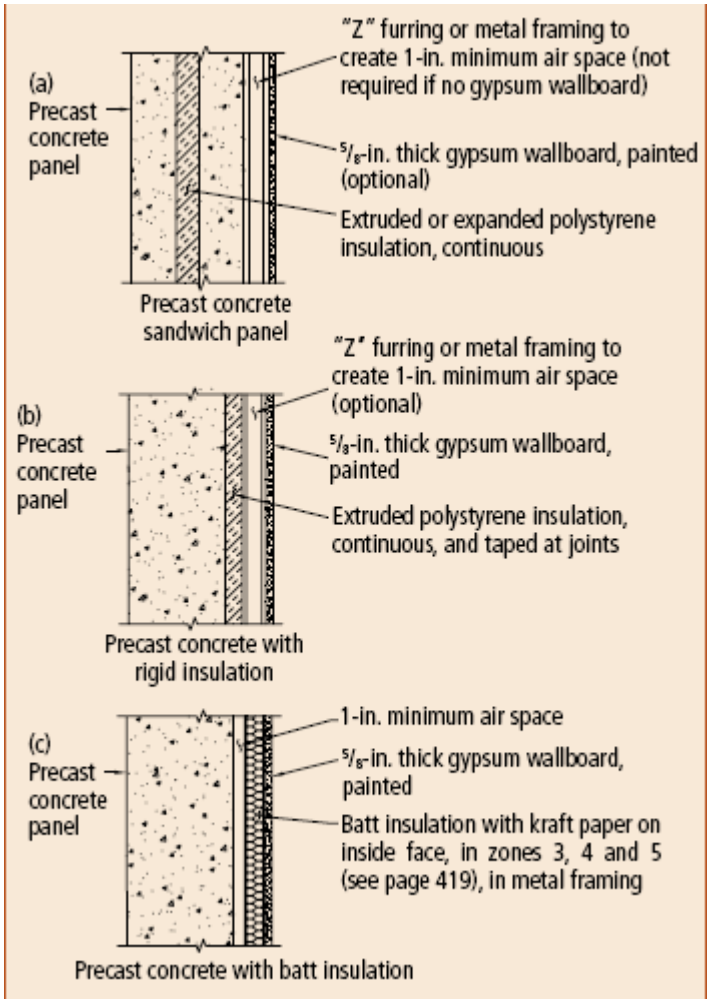

Figure 1.4 Typical cross-section of cladding panels (from Precast/Prestressed 2007, by permission)

1.2 Cladding Connections

Cladding connections are used to connect cladding panels and the primary structure. The designs of the connections are critical because they are the critical component for transferring load from the cladding systems to the primary structural systems. There are two major types of cladding connections, tieback and bearing connections. (Figure 1.5) They are combined and used in the same panels (Precast/Prestressed, 2007)

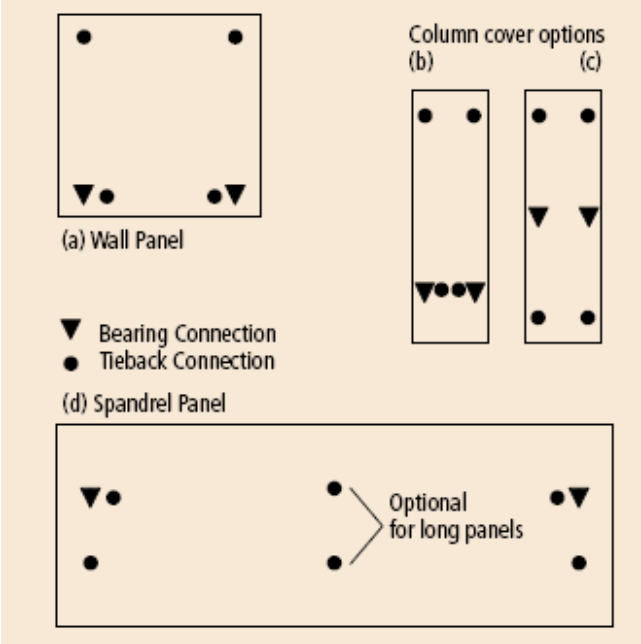

Figure 1.5 Typical panel configurations (from Precast/Prestressed 2007, by permission)

Bearing connections are typically stiff connections used to transfer vertical loads from the claddings to the structures or the foundation. These also restrict movement in the horizontal and out of plane directions. Tieback connections are flexible connections which only restrict panel out of plane deformation, but are expect to allow vertical and horizontal distortion from wind and seismic loads (Figure 1.6). Flexible tieback connections are expected to deform under lateral forces with minimal resistance.

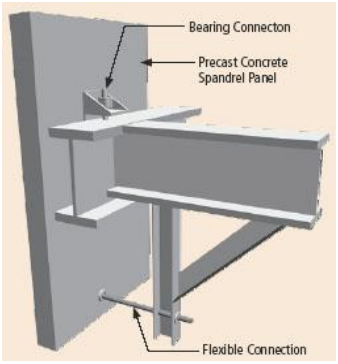

Figure 1.6 Cladding connections (from Precast/Prestressed 2007, by permission)

1.3 Scope of This Study

This research focuses on understanding the modes of energy dissipation possible through introducing flexible cladding connections and developing idealized connection response for controlling different structural behavior. OPENSEES, an advanced analysis program developed for use in seismic research, is used for the research. This program has advanced capabilities to allow cyclic loading including full hysteretic behavior of specific members and materials. Initial analysis will use the El Centro earthquake as primary reference earthquake in the simulation. A bench mark SAC 3-story and SAC 9-story building will be the reference models in the research. Two-dimension frames with corresponding connection parameters and cladding masses were used to model the structures. Varying degrees of inelasticity were introduced in the models when analyzing the effects of flexible cladding connection during moderate and major intensity earthquakes, which represented earthquakes with a 20% and 10% probability of exceedance in 50 years. This research will concentrate on analyzing the SAC 3-story model with flexible connection under a series of earthquakes. The concept of hysteretic

behaviors of the cladding connections was the primary concentration of this research, which was used in simulation model in order to maximize the effects of energy dissipation of the flexible connections. The concept of Tune Mass Damper (TMD) effect was first to used in approximating the stiffness of the flexible connections. An initial assumption is that the natural frequency of the cladding should match with the primary structure in order to experience the TMD effects. The reference literature was shown in Chapter 2. The concept of TMD was used to model elastic behavior of the nonlinear spring material for the flexible cladding connection. The results were investigated from energy dissipation of hysteretic behavior for the cladding connection and differential deflections both between cladding and structural systems and between cladding panels. Previous researchers have showed the benefits of reducing response of the primary structure under earthquake excitations using flexible connection (Pinelli et al., 1993). The goal of this study is to determine reasonable cladding connection parameters which can minimize seismic damage to structural buildings while maintaining reasonable differential deflections both between cladding and structural systems and between cladding panels. Through the hysteretic energy dissipation analysis on the structural buildings with flexible cladding connections under different earthquakes and design level, quantitative results on hysteretic energy dissipation for the structure was conducted in order to obtain how much hysteretic energy was dissipated by the flexible cladding connections.

CHAPTER II

LITERATURE REVIEWS

2.1 Introduction

In the chapter, a review of previous research is presented. It includes the study of reference buildings models used in this study, Tuned Mass Dampers, modification of reference buildings, previous research that used cladding connections as energy dissipating components and hysteretic cladding connections investigated as a direct precursor to this study.

2.2 Reference Structures

Two reference structures are considered for this research. The two buildings are 3- and 9-story structures previously used as benchmark studies which were designed by Brandow & Johnston Associates (1996) for a series of analytical studies as part of the SAC phase II Steel Project. They are good representations of typical low- and medium-rise buildings designed for the Los Angeles, California region which meet seismic codes (Ohtori et al., 2004). Both structures incorporate steel moment-resisting frames as the lateral resisting systems. The fundamental natural periods for the 3- and 9-story structures were reported as 1.01s and 2.27s (Ohtori et. al., 2004). The geometries of the structures are shown in Figure 2.1 and 2.2.

The SAC 3-story frame consists of three stories with four bays in a story. The first three frames from the left of the building are moment-resisting frames (Figure 2.1). The height for all stories is the same, set at13 ft (3.96 m). The bay widths are similar for all

locations and set at 30 ft (9.15 m). The seismic masses for the 1st and 2nd floors are 65.5 kip-sec^2/ft (9.57 x 10^5 kg). The seismic mass for the 3rd floor is 71.2 kip-sec^2/ft (1.04 x 10^6 kg) (Ohtori et al. 2004). Section sizes are shown in Figure 2.1.

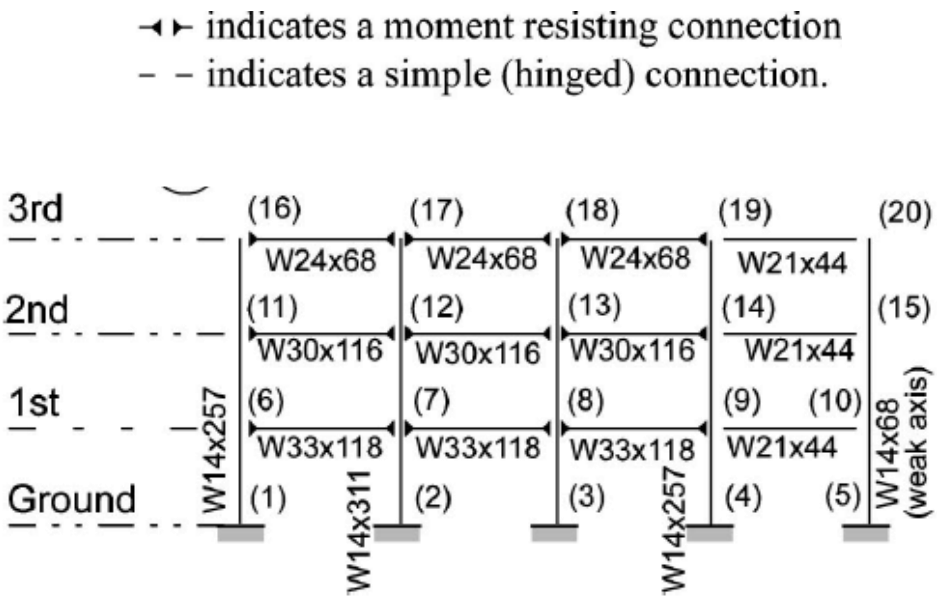

Figure 2.1 Reference SAC 3-story moment-resisting frame (Ohtori et al. 2004)

The SAC 9-story frame consists of nine stories and a basement level with five bays in each story. The first four frames from the left of the building are moment-resisting frames (Figure 2.2). Five different column sizes are used throughout the height of the building as shown in Figure 2.2. Columns were identical for each column line. For propose of simplification, the column splices were neglected. The beam sizes vary through the height of the building as well and are shown in Table 2.1. The story heights and bay widths are shown in Table 2.2. The seismic mass for ground floor is 66.1 kip-sec^2/ft (9.65 x 10^5 kg). The seismic mass for 1st floor is 69.2 kip-sec^2/ft (1.01 x 10^6 kg).

The seismic masses from 2nd to 8th floors are 67.7 kip-sec^2/ft (9.89 x 10^5 kg). The seismic mass for 9th floor is 73.3 kip-sec^2/ft (1.07 x 10^6 kg) (Ohtori et al. 2004).

Table 2.1 SAC 9-story frame beam geometry (Ohtori et al. 2004)

Floor level	Beam Size
Ground - 2nd	W36X160
3rd - 6th	W36X135
7th	W30X99
8th	W27X84
9th	W24X68

Table 2.2 SAC 9-story frame dimensions (Ohtori et al. 2004)

	Dimensions, ft (m)
Basement level height	12 (3.65)
Ground level height	18 (5.49)
1st-8th level heights	13 (3.96)
Bay widths (all)	30 (9.15)

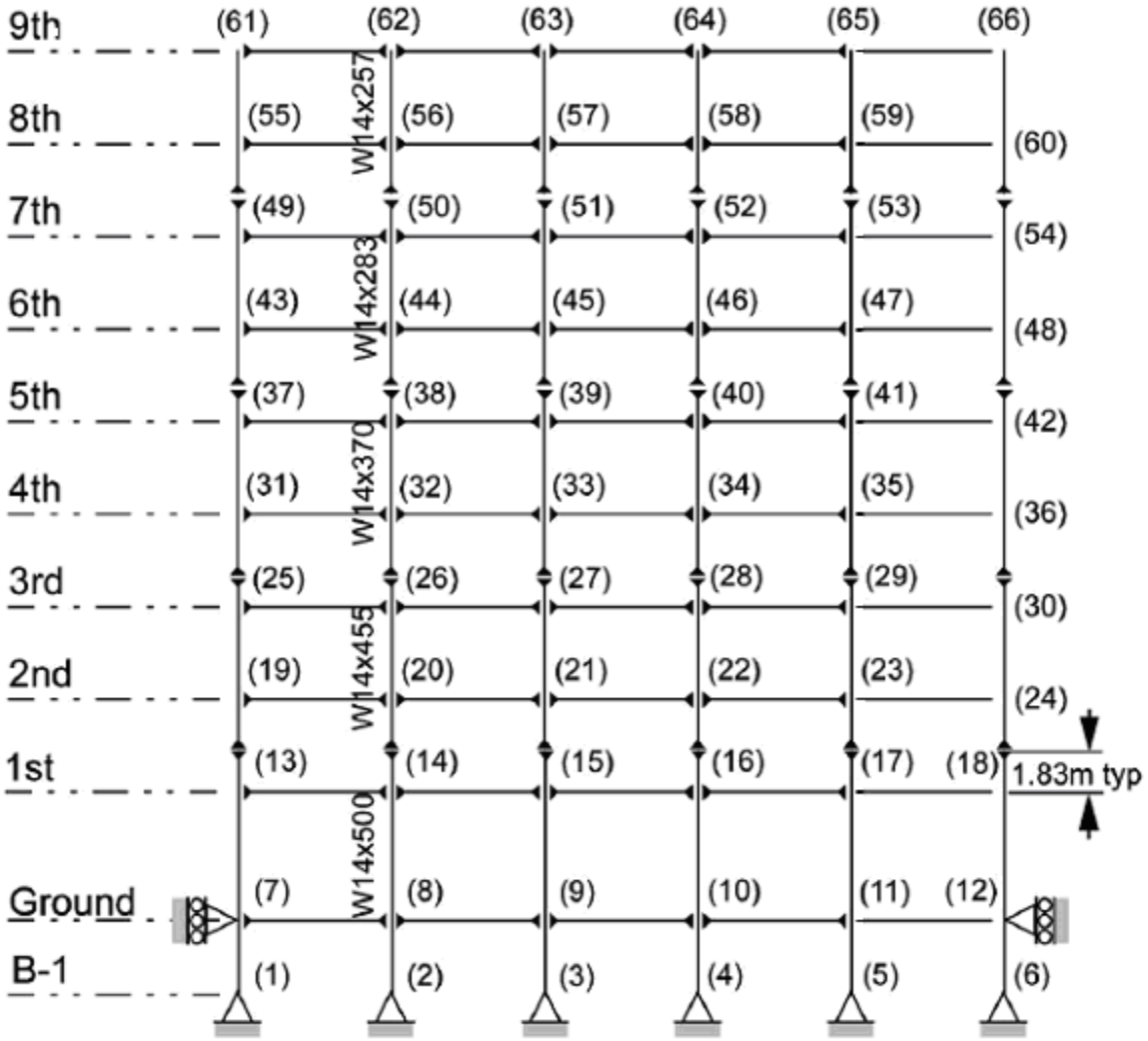

Figure 2.2 Reference SAC 9-story moment-resisting frame (Ohtori et al. 2004)

2.3 Tuned Mass Dampers

The concept of Tuned Mass Dampers (TMD) has been used since 1970s, and has been proven to be very effective in resisting lateral loading such as wind and seismic forces (Wong, 2008). In order to use the concept of TMD in a simple two degree of freedom

(DOF) system without damping, the cladding systems served as the TMD with a mass of m_2 and a spring constant of k_2. The primary structure building is given a mass of m_1 and a spring constant of k_1. A simple harmonic motion is assumed and input into the system. The harmonic force is given by $p = p_o \sin \omega t$ (Figure 2.3)

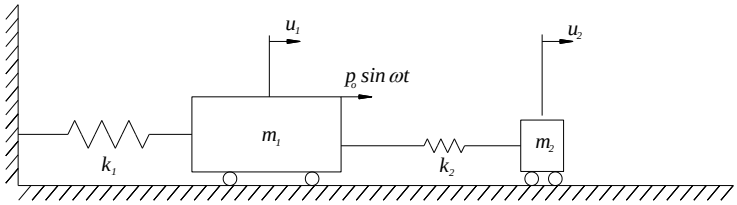

Figure 2.3 Two DOF systems with TMD (Nguyen, 2009)

Then, the equation of motion can be expressed in matrix form as following (Chopra, 2007):

$$\begin{bmatrix} m_1 & 0 \\ 0 & m_2 \end{bmatrix} \begin{Bmatrix} \ddot{u}_1 \\ \ddot{u}_2 \end{Bmatrix} + \begin{bmatrix} k_1 + k_2 & -k_2 \\ -k_2 & k_2 \end{bmatrix} \begin{Bmatrix} u_1 \\ u_2 \end{Bmatrix} = \begin{Bmatrix} p_o \\ 0 \end{Bmatrix} \sin \omega t$$

(2.1)

The steady solutions to the differential equations are:

$$\begin{Bmatrix} u_1(t) \\ u_2(t) \end{Bmatrix} = \begin{Bmatrix} u_{1o} \\ u_{2o} \end{Bmatrix} \sin \omega t$$

(2.2)

Where,

$$u_{1o} = \frac{p_o}{k_1} \frac{1 - \left(\frac{\omega}{\omega_2^*}\right)^2}{\left[1 + \mu\left(\frac{\omega_2^*}{\omega_1^*}\right)^2 - \left(\frac{\omega}{\omega_1^*}\right)^2\right]\left[1 - \left(\frac{\omega}{\omega_2^*}\right)^2\right] - \mu\left(\frac{\omega_2^*}{\omega_1^*}\right)^2}$$

(2.3)

$$u_{2o} = \frac{p_o}{k_1} \frac{1}{\left[1 + \mu\left(\frac{\omega_2^*}{\omega_1^*}\right)^2 - \left(\frac{\omega}{\omega_1^*}\right)^2\right]\left[1 - \left(\frac{\omega}{\omega_2^*}\right)^2\right] - \mu\left(\frac{\omega_2^*}{\omega_1^*}\right)^2}$$

(2.4)

Where,

$$\omega_1^* = \sqrt{\frac{k_1}{m_1}}; \quad \omega_2^* = \sqrt{\frac{k_2}{m_2}}; \quad \mu = \frac{m_2}{m_1}$$

u_{1o} is a representation of the motion of the primary structure. From Equation (3), we can see that u_{1o} equals to zero when $\omega_2^* = \omega$. However, if damping is included into the system which is true in most of the cases, u_{1o} will not equal to zero but a number close to zero. From this TMD analysis, if the natural frequency of attached systems ω_2^* is tuned to the excitation frequency ω, the response of the primary structure can be reduced significantly under wind or seismic loadings. The same concept can be used in a multiple DOF system.

Conceptually, cladding systems could be used as distributed masses for the TMD. In order to use this concept, the natural frequency of the cladding should be equal to that of the primary structure. However, a typical structure can have many natural frequencies which can be excited by a ground motion. It is assumed that most mass participation occurs in the first few modes, so these should be matched with the cladding system frequency. The natural frequencies of the reference structures are relatively high. In order for the frequency of the cladding match the structure frequency, low cladding connection stiffness is required to be effective. Low connection stiffness can cause excessive differential connection deflections which is one of the negative effects of using cladding as a TMD system as reported by Nguyen (2009).

2.4 Energy Dissipation Research Of Engineered Cladding Connection From Pinelli Et Al.

Since large deformations were not acceptable, some energy must be dissipated through yielding. Through the hysteretic behaviors of the cladding connections, the energy dissipated in the primary structure would be able to reduce. The intent of energy dissipation due to material yielding was to minimized damage on the primary structure except in extreme events.

Pinelli et al. (1990, 1992, 1993, 1995, and 1996) published results on energy dissipation using engineered cladding connection as an energy absorber during earthquakes. Through the hysteresis behaviors of the cladding-to-frame connection, the energy dissipated in the primary structure was reduced significantly. A moment-resisting steel building was modeled as a six-story frame building with three moment-resisting bays.

The height of the frame was 216 in (546 cm). The width of the frame is 144 in (366 cm). The weight of the building frame was 42 k (19.05 kg). The first two periods of the frame were 0.85 s and 0.26 s. The model was analyzed under three different earthquake records (Table 2.3) with the engineered cladding connection (Figure 2.4). The hysteresis behavior of the cladding connection with shears against displacements was shown in Figure 2.5.

Table 2.3 Earthquake information (Pinelli et al. 1995, permission from ASCE)

Earthquake (1)	Unit (2)	Imperial Valley, 00°SE El Centro, May 18, 1940 (3)	20°SW Viña del Mar, Chile, 1985 (4)	Kern County, 48°SE Santa Barbara courthouse, July 21, 1952 (5)
Duration	s	53	100	50
Maximum acceleration	g	0.35	0.36	0.13
Critical frequency	Hz	1.5–1.8	1.1–1.4	0.5–1
Acceleration scale	%	125	100	200

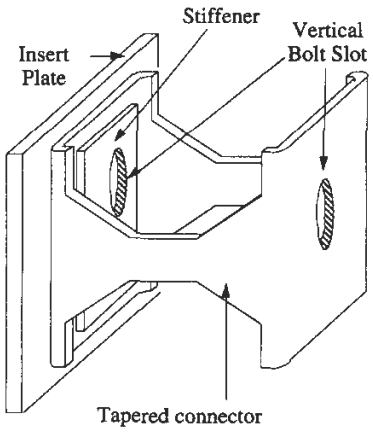

Figure 2.4 Engineered cladding connection from Georgia Tech (Pinelli et al. 1995, permission from ASCE)

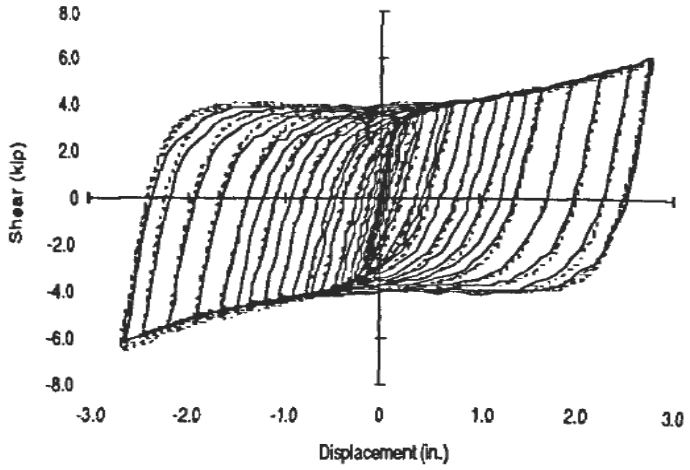

Figure 2.5 Hysteretic behavior of the engineered cladding connection (Pinelli et al. 1995. permission from ASCE)

During an earthquake, the total seismic energy input to the structure (E_i) equals to the sum of the relative kinetic energy (E_k), the recoverable elastic strain energy (E_e), the viscous damping energy (E_d) and the irrecoverable hysteretic energy (E_h). This relation was shown as following equation (Uang and Bertero, 1990).

$$E_i = E_k + E_e + E_d + E_h$$

(2.5)

Pinelli et al. (1993) further divided the hysteretic energy (E_h) into the hysteretic energy dissipated in the structure (E_s) and hysteretic energy dissipated in the cladding connections (E_c). The ratio of $\frac{E_c}{E_i}$ was defined as the effectiveness of the energy dissipation of the cladding connection.

The results on the steel frame with different cladding connections under the three different earthquakes were shown in Table 2.4. The reference case was the case with rigid cladding connection which dissipated no energy. The ideal case was the case with hypothetical elastoplastic cladding connection. The tapered case was the cases with the engineered cladding connection shown in Figure 2.4.

Table 2.4 Results of energy dissipation from Georgia Tech (Pinelli at el. 1993)

	125% El Centro			100% Chile			200% Santa Barbara		
	f (Hz)	E_s/E_i (%)	E_c/E_i (%)	f (Hz)	E_s/E_i (%)	E_c/E_i (%)	f (Hz)	E_s/E_i (%)	E_c/E_i (%)
Reference Case	1.11	37	0	1.1	34	0	1.1	32	0
Ideal Case	1.39	0	75	1.4	4	70	1.4	0	79
Tapered Case	1.35	0	74	1.4	4	70	1.3	0	64

The results showed no damage on the structures for both ideal and tapered cases under El Centro and Santa Barbara earthquakes. There was a 96% reduction on the energy dissipated by the primary structure for both ideal and tapered case under the Chile earthquake. Most of the hysteretic dissipated energy was transferred from the structure to the cladding systems for the last two cases. This research showed the benefits of using flexible cladding connection to reduce the energy dissipation in the primary structure members during an earthquake. However, deflections associated with cladding and connections were not reported in any of the studies, so it is not clear if the researchers were able to overcome the problems reported by Nguyen (2009).

2.5 Modification of SAC 3-story Model From Nguyen

Nguyen (2009) used a 2-D inelastic material to model the frame elements for the SAC 3-story building in OPENSEES. In order to account for the inelastic behavior of the frame elements, a series of patches were used to represent the member cross-section geometry, the "fiber" method used in OPENSEES. Patches are defined as a fiber section which has a general geometric configuration formed by sub-regions of simpler, regular shapes (OPENSEES Command Language Manual). There were 64 patches in each flange and 32 patches in the web used (Figure 2.6).

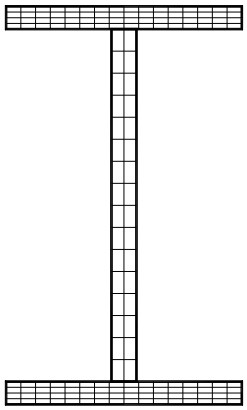

Figure 2.6 Member cross-sections with fiber meshing (Nguyen, 2009)

Cladding components were represented by lumped masses. The mass of one single bay was calculated to be about 1 kip-sec^2/ft (1.46 x 10^4 kg). Cladding was connected to the structure through multiple non-linear springs representing the connections. The length of the cladding to frame connections was assumed to be 10 in (25.4 cm). The bay tributary area determined the cladding mass used at each node. For example, nodes at the center

were lumped to a mass with the whole bay tributary area which equals 1 kip-sec^2/ft (1.46 x 10^4 kg). Nodes at the perimeter were lumped to a mass with half of the bay tributary area which equals .5 kip-sec^2/ft (7.3 x 10^3 kg). Finally, the nodes at the corner lumped with a mass equals to .25 kip-sec^2/ft (3.65 x 10^3 kg) (Figure 2.7). Non-linear springs were introduced to the model with a fixed condition to the frame nodes and free lateral force restriction at the cladding nodes (Figure 2.8). Therefore, regardless of the final details of a connection system, the dynamic properties are effectively captured by the uniaxial spring.

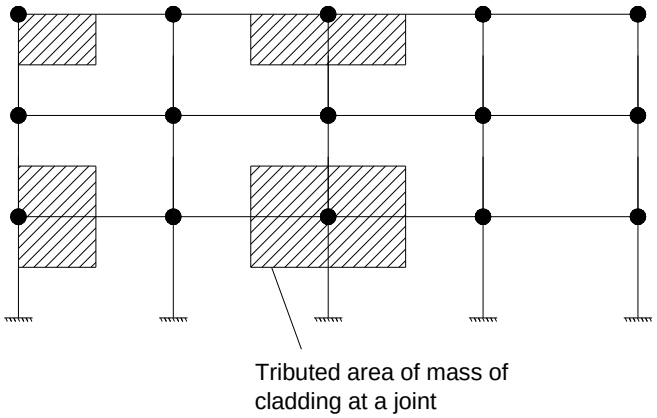

Figure 2.7 Cladding masses distributions on different node locations (Nguyen, 2009)

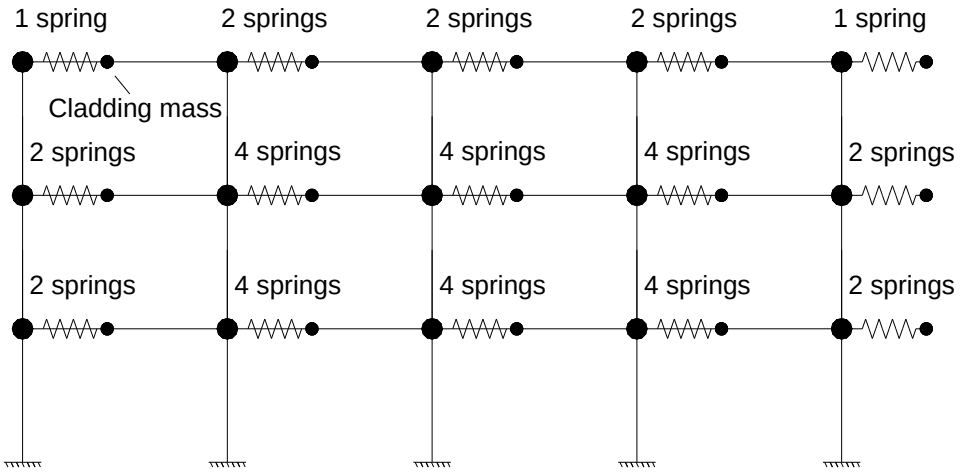

Figure 2.8 Non-linear springs model as cladding connections (Nguyen, 2009)

The behaviors of the claddings were also affected by higher modes. Table 2.5 shows the modal analysis results, indicating that the participation ratio for higher modes increased as the stiffness of cladding connections increased. The participation ratio for the first mode was reduced. The behaviors of the higher modes became more critical for building with flexible cladding. Therefore, the behaviors of the claddings were affected by higher modes of the building.

Table 2.5 Dynamic analysis results of SAC 3-story model (Nguyen, 2009)

Connecti-on stiffness (kip/ft)	Natural Period of Cladding Units (s)	1st Period (s)	Particip-ation Ratio	2nd Period (s)	Partici-pation Ratio	3rd Period (s)	Particip-ation Ratio	Sum of participate-on of first three modes	Δ* (%)
No cladding	-	0.97	0.84	0.32	0.13	0.17	0.02	0.99	-
1.04E+09	0	1.01	0.82	0.33	0.12	0.18	0.02	0.967	99.98
1.31E+08	0.001	1.01	0.82	0.33	0.12	0.18	0.02	0.969	99.95
1.04E+06	0.006	1.01	0.82	0.33	0.12	0.18	0.02	0.97	99.39
1.31E+05	0.017	1.01	0.82	0.33	0.12	0.18	0.02	0.97	98.27
1.63E+04	0.049	1.01	0.82	0.33	0.12	0.18	0.02	0.97	95.11
1.04E+03	0.194	1.01	0.82	0.34	0.12	0.17	0.01	0.957	80.68
130.5	0.55	1.01	0.82	0.31	0.09	0.17	0.02	0.937	45.78
66.82	0.769	1.03	0.81	0.31	0.11	0.17	0.02	0.934	25.37
57.29	0.83	1.04	0.79	0.31	0.11	0.17	0.02	0.915	20.07
44.76	0.939	1.07	0.68	0.32	0.11	0.17	0.02	0.815	11.86
34.21	1.074	1.14	0.41	0.96	0.37	0.32	0.11	0.895	5.5
28.19	1.183	1.22	0.25	1	0.48	0.32	0.11	0.845	18.66
22.92	1.312	1.34	0.16	1.04	0.45	0.32	0.11	0.723	26.74
16.31	1.556	1.57	0.1	0.93	0.51	0.32	0.11	0.722	66.89
11.12	1.884	1.9	0.08	0.98	0.39	0.32	0.11	0.58	92.16
8.35	2.174	2.18	0.07	0.95	0.66	0.32	0.11	0.843	128.12
6.09	2.546	2.56	0.06	0.96	0.72	0.32	0.11	0.891	164.65

* Δ = Difference between period of the highest participation and natural period of cladding units

2.6 Hysteretic Cladding Connection Research from Nguyen

Nguyen (2009) explained the benefits of hysteretic behavior in flexible cladding connections. Hysteretic behavior is the behavior after yielding under cycling loadings. This behavior in the cladding to structural member connections may reduce the structural response of structural frame and minimize structural damage. However, excessive differential deflections between the cladding and primary structure were noted as a major

issue to overcome. In addition, resulting damage in the connections must be fairly minimal to avoid the need to replace these elements after a moderate earthquake.

In further models developed by Nguyen (2009), yielding connection materials were included to account for a variety of elastic and inelastic response when subjected to a specific ground motion. Material properties were identified as "Steel02" in the OPENSEES Command Language Manual to represent the hysteretic behaviors of the cladding connections. "Steel02" is one of the default hysteretic materials in OPENSEES. The input earthquake was El Centro with PGA of .35g and a 40-second time frame, and the reference structure was SAC 3-story moment-resisting frame. From a series of OPENSEES simulations, a hysteretic behavior resulting in the most base shear reduction of those studied was reported (HLOOP2 shown in Figure. 2.9).

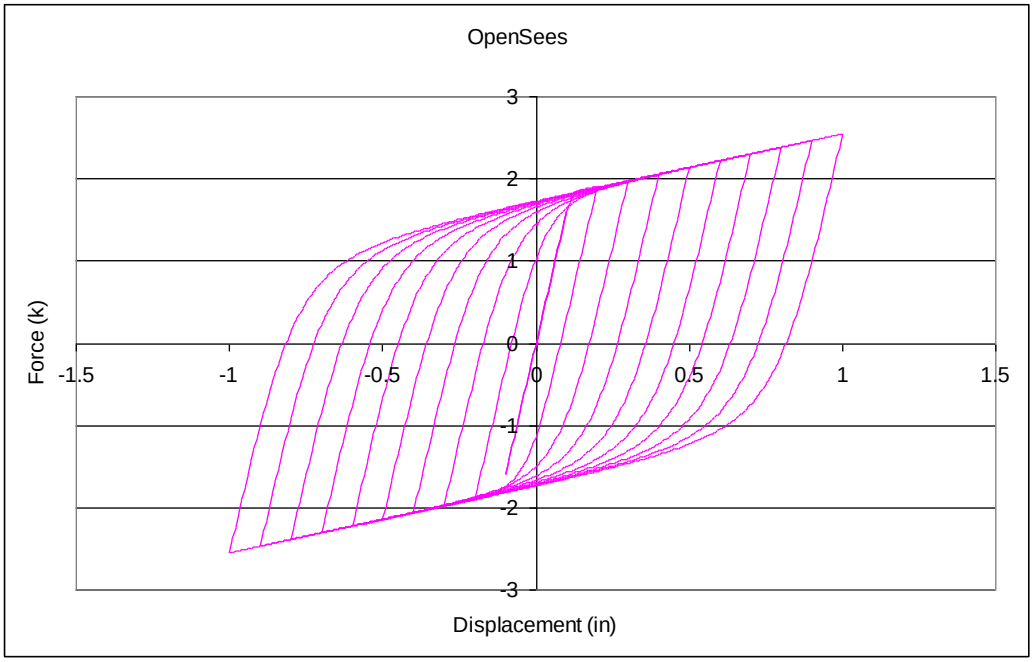

Figure 2.9 Steel02 spring hysteretic behaviors HLOOP2 (Nguyen, 2009)

From the results of hysteretic behavior of cladding connections of SAC 3-story model using HLOOP2, the maximum base shear was reduced from 1116.5 to 1070.3 k (4966.2 to 4760.7 kN), a 4% reduction. However, the maximum differential connection deflection (measured between the steel frame and cladding mass) was about 7 in (17.78 cm) (Figure 2.10).

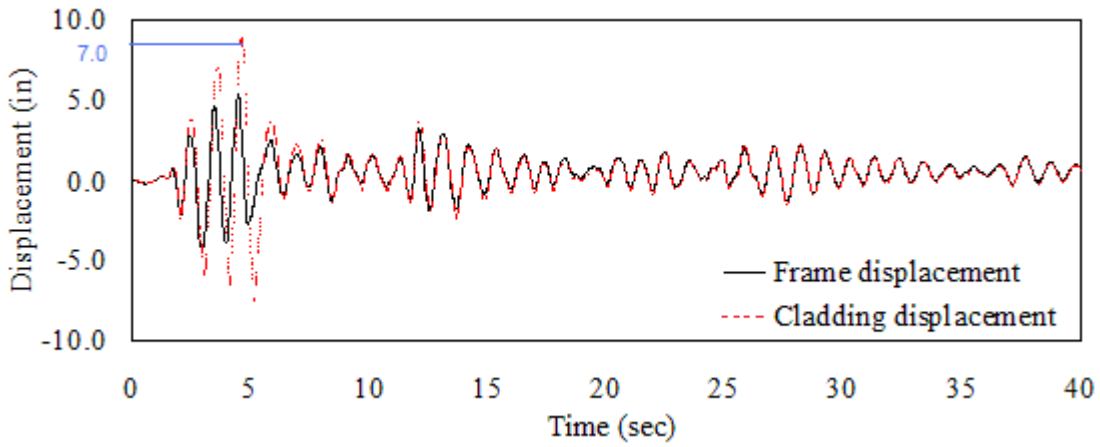

Figure 2.10 Third floor maximum differential connection displacement when HLOOP2 was used (Nguyen, 2009)

CHAPTER III

PRELIMINARY ANALYSIS AND RESULTS WITH FLEXIBLE CLADDING CONNECTION ON SAC 3-STORY BUILDING

3.1 Introduction

The results of Nguyen (2009) provided guidance for this research project. In this Chapter, further modifications of the SAC 3-story structure based on its elastic and inelastic behaviors will be discussed. In order to solve the excess of connection displacements, the effect of hardening/stiffening in the hysteretic materials was investigated through use of different non-linear spring materials modeling flexible cladding connections. All structures were subjected to the El Centro earthquake excitation for these analyses. The analysis objective of this Chapter was to fix an input earthquake record and vary the material properties of the flexible cladding connections.

3.2 Elastic and Inelastic Analysis

The analysis model was developed in OPENSEES based on the SAC 3-story building. Inelastic fiber elements were used for all yielding elements in these analyses, while the majority of non-yielding elements were modeled as elastic elements to minimize computation time. An elastic element was defined as a single 2 nodded frame element with 6 degrees of freedom per node and was a default element type in OPENSEES. Inelastic element was defined as multiple fiber elements in terms of geometry, and it was also one of the element types in OPENSEES. To verify behavior of elastic and inelastic elements, a simple two dimensional cantilever W30X116 I-beam was used. The base

support was fixed on one end of the beam and an incremental deflection was applied at other end of the beam until the deflection reached 100 in. 50 ksi steel was used in the analysis. After the model was run, the moments induced in the beam were plotted against the applied deflection (Figure 3.1). Then, the inelastic fiber elements (128 fibers) with strain hardening effect were used to model the same section. The moments induced in the beam were also plotted against the applied deflection (Figure 3.1).

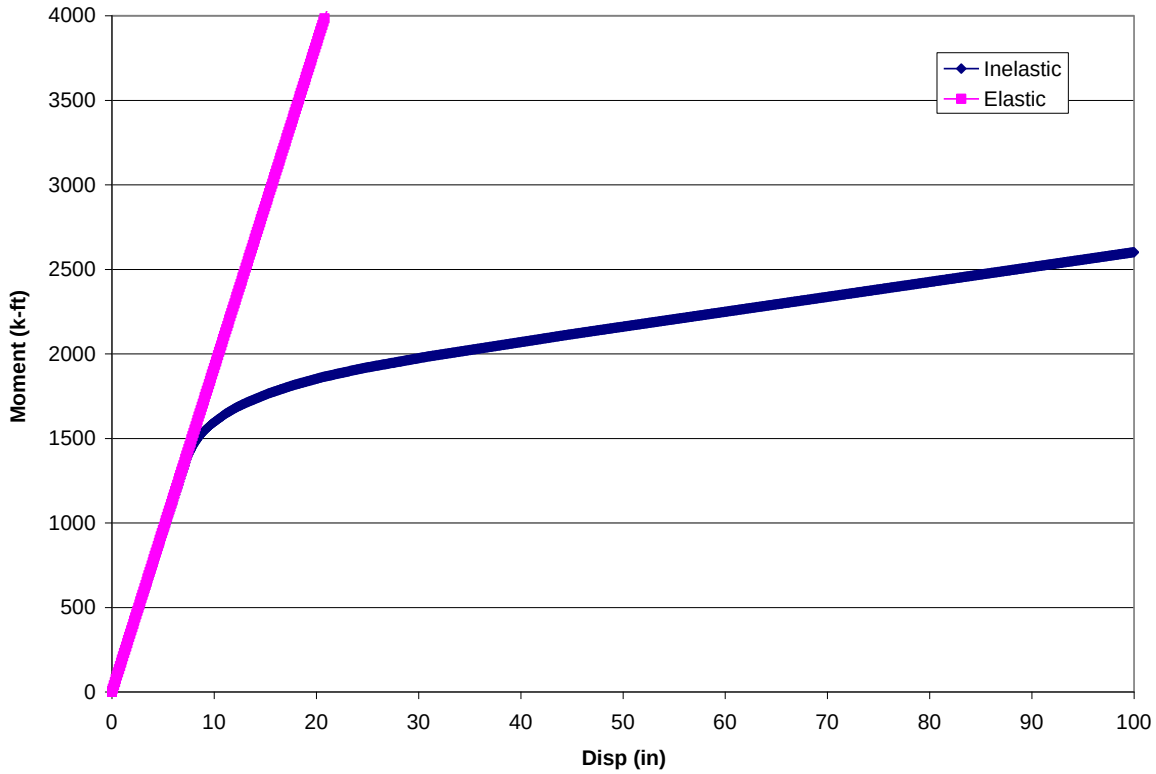

Figure 3.1 Moments vs. displacements plot for W30X116

Using basic structural analysis, the moment and deflection relationship for a simple cantilever beam is represented by equation 3.1:

$$\Delta = \frac{ML^2}{3EI} \quad (3.1)$$

Where, Δ = the end beam deflection (in).

L = length of the beam (432 in)

M = moment (k-in);

E = Elastic Modulus (29000 ksi)

I = moment of inertia along the strong axis (4930 in^4)

The yield moment (M_y) for W30X116 equals to 1370.8 k-ft (1.86 x 10^6 N-m). From Equation 3.1, deflection can be calculated to be 7.2 in (18.3 cm) if the moment reaches yield moment. From Figure 3.1 and Table 3.1, when deflection equals to 7.2 in (18.3 cm), moment is 1379.0 k-ft (1.87 x 10^6 N-m). From Figure 3.2, when the deflection equals to 7.2 in (18.3 cm), the moment is 1358.2 k-ft (1.84 x 10^6 N-m). The results from the elastic and inelastic analysis are very close to the calculated result. The difference of percentage between the calculated value and the value from elastic analysis was 0.6%. The difference of percentage for the inelastic analysis was 0.9%. The analysis results showed very good agreements with calculated result.

Comparing the moment for both elastic and inelastic moment under the elastic range, the difference was very small which equaled to 1.53% (Table 3.1).

Table 3.1 Moment difference for both elastic and inelastic cantilever beam

Displacement (in)	Inelastic moment (k-ft)	Elastic moment (k-ft)	Difference %	% of M_y
1	188.64	191.52	1.53	14.0
2	377.28	383.04	1.53	27.9
3	565.93	574.56	1.53	41.9
4	754.57	766.08	1.53	55.9
5	943.21	957.6	1.53	69.9
6	1131.85	1149.13	1.53	83.8
7	1320.5	1340.65	1.53	97.8
7.2	1358.17	1378.96	1.53	100.6
7.3	1376.29	1398.11	1.59	102.0
7.4	1392.92	1417.26	1.75	103.4
8	1463.44	1532.18	4.70	111.8
9	1542.82	1723.69	11.72	125.7
10	1595.73	1915.22	20.02	139.7
11	1650.1	2106.73	27.67	153.7
12	1676.64	2298.26	37.08	167.7
13	1706.38	2489.78	45.91	181.6
14	1732.61	2681.3	54.75	195.6
15	1757.18	2872.83	63.49	209.6

From Table 3.1, both elastic and inelastic model shared a similar behavior in term of moments in the beam, when the moments were below the M_y which equals to 1370.8 k-ft (1.86×10^6 N-m). After the moments induced in the beam exceeded M_y, the differences of moments between elastic and inelastic model would increase proportionally.

3.3 Modifications on the SAC 3-story model

The partial inelastic SAC 3-story model with rigid claddings was built in OPENSEES according to Ohtori's original model and modifications from Nguyen on claddings. In

order to account for the geometric non-linearity, Eigen-value solver was used as analysis method. Both elastic and inelastic behaviors from previous section were used in the development of the SAC 3-story model. In order to minimize computation effort, an iterative effort of reducing inelasticity in the models was completed. Members with maximum moment below the M_y were modeled as elastic sections, with remaining members modeled as inelastic sections. This would help reducing the run time for the final model in OPENSEES. This is important as a goal for these runs would be to eventually verify frame and connection behavior through dynamic hybrid testing. Table 3.2 shows results in run time for inelastic and partial inelastic SAC 3-story with rigid cladding connection under El Centro earthquake (Figure 3.2). There was a 30% reduction on the model run time between the partial inelastic and fully inelastic models.

Table 3.2 Model run time

	Earthquake Duration (s)	Model run time (s)
Inelastic SAC 3-story model	40	34.5
Partial inelastic SAC 3-story model	40	24.3

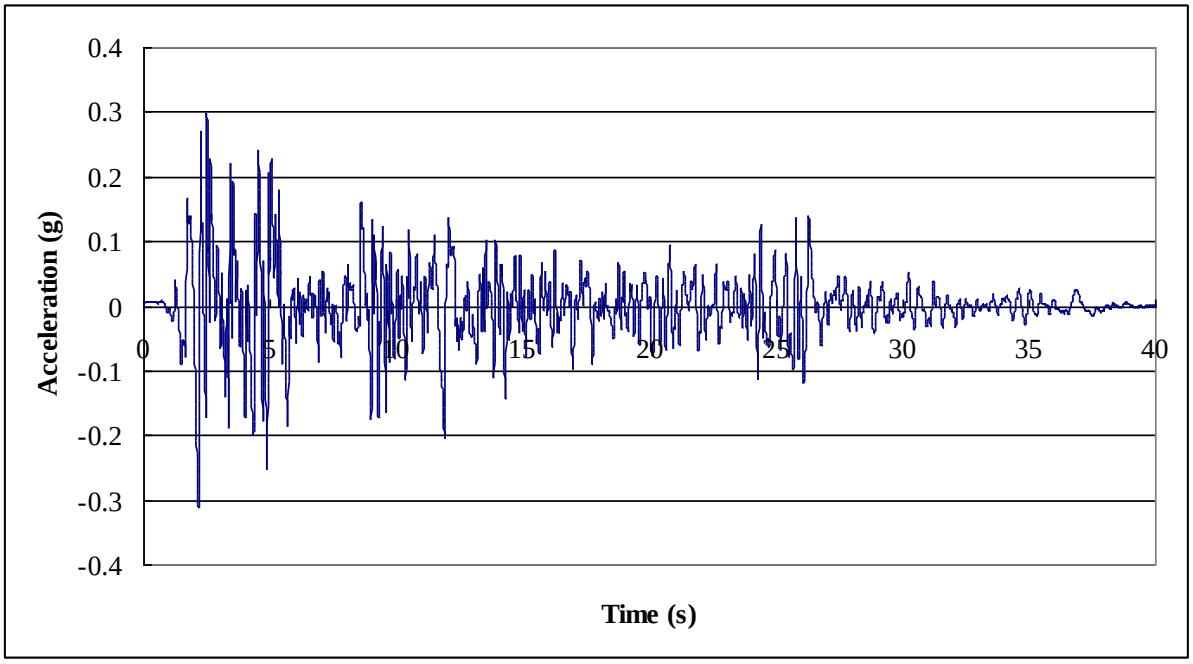

Figure 3.2 El Centro earthquake acceleration time-history

There are a total of 27 structural elements and 35 nodes in the partial inelastic SAC 3-story model with claddings, as shown in Figure 3.3. When the model with rigid cladding connections was subjected to the El Centro earthquake, the maximum moment in each member was obtained. Ten elements remained elastic when rigid cladding connections were used. Seventeen elements were yielded, indicated by maximum moments exceeding M_y. These 17 members were modeled as inelastic fiber elements which were shaded with light and dark color in Table 3.4. Notice that for elements with dark shading, the maximum moments exceed $M_{p.}$ When modeling the inelastic members, hardening effect was included, which allowed the moment induced on the member to exceed M_p. There were a total of 8 elements exceeding $M_{p.}$ This indicates severe damage in the elements and connections. The maximum story drift ratios at the center column for each story were shown in Table 3.3, in order to show if the structure still behave in a

reasonable manner. The peak story drift ratios are under the allowable story drift ratio which is 0.025. Therefore, the partial inelastic SAC 3-story model was built according to the elastic and inelastic behaviors shown in Table 3.4.

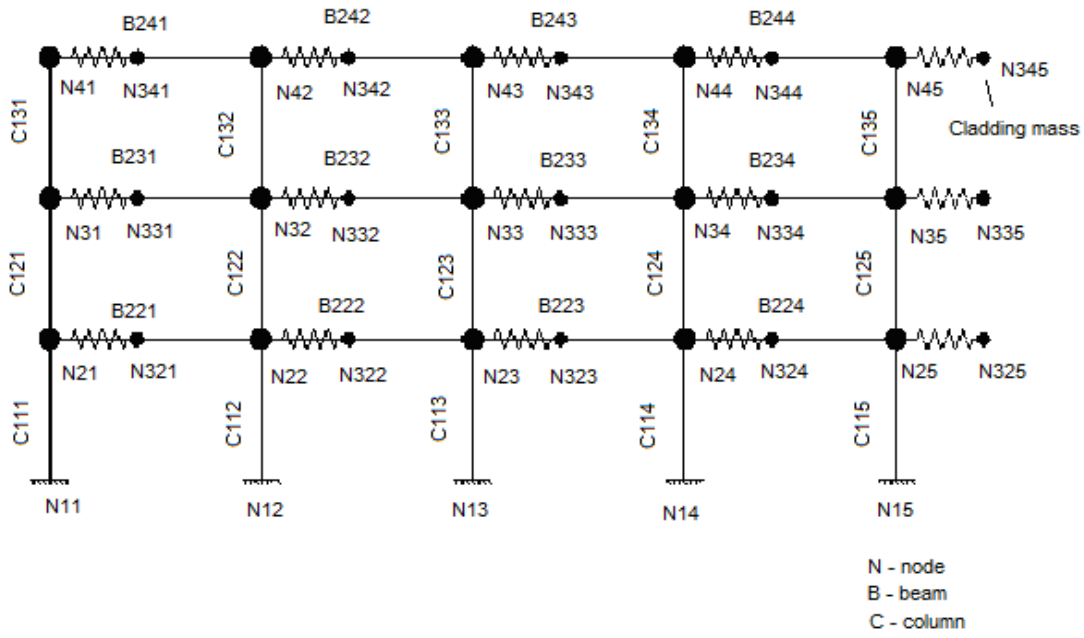

Figure 3.3 SAC 3-story model with claddings

Table 3.3 Peak story drift ratio of partial inelastic SAC 3-story model with rigid cladding connections

Story	Peak story Drift ratio
1st	0.010
2nd	0.014
3rd	0.013

Table 3.4 Partial inelastic SAC 3-story model with rigid cladding connections

Column 1 (W14X257)		M_u (k-ft)	M_y (k-ft)	M_p (k-ft)	Yielded	Elasticity
Element	111	1953.6	1729.2	2033.3	Yes	Inelastic
	121	1065.9			No	Elastic
	131	1953.6			Yes	Inelastic
Column 2 (W14X311)						
Element	112	2533.6	2108.3	2511.1	Yes	Inelastic
	122	2027.4			Yes	Elastic
	132	2533.6			Yes	Inelastic
Column 3 (W14X311)						
Element	113	2538.3	2108.3	2511.1	Yes	Inelastic
	123	2044.5			No	Elastic
	133	2538.3			Yes	Inelastic
Column 4 (W14X257)						
Element	114	1977.2	1729.2	2033.3	Yes	Inelastic
	124	1099.3			No	Elastic
	134	1977.2			Yes	Inelastic
Column 5 (W14X68)						
Element	115	373.1	429.2	478.9	No	Elastic
	125	102.6			No	Elastic
	135	373.1			No	Elastic
Beam 1 (W33X118)						
Element	221	1766.8	1495.8	1733.3	Yes	Inelastic
	222	1700.8			Yes	Inelastic
	223	1768.4			Yes	Inelastic
Beam 2 (W30X116)						
Element	231	1593.3	1370.8	1577.8	Yes	Inelastic
	232	1562.3			Yes	Inelastic
	233	1606.5			Yes	Inelastic
Beam 3 (W24X68)						
Element	241	696.7	641.7	737.8	Yes	Inelastic
	242	678.5			Yes	Inelastic
	243	694.9			Yes	Inelastic
Beam 4 (W21X44)						
Element	224	0	340	397.8	No	Elastic
	234	0			No	Elastic
	244	0			No	Elastic

The first two periods of the SAC 3-story models were recorded in Table 3.5, which included Ohtori's SAC 3-story model without claddings, elastic SAC 3-story model without cladding, and partial inelastic model with rigid and flexible cladding connections. By comparing results between the elastic model without claddings and Ohtori's results, they had the same 1st period and 2% difference in the 2nd period. The results of the elastic SAC 3-story model agreed with Ohtori's references. The differences in periods between the partial inelastic models and Ohtori's model were because cladding masses were included in the partial inelastic model. The model with the flexible cladding connection (Hys.6) will be discussed later in this Chapter.

Table 3.5 Periods of the SAC 3-story models

	1st period (s)	2nd period (s)
Ohtori's model (no claddings)	1.01	0.327
Elastic SAC 3-story model (no claddings)	1.01	0.335
Partial inelastic SAC 3-story model (with rigid cladding connections)	1.055	0.353
Partial inelastic SAC 3-story model (with flexible cladding connections)	1.058	0.396

3.4 Non-linear Springs Materials As Flexible Cladding Connections

Non-linear springs were used to model the flexible cladding connections. Several material properties were investigated to model the hysteretic behaviors of the non-linear springs (representing the cladding to primary structure connections) in OPENSEES. Specifically, "Pinching4", "Steel02", and "Hysteretic" materials were used. "Pinching4" is a uniaxial material which has "pinched" load-deflection response with degradation under cyclic loading. "Steel02" material is a uniaxial steel material with isotropic strain hardening. "Hysteretic" material is a uniaxial bilinear hysteretic material with "pinched" effects, damage due to ductility and energy, and unloading stiffness degradation based on ductility (OPENSEES Command Language Manual). Each of these will be described in more detail in the following paragraphs.

The "Pinching4" material model is a pre-set material in OPENSEES, which includes 39 parameters. Large variations in material properties can result from relatively small changes to parameters, showing high sensitivity to some parameters. Parameters defined in the OPENSEES Command Language Manual are (Figure 3.4):

ePf1 ePf2 ePf3 ePf4	floating point values defining force points on the positive response envelope
ePd1 ePd2 ePd3 ePd4	floating point values defining deformation points on the positive response envelope
eNf1 eNf2 eNf3 eNf4	floating point values defining force points on the negative response envelope (optional, default: negative of positive envelope values)
eNd1 eNd2 eNd3 eNd4	floating point values defining deformations points on the negative response envelope (optional, default: negative of positive envelope values)

rDispP	floating point value defining the ratio of the deformation at which reloading occurs to the maximum historic deformation demand
rForceP	floating point value defining the ratio of the force at which reloading begins to force corresponding to the maximum historic deformation demand
uForceP	floating point value defining the ratio of strength developed upon unloading from negative load to the maximum strength developed under monotonic loading
rDispN	floating point value defining the ratio of the deformation at which reloading occurs to the minimum historic deformation demand (optional, default: $rDispP)
rForceN	floating point value defining the ratio of the force at which reloading begins to the force corresponding to the minimum historic deformation demand (optional, default: $rForceP)
uForceN	floating point value defining the ratio of the strength developed upon unloading from a positive load to the minimum strength developed under monotonic loading (optional, default: $rForceP)
gK1 gK2 gK3 gK4 gKLim	floating point values controlling cyclic degradation model for unloading stiffness degradation
gD1 gD2 gD3 gD4 gDLim	floating point values controlling cyclic degradation model for reloading stiffness degradation
gF1 gF2 gF3 gF4 gFLim	floating point values controlling cyclic degradation model for strength degradation
gE	floating point value used to define maximum energy dissipation under cyclic loading. Total energy dissipation capacity is defined as this factor multiplied by the energy dissipated under monotonic loading.
dmgType	string to indicate type of damage (option: “cycle”, “energy”)

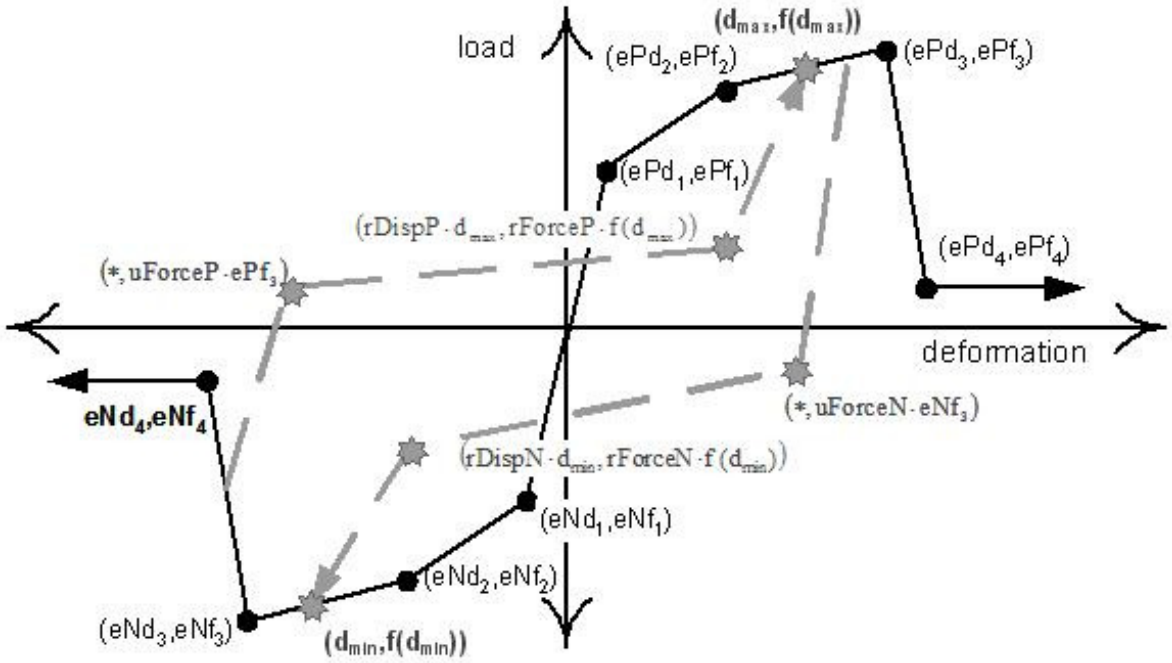

Figure 3.4 Pinching4 material properties (from OPENSEES)

Typical hysteretic responses from "Pinching4" material with different degradations were shown in Figure 3.5.

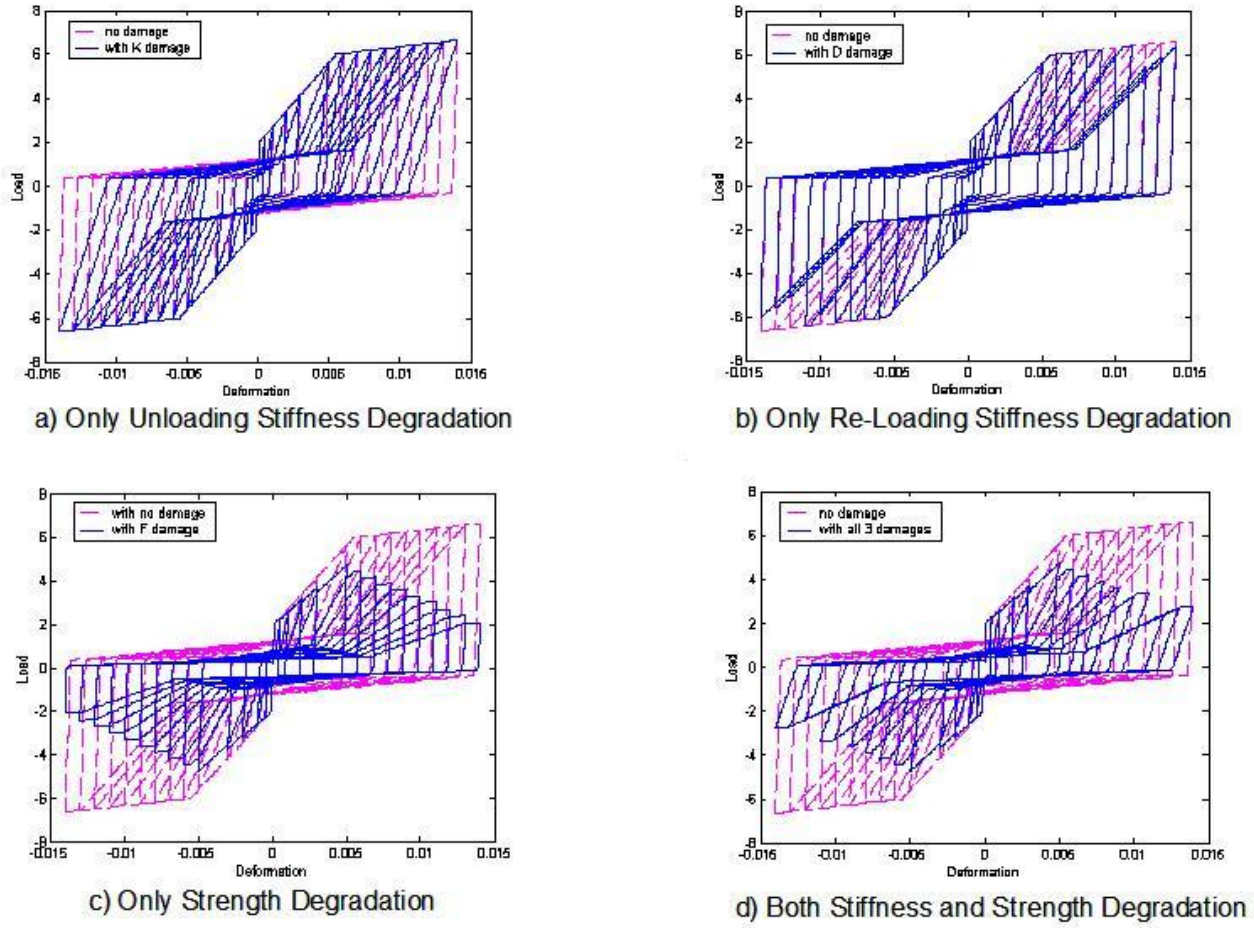

Figure 3.5 Hysteresis loop of "Pinching4" material with different degradation (from OPENSEES)

The "Steel02" material model is another pre-set material in OPENSEES. The "Steel02" parameters are defined from OPENSEES Command Language Manual as following:

F_y	yield strength
E	initial elastic tangent
b	strain-hardening ratio (ratio between post-yield tangent and initial elastic tangent)

R0, cR1, cR2 control the transition from elastic to plastic branches.

A typical hysteretic loop for "Steel02" with positive strain was shown in Figure 3.6

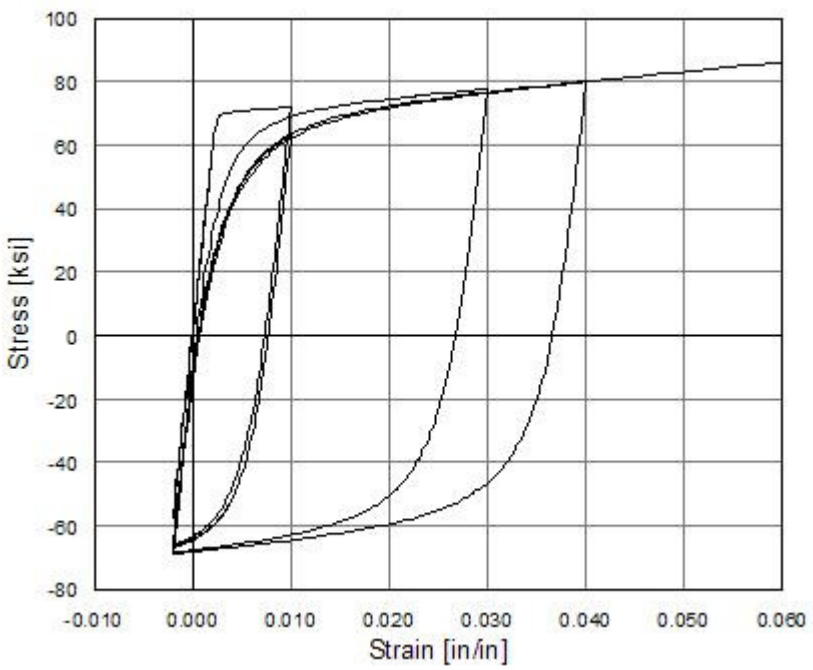

Figure 3.6 Hysteretic loop of "Steel02" material (from OPENSEES)

"Hysteretic" material was also introduced which includes hardening effects. Hardening may benefit in control of cladding connection deflections. The parameter of this material can be found in OPENSEES Command Language Manual (Figure 3.7).

s1p e1p	stress and strain (or force & deformation) at first point of the envelope in the positive direction
s2p e2p	stress and strain (or force & deformation) at second point of the envelope in the positive direction
s3p e3p the	stress and strain (or force & deformation) at third point of envelope in the positive direction (optional)
s1n e1n	stress and strain (or force & deformation) at first point of the envelope in the negative direction*

s2n e2n	stress and strain (or force & deformation) at second point of the envelope in the negative direction*
s3n e3n	stress and strain (or force & deformation) at third point of the envelope in the negative direction (optional)*
pinchX	pinching factor for strain (or deformation) during reloading
pinchY	pinching factor for stress (or force) during reloading
damage1	damage due to ductility: D1(mu-1)
damage2	damage due to energy: D2(E_{ii}/E_{ult})
beta	power used to determine the degraded unloading stiffness based on ductility, mu-beta (optional, default=0.0)

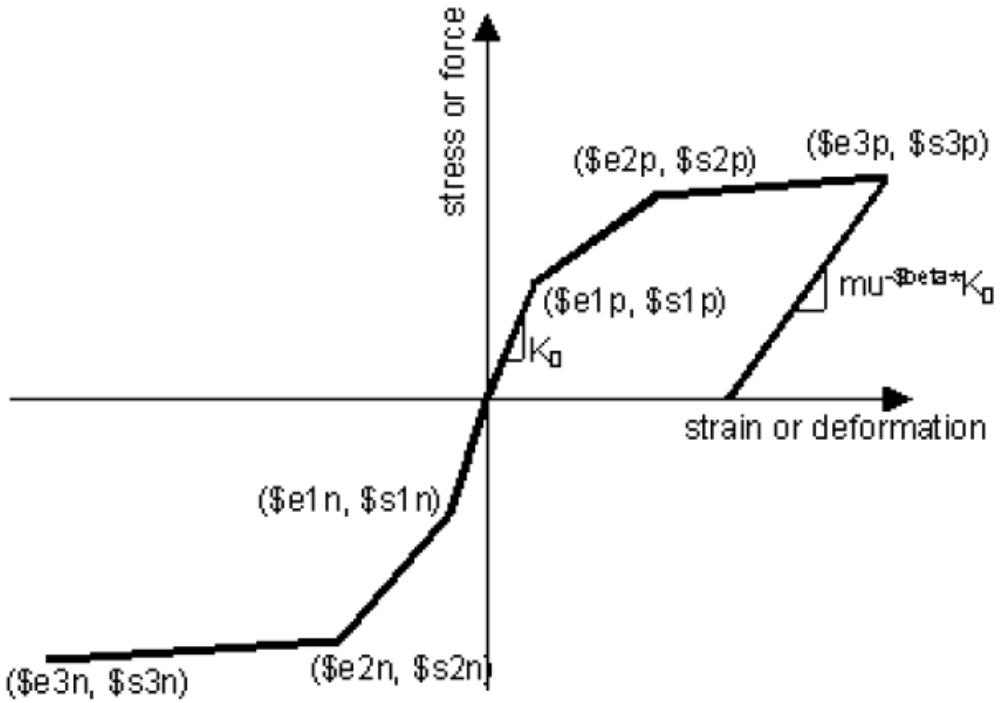

Figure 3.7 "Hysteretic" material properties (from OPENSEES)

In order to minimize response of the structural frame when the cladding connections are still behaving elastically, the natural period of the springs should match the natural period of the primary frame which is 1.01s. The mass of cladding attached to one spring is .25 kip-sec^2/ft. From equation 3.2, connection stiffness was calculated to be 0.8 k/in.

$$k = \omega^2 m = \frac{4\pi^2 m}{T^2}$$

(3.2)

However, such low connection stiffness would create cladding connection deflection problems, as noted previously. A series of analysis were conducted by incrementally increasing the connection stiffness in order to get an optimized result both in terms of maximum displacement between the cladding and the steel frame (maximum differential connection deflection) and maximum base shear on the SAC 3-story model with El Centro earthquake. Finally, hysteretic response loops with elastic stiffness from 8 to 12 k/in were used to model the non-linear spring materials. The elastic stiffness was calculated by equation 3.3:

$$k = \frac{EA}{L}$$

(3.3)

Where,

k = elastic stiffness of the non-linear spring (k/in);

E = modulus of elasticity of the non-linear spring (ksi); $\frac{\sigma}{\varepsilon}$

L = length of the non-linear spring (10 in).

Figure 3.8 to 3.11 shows the different "Steel02" hysteretic response loops. Table 3.6 shows the parameters and results of different "Steel02" hysteretic response loops. After a series of analysis were conducted by incrementally increasing the connection stiffness and changing the other parameters, the hysteretic response of "Steel02 HLoop5" with an elastic stiffness of 12 k/in was used as the model of the non-linear spring for the flexible cladding connection. From Table 3.6, "Steel02 HLoop5" showed the best results both in terms of maximum base shear and differential connection deflection.

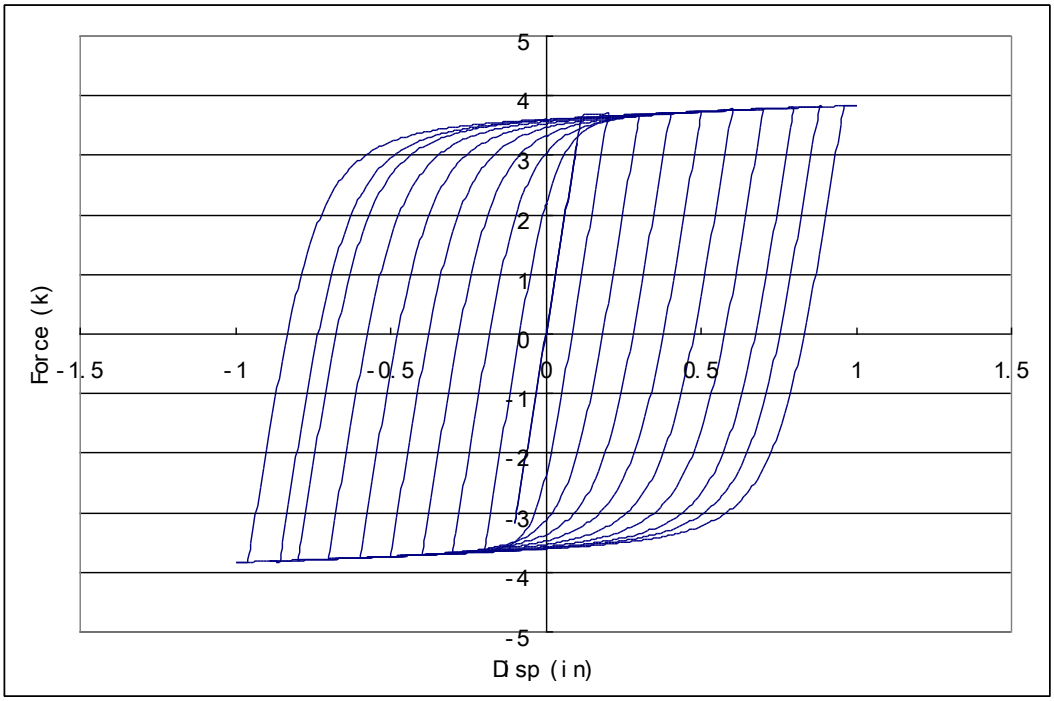

Figure 3.8 Hysteretic behavior of Steel02 Hloop4

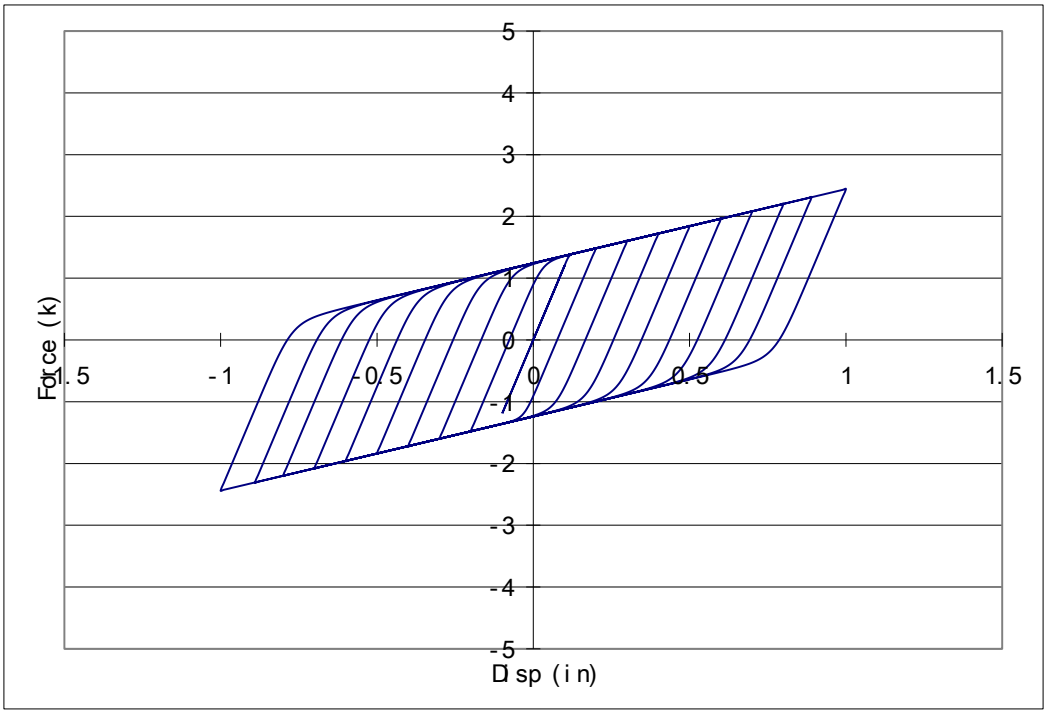

Figure 3.9 Hysteretic behavior of Steel02 Hloop5

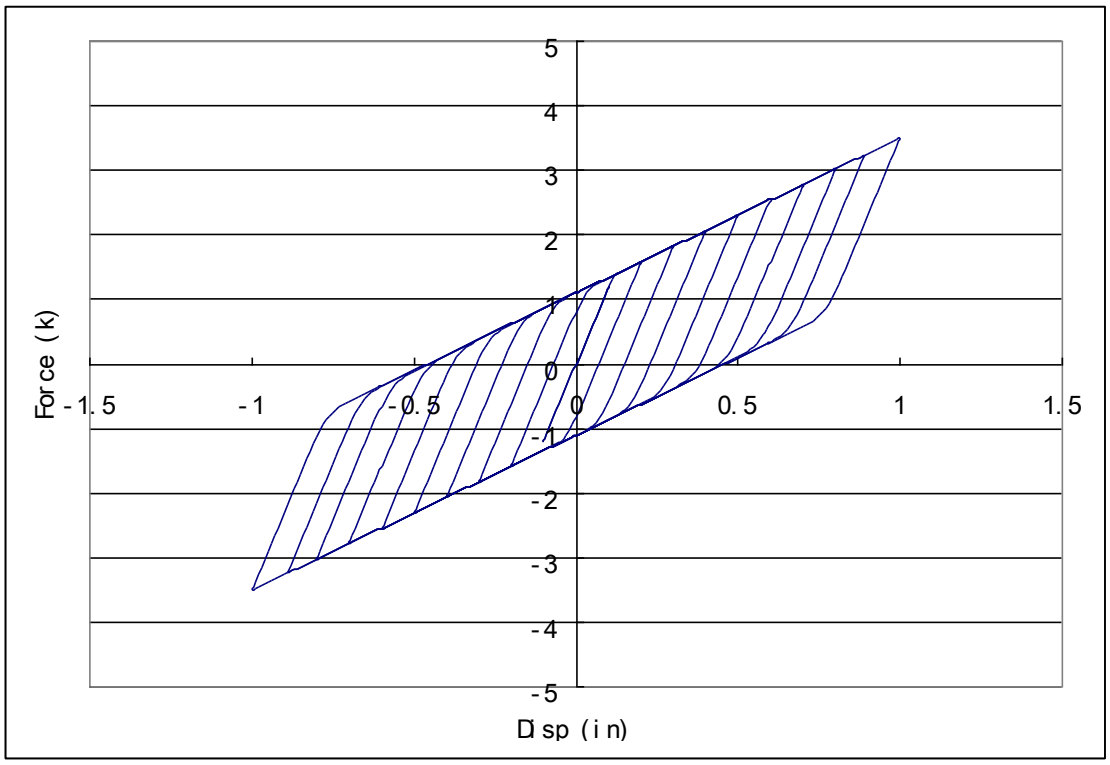

Figure 3.10 Hysteretic behavior of Steel02 Hloop6

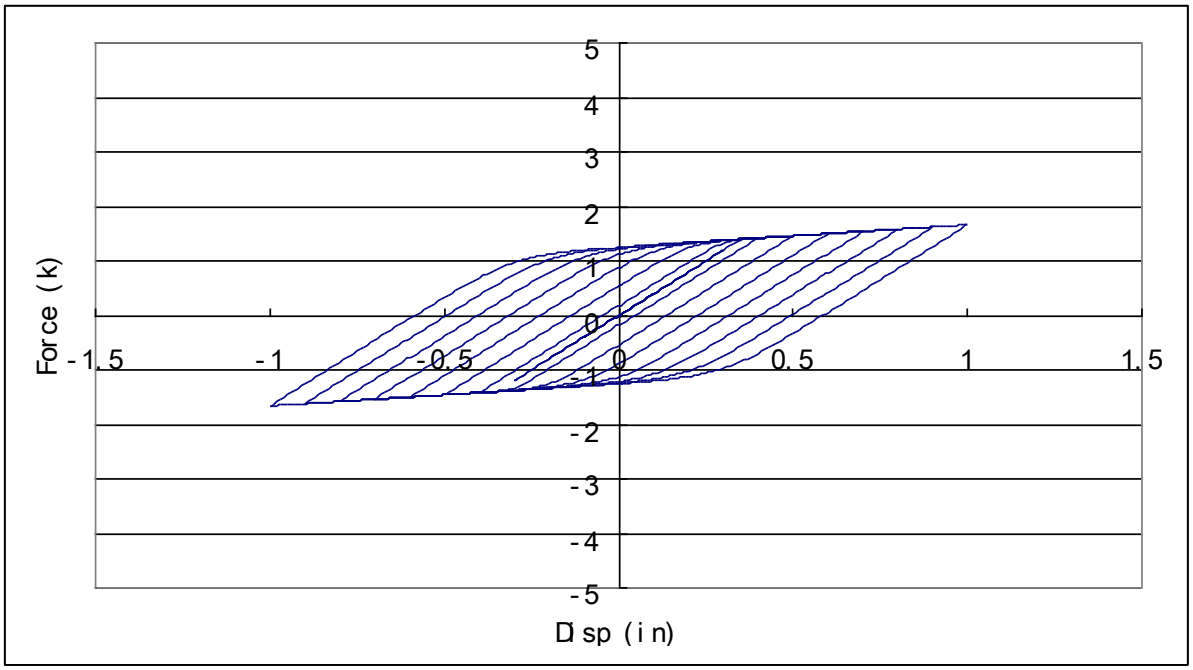

Figure 3.11 Hysteretic behavior of Steel02 Hloop9

Table 3.6 Parameters and results of "Steel02" non-linear spring materials

Parameters and results	Steel02 Hloop4	Steel02 Hloop5	Steel02 Hloop6	Steel02 Hloop9
A (in^2)	0.08	0.03	0.03	0.02
Fy (ksi)	46	46	46	70
E (ksi)	4000	4000	4000	2000
b	0.006	0.1	0.2	0.1
R0	35	100	150	100
cR1	0.925	0.925	0.925	0.925
cR2	0.1	0.1	0.1	0.1
k	32	12	12	4
Max. Differential Connection Deflection (in)	0.7	5.64	1.88	9.23
Max. Base Shear (k)	1108.1	1047.3	1088.3	1085.4

To more closely match the hysteretic behavior of engineered cladding connection (Figure 2.5), a combination of "Pinching4" and "Steel02" were applied in parallel as shown in Figure 3.9. The hysteretic responses of the two materials were simply "stacked" together. "Pinching4.11" material was defined specifically so that it could be added to "Steel02halfloop". The material properties of "Steel02halfloop" were identical to "Steel02 HLoop4" except the cross-section area was only half of the "Steel02 HLoop4". Figure 4.12 and 4.13 shows the hysteretic behaviors of "Pinching4.11" and "Steel02halfloop". The force component of "Pinching4.11" was directly added to "Steel02halfloop", while the displacement component of the hysteretic loop of the two remained the same. The parameters and hysteretic loop of "Pinching4.11&Steel02halfloop" are shown in Table 3.7 and Figure 3.14.

Table 3.7 Non-linear spring parameters of "Pinching4.11&Steel02halfloop"

parameters	Pinching4.11&Steel02halfloop
A (in^2)	0.04
Fy (ksi)	46
E (ksi)	4000
b	0.006
R0	35
cR1	0.925
cR2	0.1
pEnvelopeStress	[3.0 13.0 70.0 1.0]
nEnvelopeStress	[-3.0 -13.0 -70.0 -1.0]
pEnvelopeStrian	[0.0005 0.05 0.1 0.15]
nEnvelopeStrian	[-0.0005 -0.05 -0.1 -0.15]
rDisp	[1.0 1.0]
rForce	[0.0001 0.0001]
uForce	[0.0 0.0]
gammaK	[0.5 0.1 0.15 0.1 0.45]
gammaD	[0.0 0.0 0.0 0.0 0.0]
gammaF	[0.0 0.0 0.0 0.0 0.0]
gammaE	10
dam	energy

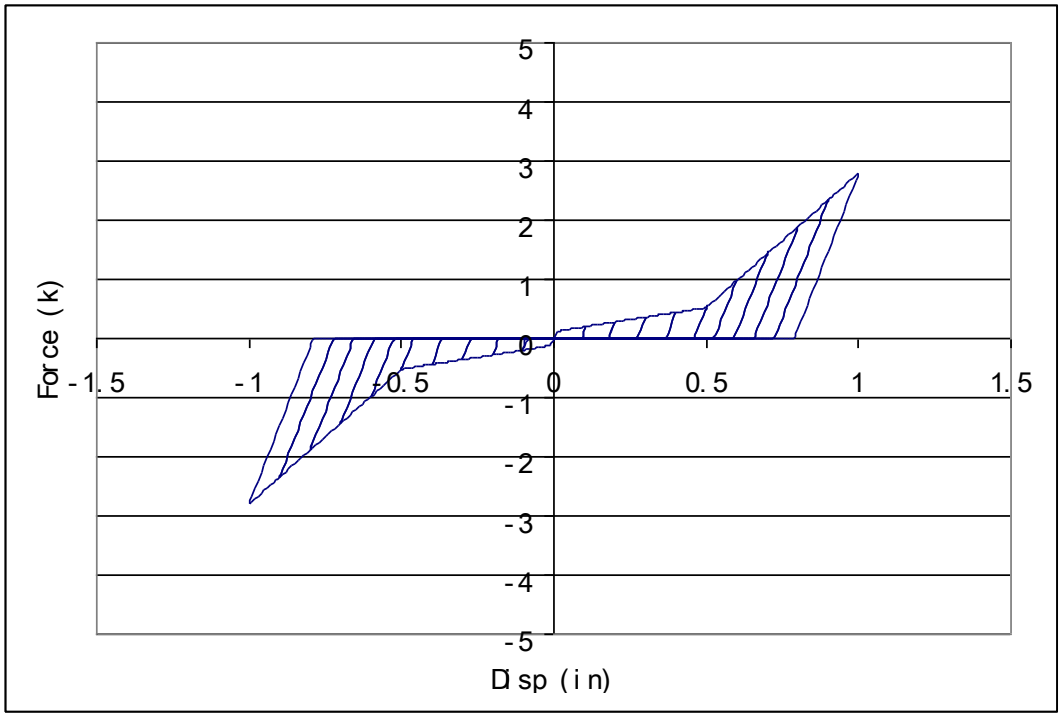

Figure 3.12 Hysteretic behavior of Pinching4.11

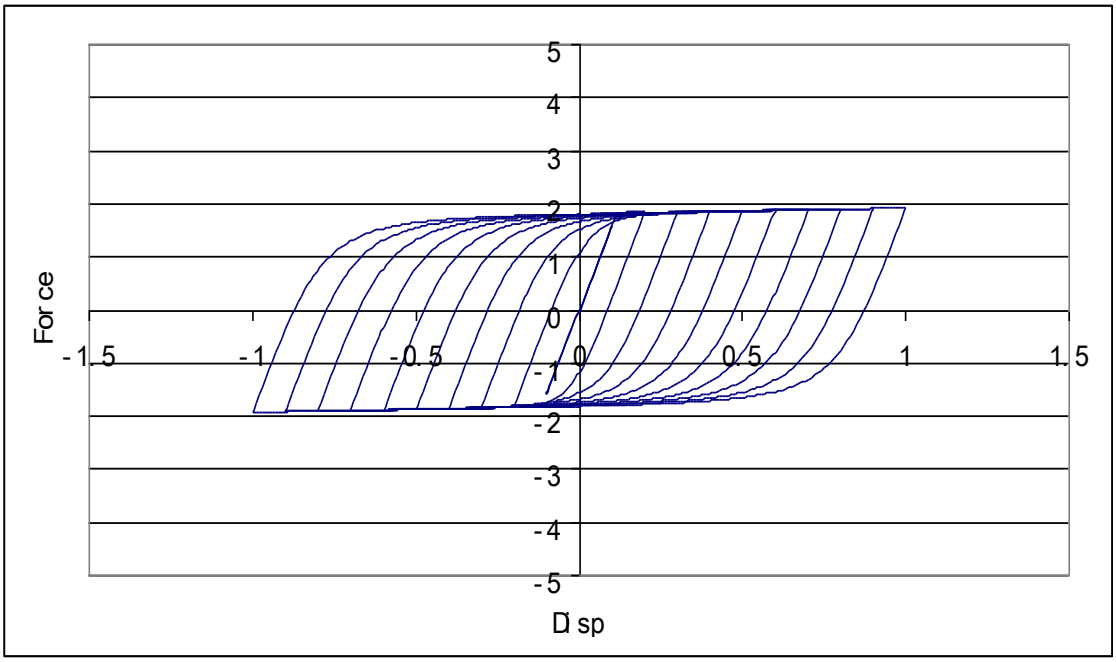

Figure 3.13 Hysteretic behavior of Steel02halfloop

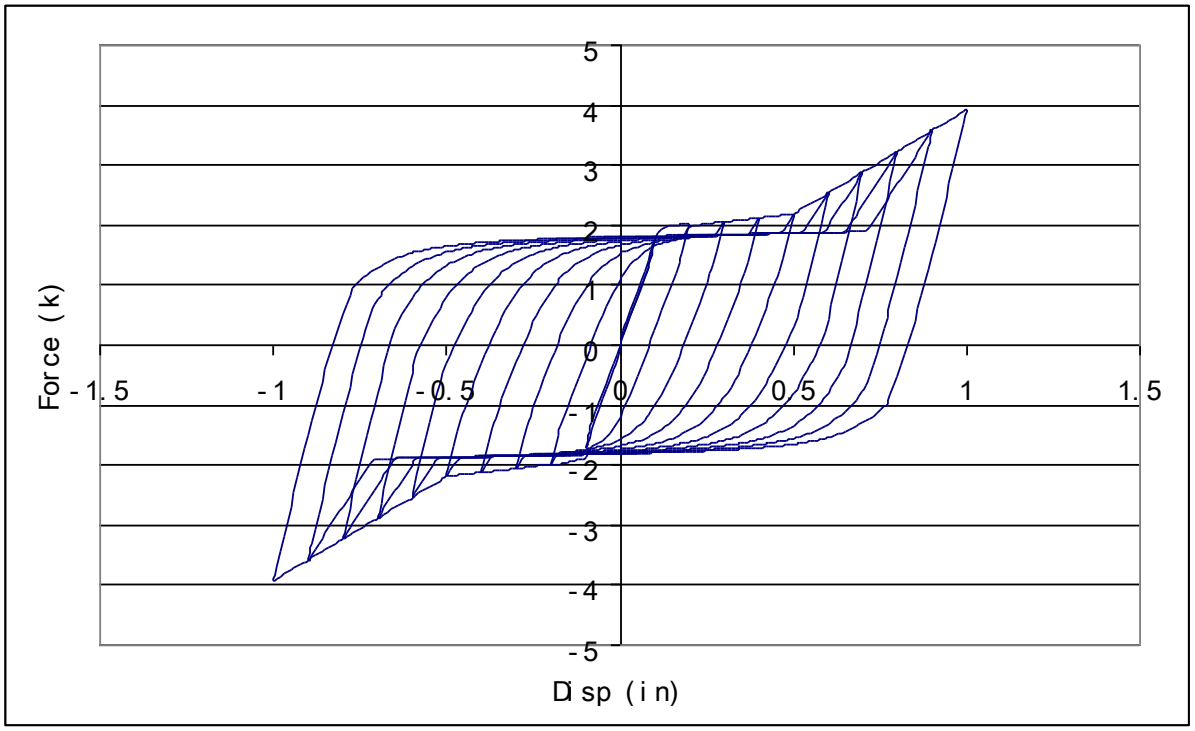

Figure 3.14 Hysteretic behavior of Pinching4.11&Steel02halfloop

A series of trials for this "Hysteretic" material with an elastic stiffness range from 4 to 8 k/in have been conducted. The hysteretic behaviors and parameters of "Hysteretic" materials used are shown in Table 3.8 and Figures 3.15 – 3.18. Hardening effects were modified by increasing the ultimate stress (s3p; s3n), s3p and s3n were increase from 85 ksi to 160 ksi (Table 3.8).

Table 3.8 Hysteretic material parameters

parameters	Hys. 3	Hys.4	Hys. 5	Hys. 6
A (in^2)	0.04	0.04	0.04	0.04
s1p;s1n (ksi)	2	2	2	2
e1p;e1n	0.001	0.001	0.002	0.001
s2p;s2n (ksi)	10	10	10	10
e2p;e2n	0.05	0.06	0.05	0.06
s3p;s3n (ksi)	85	160	150	160
e3p;e3n	0.3	0.35	0.04	0.043
pinchX	0.4	0.4	0.4	0.4
pinchY	0.6	0.6	0.6	0.6
damage1	0	0	0	0
damage2	0.02	0.02	0.02	0
beta	0.01	0.01	0.0001	0.0001
k (k/in)	8	8	4	8

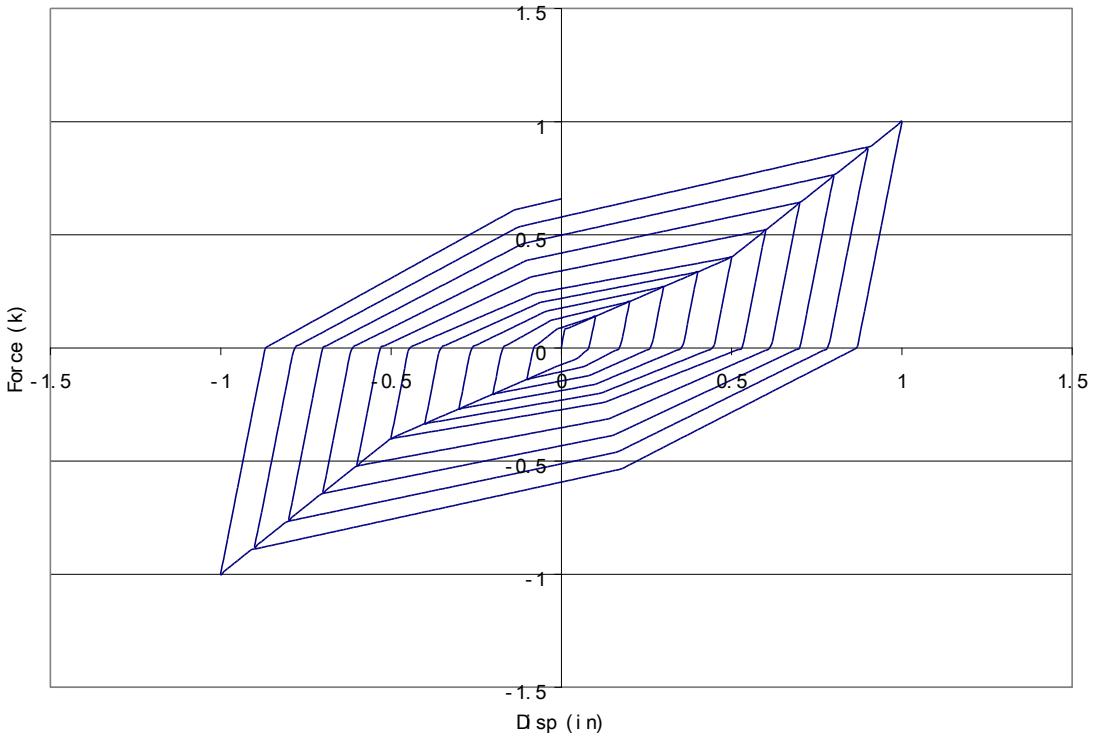

Figure 3.15 Hysteretic behaviors of "Hys.3"

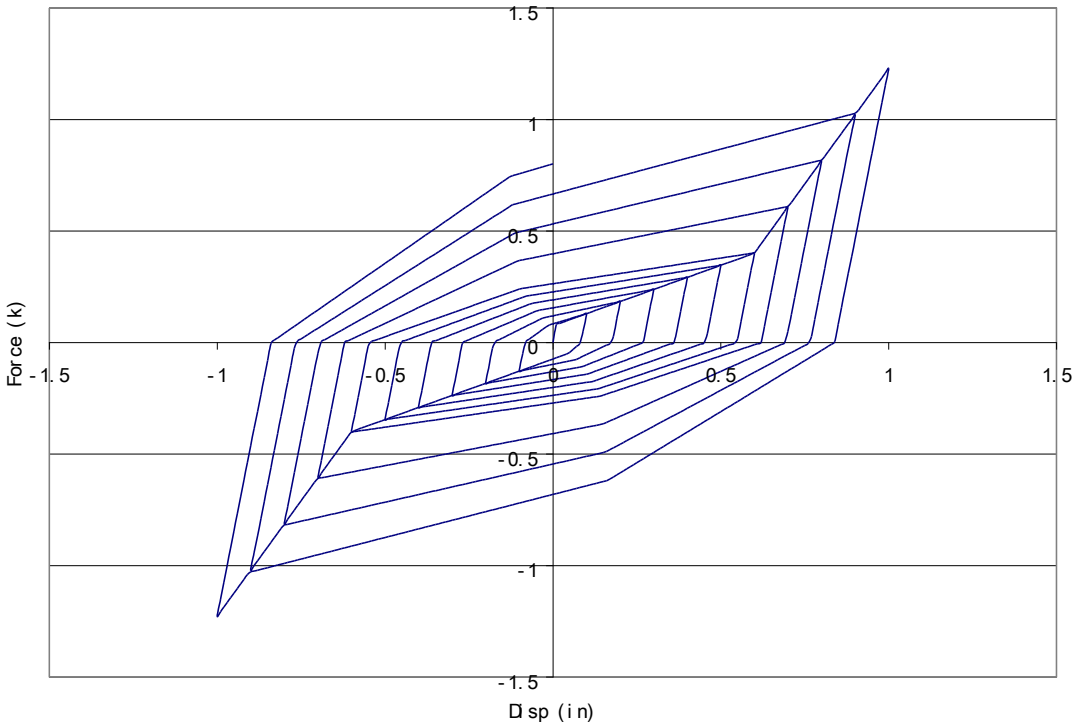

Figure 3.16 Hysteretic behaviors "Hys.4"

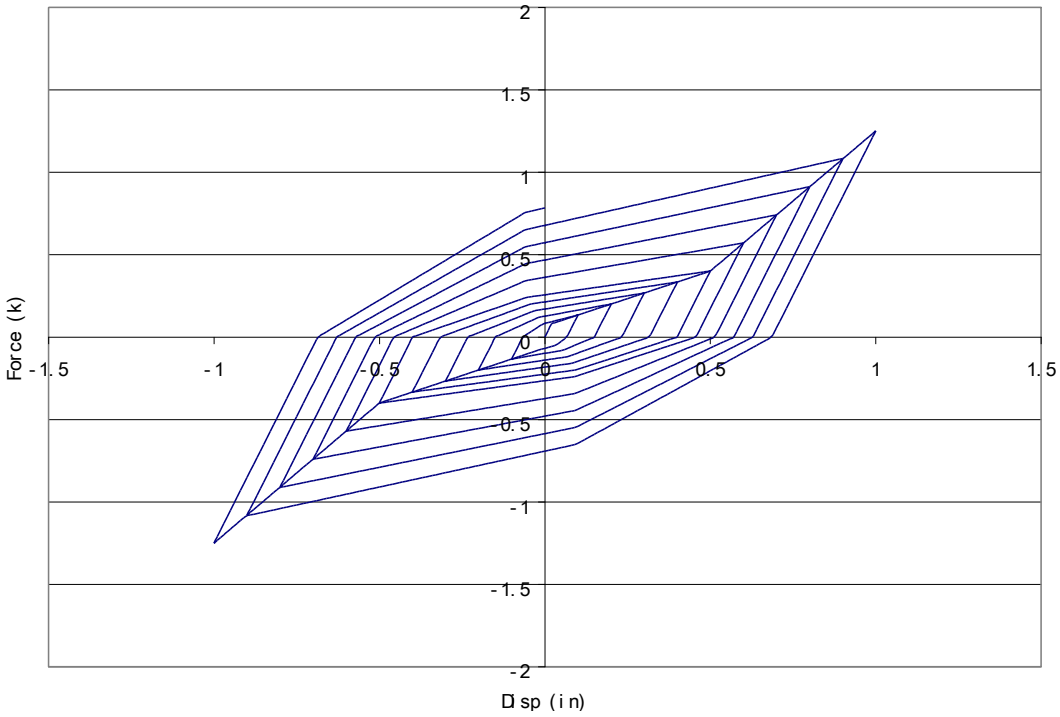

Figure 3.17 Hysteretic behaviors "Hys.5"

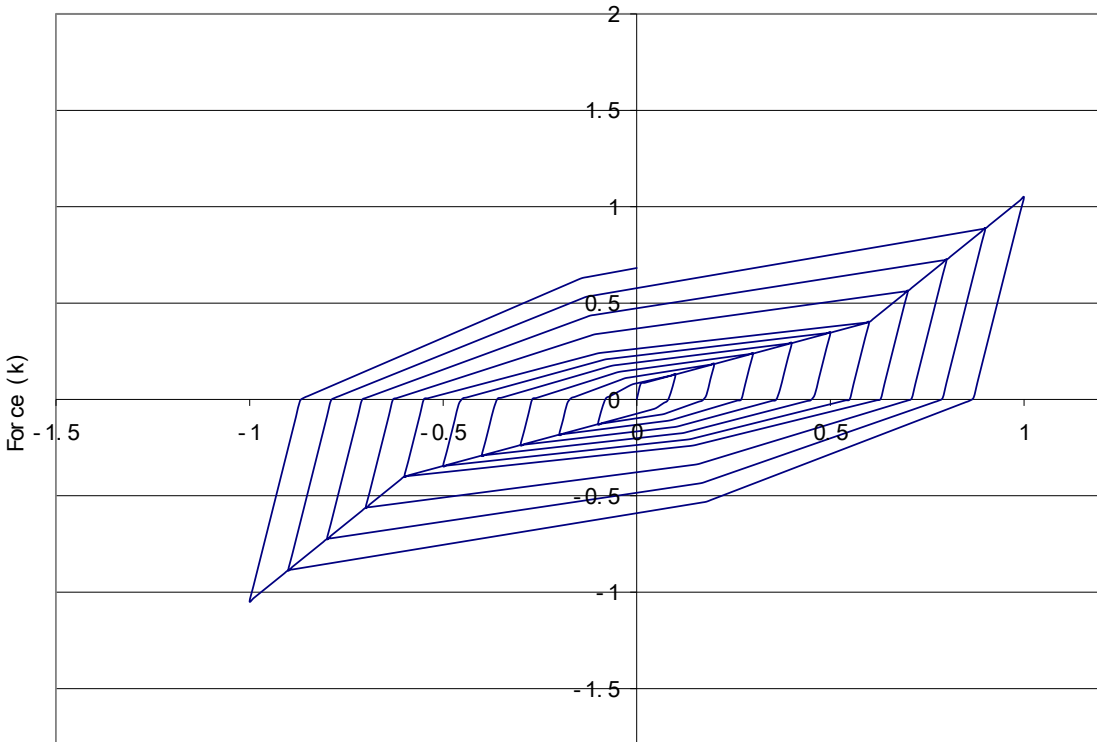

Figure 3.18 Hysteretic behaviors "Hys.6"

3.5 Results of SAC 3-story model with different spring properties

The non-linear spring materials were used as the flexible cladding connection in modeling the SAC 3-story model under the El Centro ground motion. The parallel spring's material (Pinching4.11&Steel02halfloop) was first used to model the cladding connection of the SAC 3-story frame in OPENSEES (Figure 3.14). The results showed minimum reduction in base shear, although the maximum differential connection deflections were reduced to 3.75 in (9.53 cm). The differential connection deflection was defined as the relative connection from the structural frame and cladding. The maximum moments from three members of the structure exceeded M_p (Table 3.9).

"Steel02 Hloop5" spring material was next used as the flexible cladding connection in the model (Figure 3.9). It showed a better effect on reduction of maximum base shear, which the maximum base shear was reduced to 1048.6 k (4664.2 kN) (Table 3.9). Maximum moments from none of members exceeded $M_{p.}$

The results of SAC 3-story model with "Hysteretic" materials (Figure 3.15-3.18) as flexible cladding connections under El Centro earthquake were obtained from OPENSEES. The summary and results of all the spring materials were shown in Table 3.9.

Table 3.9 Analysis results for SAC 3-story model with different spring materials as flexible cladding connections under El Centro Earthquake

Connection types	Rigid	Pinching 4.11&Steel02halfloop	Steel02 Hloop5	Hys.3	Hys.4	Hys.5	Hys.6
Max. Base shear (k)	1118.2	1077.9	1048.6	1062.6	1068.7	1070.5	1065.3
Number of members exceeded M_p	8	3	0	0	2	1	0
Max. differential connection deflection (in.)	N/A	3.75	5.65	4.67	3.07	3.97	3.65

From the summary Table 3.9, among the "Hysteretic" materials, "Hys.3" and "Hys.6" showed no members exceeded M_p. However, the maximum differential connection deflection was reduced from 4.67 to 3.65 in (11.86 to 9.27 cm). The maximum base shear for "Hys.3" and "Hys.6" was reduced by 5% from the rigid case. From Table 3.9, "Hys.6" presented the best results in both reducing the response of the SAC 3-story frame

and controlling deflection. The maximum differential connection deflections between the cladding and the primary structure for using "Hys.6" material were 1.70, 3.14, and 3.65 in (4.32, 7.98, and 9.27 cm) for the 1st through 3rd floor respectively (Figure 3.19).

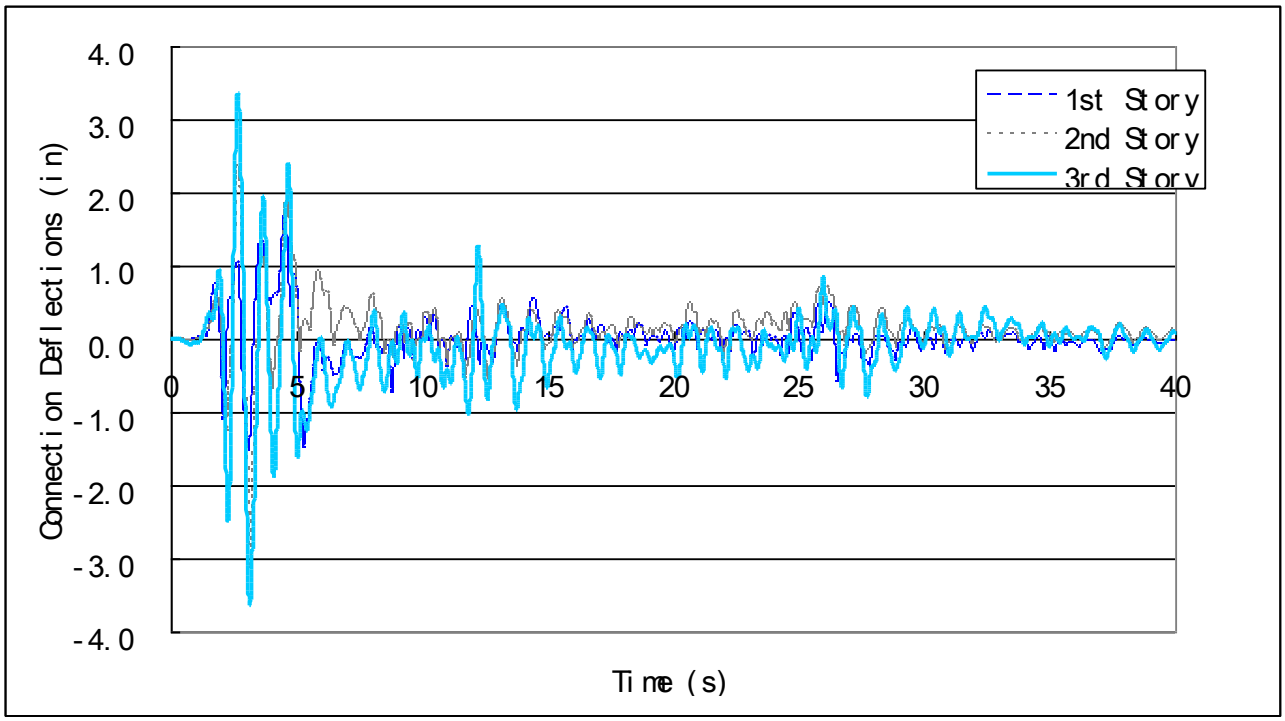

Figure 3.19 Differential connection deflections for SAC 3-story model

3.6 Conclusions

In this Chapter, a partial inelastic model of the SAC 3-story building was built according to the elastic and inelastic behaviors of each element in the structure. Different non-linear springs were discussed and used to model the flexible cladding connections on the SAC 3-story model. The results has demonstrated the possible benefits of using flexible instead of rigid cladding connections to reduce response of the primary structure when

subjected to the El Centro earthquake. Among all the hysteretic behaviors, "Hys6" has demonstrated the best results for the structure and load considered, both in terms of reducing the response of the primary structure and controlling connection deflections. By comparing the result with previous research (Nguyen 2009), Nguyen used "Steel02 Hloop2" (Figure 2.7) as the material properties for the flexible connection, the differential connection deflections reduced from 7 to 3.65 in (17.78 to 9.27 cm) and the maximum base shear reduced from 1070.3 to 1065.3 k (4760.7 to 4738.5 kN). Therefore, it appeared that with further modifications of connection properties it may be possible to both reduced base shear in the structure members and limit cladding deformations.

CHAPTER IV

ANALYSIS RESULTS ON HYSTERETIC ENERGY DISSIPATION OF FLEXIBLE CLADDING CONNECTIONS

4.1 Introduction

From the previous analysis results, "Hysteretic" non-linear springs for the flexible cladding connection showed the best results both in terms of reducing maximum moments in the members and controlling connection deflections. Hys.6 hysteretic material was chosen for the flexible cladding connections to analyze the behaviors of the SAC 3-story model under different seismic excitations. The case of rigid connections was used as the baseline case for comparison of structural frame behavior. Detailed connection behaviors such as differential deflections between claddings and frame, panel to panel deflections and extent of damage were compared. An initial analysis of the SAC 9-story model with the flexible connection was also conducted. The analysis objective of this Chapter was to fix material properties of the flexible cladding connections and vary the earthquake excitation input including different earthquake design levels in order to evaluate the effectiveness of the flexible cladding connections.

4.2 Targeted Ground Motions

The fundamental period of the SAC 3-story model with the rigid cladding connection was 1.055s. A series of earthquake records were chosen based on this fundamental period. Table 4.1 provides the details information of the earthquake records for the analysis. All

information including acceleration data and response spectra data were obtained from the PEER Strong Motion Database (Silva, 2000).

Table 4.1 Historic earthquake information for analysis (Silva, 2000).

Earthquake Records	Magnit-ude	Date	Compo nent (Degree to N, o)	Statio n	Location	D_t (s)	Total Time (s)	PGA (g)	Site Class	Eipcen-tral Dist (km)
El Centro	7.0	5/19/ 1940	180	USG S 117	El Centro Array #9	0.01	40	0.313	D	12.99
San Fernando	6.6	2/9/1 971	180	USG S 135	LA - Hollywood Stor. Lot	0.01	28	0.174	D	21.2
Loma Prieta	6.9	10/18 /1989	0	CDM G 58117	TREASUR E ISLAND	0.005	30	0.1	D	97.43
Big Bear	6.4	6/28/ 1992	90	USG S 23542	San Bernardino -E &Hospitalit y	0.01	50	0.092	D	45.5
Northridge	6.7	1/17/ 1994	90	CDM G 24400	LA - Obregon Park	0.02	40	0.355	D	39.4

Figures 4.1 to 4.5 show the time-acceleration history of the five different earthquakes. Figures 4.6 to 4.10 show the Pseudo-acceleration spectra for five different earthquake records with damping ratio of 5%. From the Pseudo-acceleration spectra, it can be seen that each earthquake record represents a different level of frequency excitation. Loma Prieta and Big Bear earthquake records had high excitation levels near the structure

fundamental period. El Centro earthquake record had medium excitation level at the structure fundamental period. The Northridge and San Fernando earthquake records had low excitation level at the structure fundamental period. The variation of the earthquake excitation level with respect to the structure fundamental period would show whether the flexible cladding connections were effective under the different earthquake records.

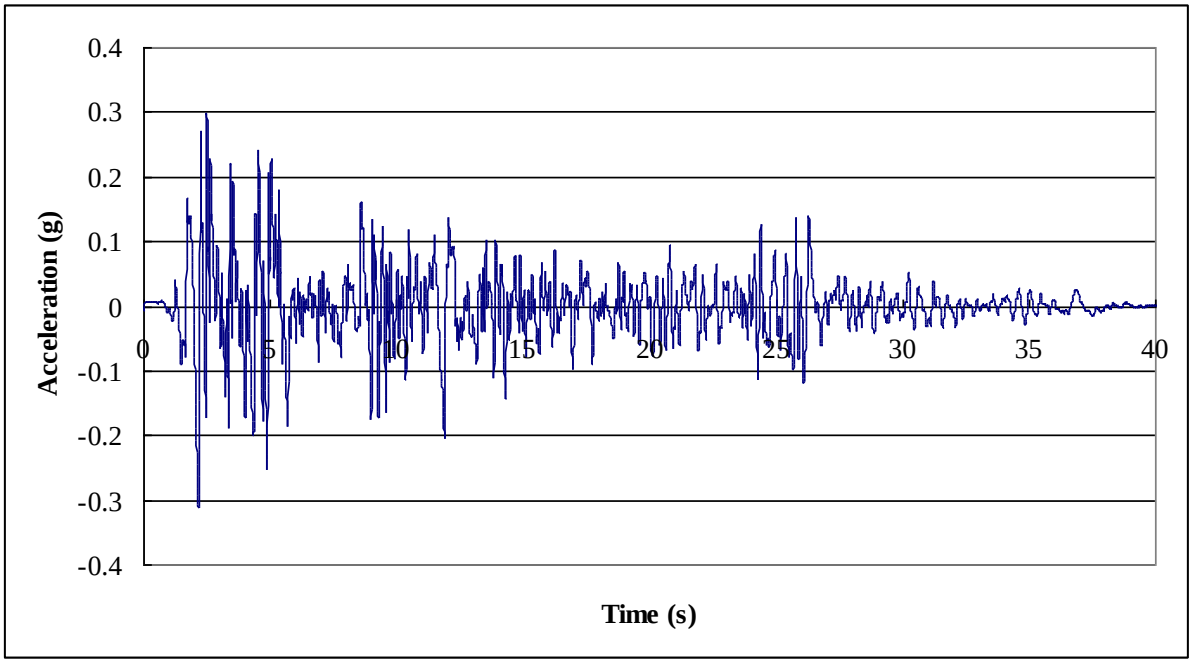

Figure 4.1 Time-acceleration history for El Centro earthquake

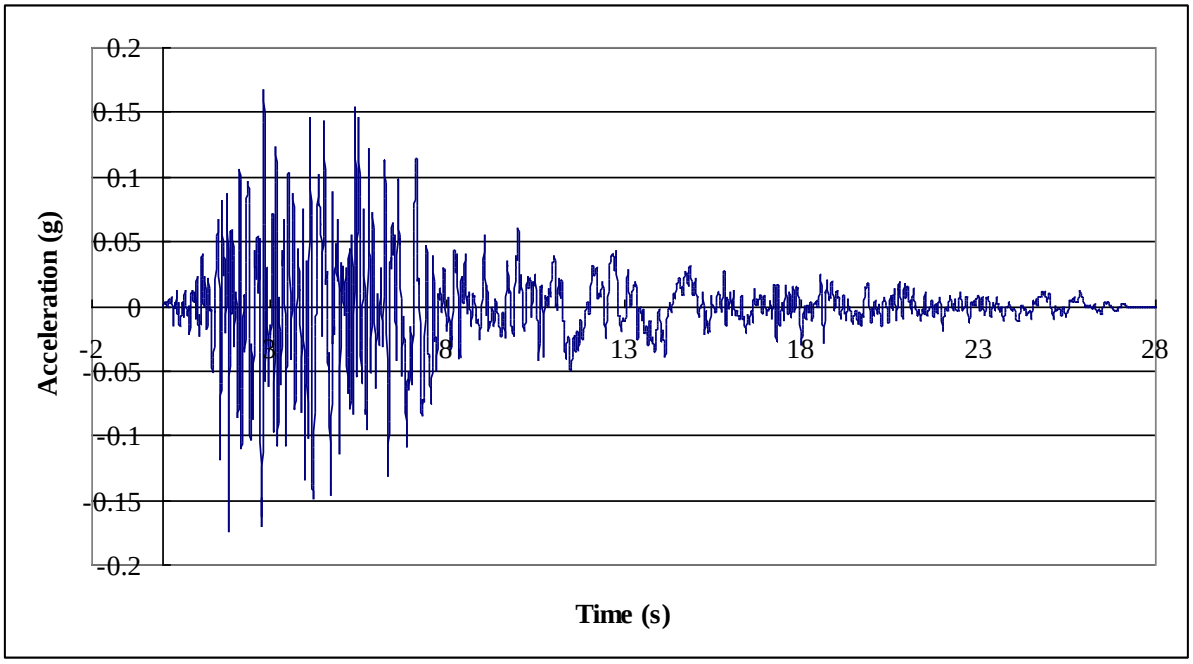

Figure 4.2 Time-acceleration history for San Fernando earthquake

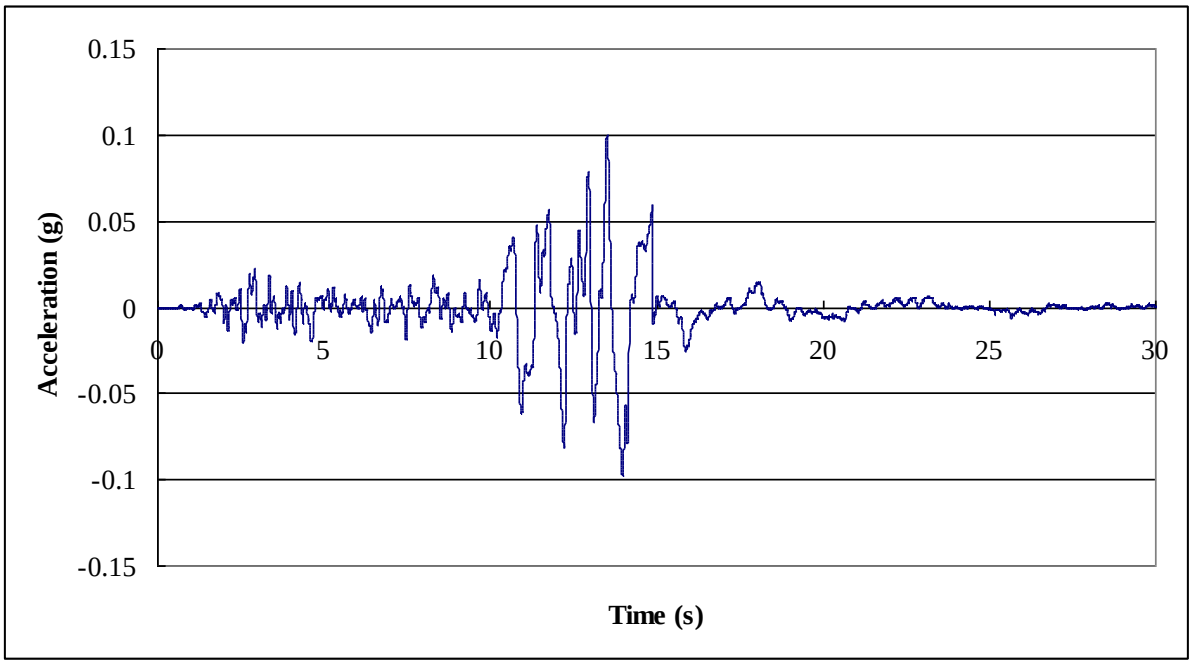

Figure 4.3 Time-acceleration history for Loma Prieta earthquake

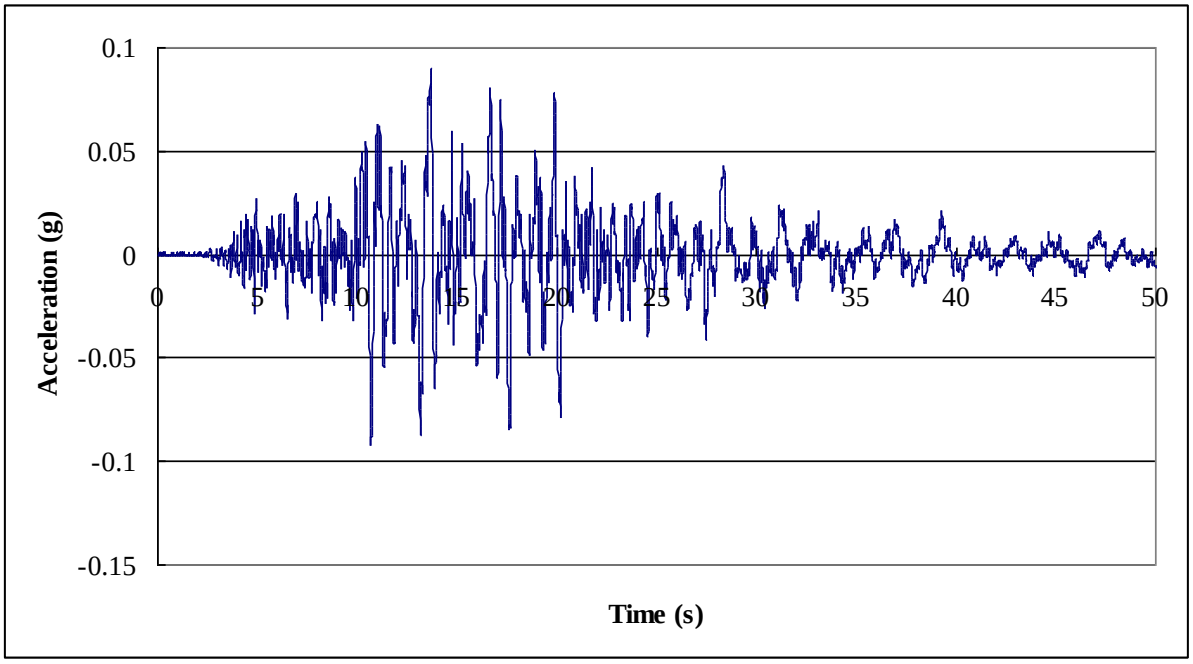

Figure 4.4 Time-acceleration history for Big Bear earthquake

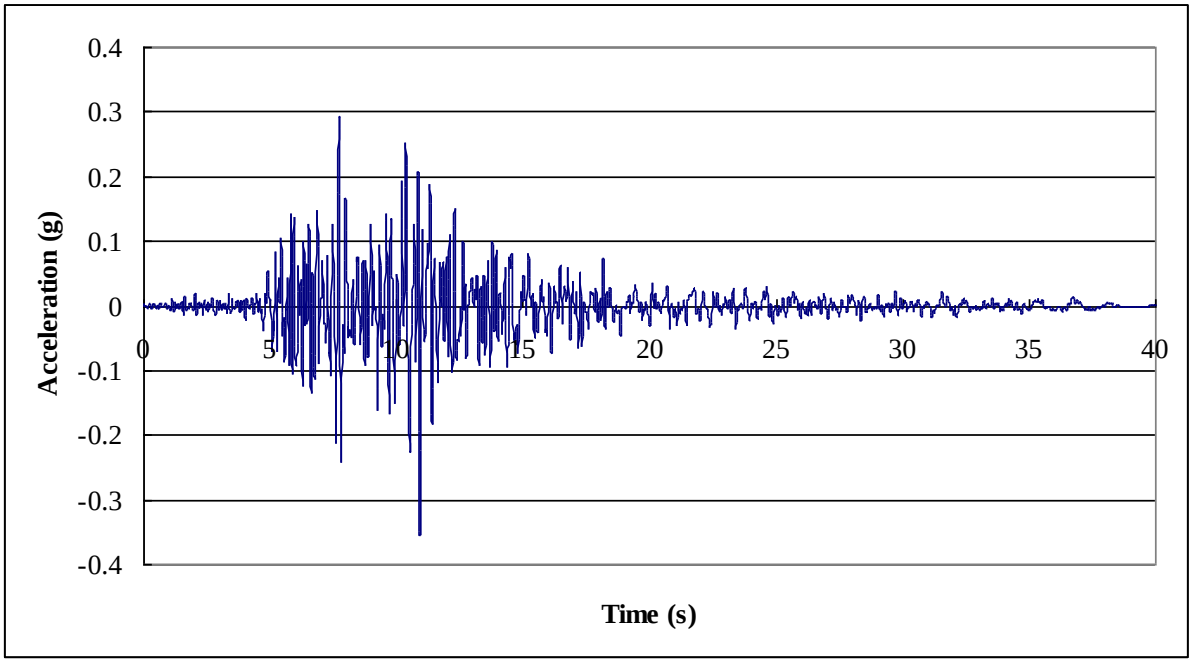

Figure 4.5 Time-acceleration history for Northridge earthquake

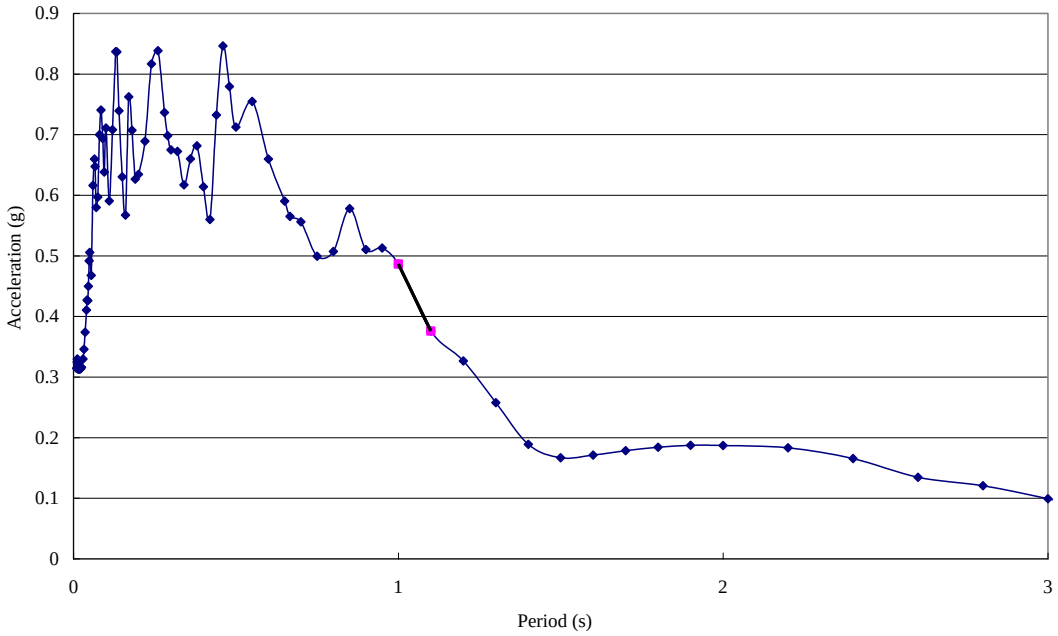

Figure 4.6 Pseudo-acceleration spectrum of El Centro earthquake record, ζ=5%

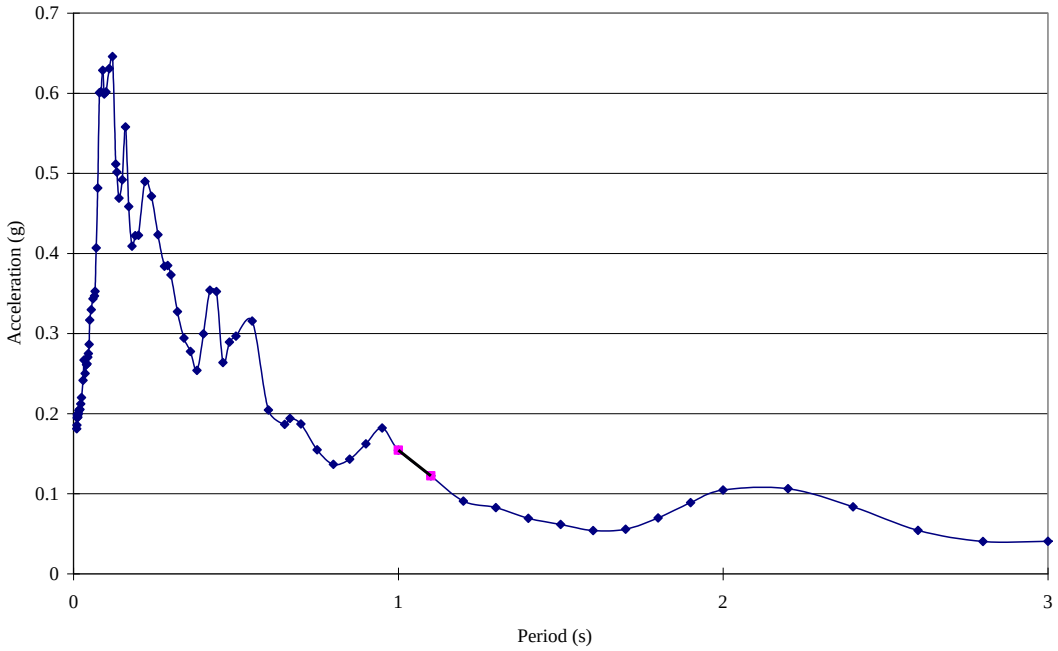

Figure 4.7 Pseudo-acceleration spectrum of San Fernando earthquake record, ζ=5%

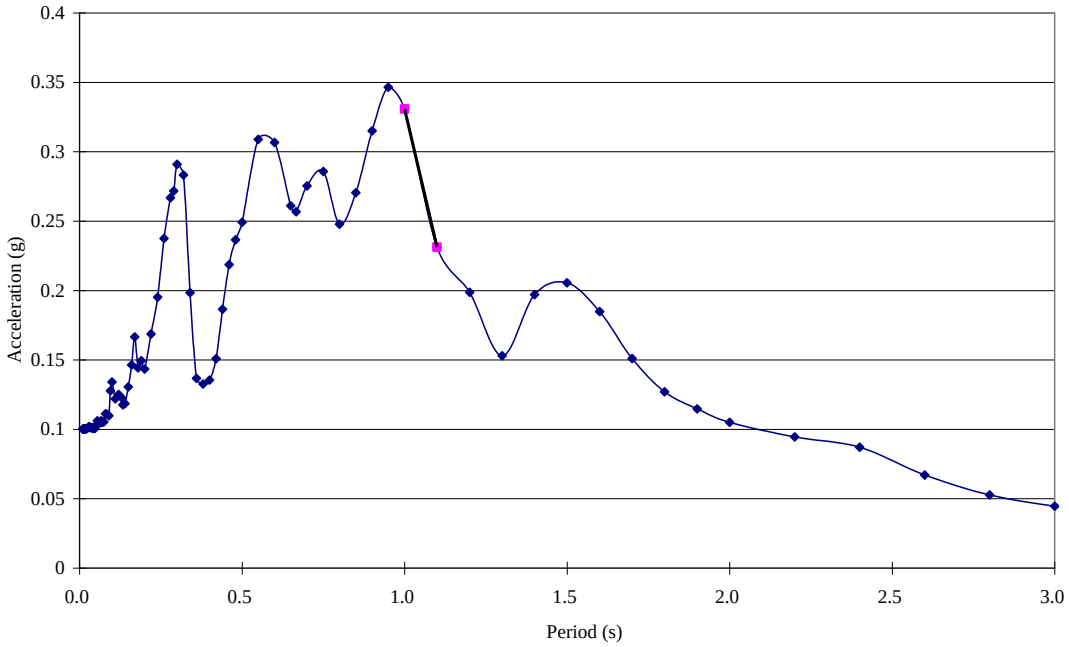

Figure 4.8 Pseudo-acceleration spectrum of Loma Prieta earthquake record, ζ=5%

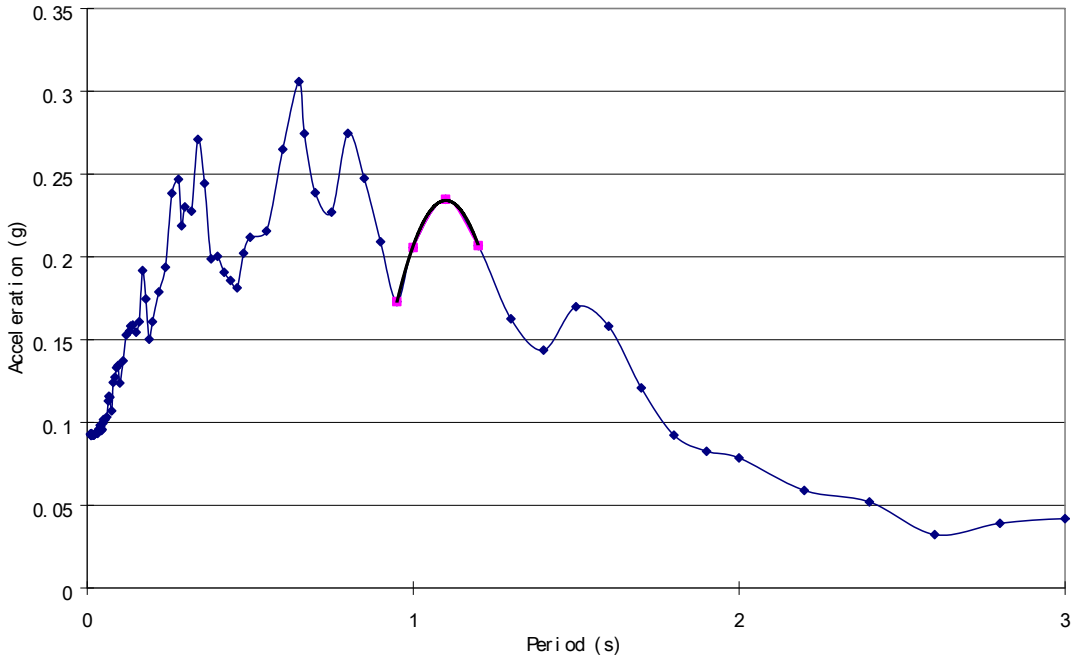

Figure 4.9 Pseudo-acceleration spectrum of Big Bear earthquake record, ζ=5%

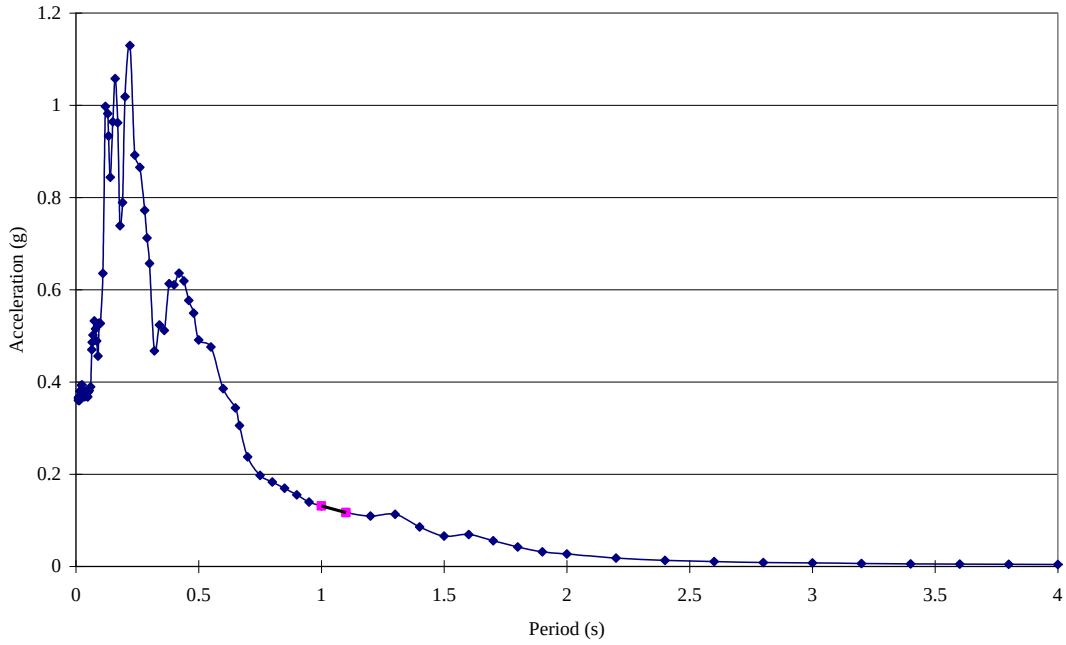

Figure 4.10 Pseudo-acceleration spectrum of Northridge earthquake record, ζ=5%

4.3 Design Spectra for Analysis

For the purpose of consistence and comparability, all selected earthquake records were recorded on class D sites. Referring to the International Building Code (IBC) and ASCE 7-05, a set of design spectra were generated using NSHMP Hazard Map program developed by United States Geological Survey (USGS). The design spectra were used as reference points so that different earthquake response spectra could be scaled to specific design level. The location for the analysis was in Los Angeles (LA), California region with a zip code of 90002. This location has a relatively low seismic activity compared to other regions in LA and is not a near fault region. For a design spectrum with 10%

probability in 50 years of exceedance (10%/50yrs), the mapped short-period spectral acceleration (S_S) is 0.916g and the mapped long-period spectral acceleration (S_1) is 0.337g. These values can be obtained by inputting zip code and probability of exceedance into the NSHMP Hazard Map program. According to Table 11.4-1 and 11.4-2 in ASCE 7-05; using previous S_S and S_1 value for site class D, F_a and F_v were obtained to be 1.133 and 1.726. These parameters (S_S, S_1, F_a and F_v) were input to NSHMP Hazard Map program which a design spectrum was generated and plotted in Figure 4.11. At the structural fundamental period, the level of excitation equals to 0.552g. The detail information for 10%/50yrs design level is shown in Table 4.2. The predominant periods (the periods at which the peak excitations of the Pseudo-acceleration spectrum occurred), scaling factors required to scale each earthquake the design levels, and peak acceleration for each earthquake were shown in Table 4.2 and 4.3. For a design spectrum with 20% probability in 50 years of exceedance (20%/50yrs), S_S and S_1 are 0.677g and 0.250g. Same procedure was used to obtain F_a and F_v, which were 1.258 and 1.900. The design spectrum was generated with these set of parameters by NSHMP Hazard Map program which was plotted in Figure 4.12. At the structural fundamental period, the level of excitation equals to 0.451g. The detail scaling information for 20%/50yrs design level is shown in Table 4.3. In order to compare these design spectra with the specific earthquake response spectra, all response spectra were scaled to the design spectra. The excitation level for each design spectrum was scaled to match at the fundamental period of the SAC 3-story model with rigid cladding connections, which was at 1.055s. Figure 4.11 and 4.12 showed the scaled response spectra and original design spectrum. For the design spectrum with 10% probability in 50 years of exceedance, all the earthquake

response spectra were scaled to 0.552g at period of 1.055 seconds. For the design spectrum with 20% probability in 50 years of exceedance, all the earthquake response spectra were scaled to 0.451g at period of 1.055 seconds.

Table 4.2 Scaled earthquake records with 10%/50yrs

Earthquakes	Predominant period (s)	Scale Factor	Peak Acc. (5% damping), g
El Centro	.08-1	1.30	1.10
San Fernando	.08-.55	4.04	2.61
Loma Prieta	.5-1	2.00	0.69
Northridge	.2-.6	4.49	5.07
Big Bear	.2-1.3	2.45	0.75

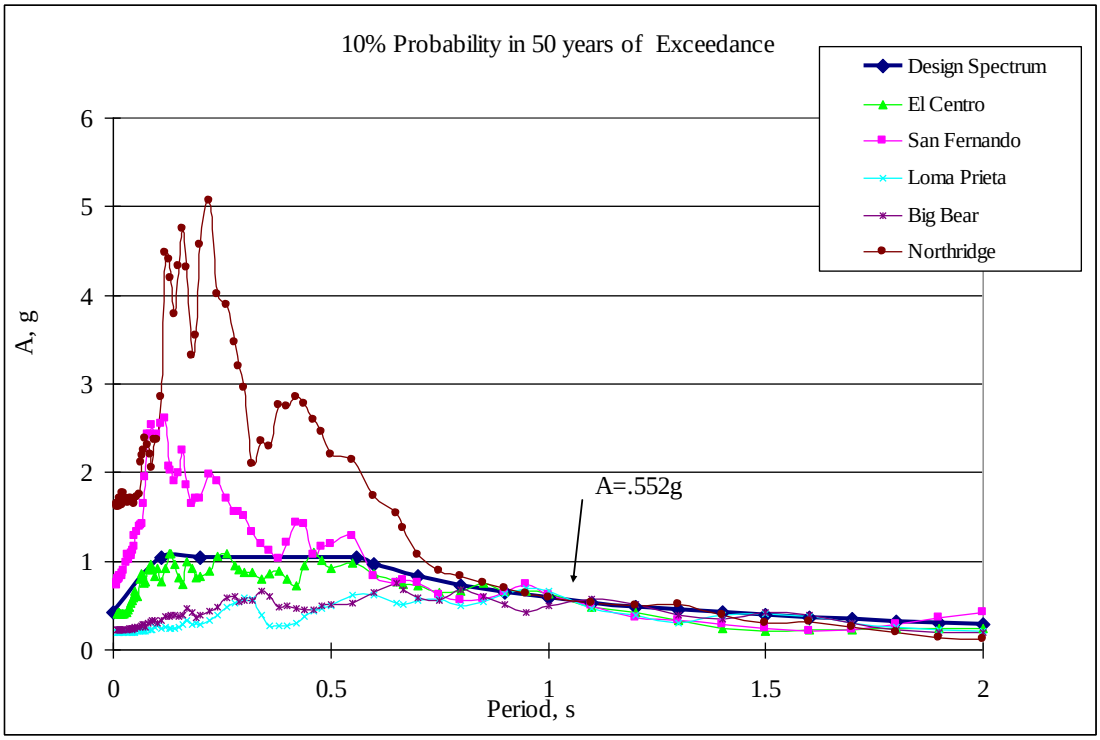

Figure 4.11 Design spectrum with different response spectra for 10%/50yrs

Table 4.3 Scaled earthquake records with 20%/50yrs

Earthquakes	Predominant period (s)	Scale Factor	Peak Acc. (5% damping), g
El Centro	.08-1	1.06	0.90
San Fernando	.08-.55	3.30	2.13
Loma Prieta	.5-1	1.63	0.57
Northridge	.2-.6	3.67	4.14
Big Bear	.2-1.3	2.00	0.61

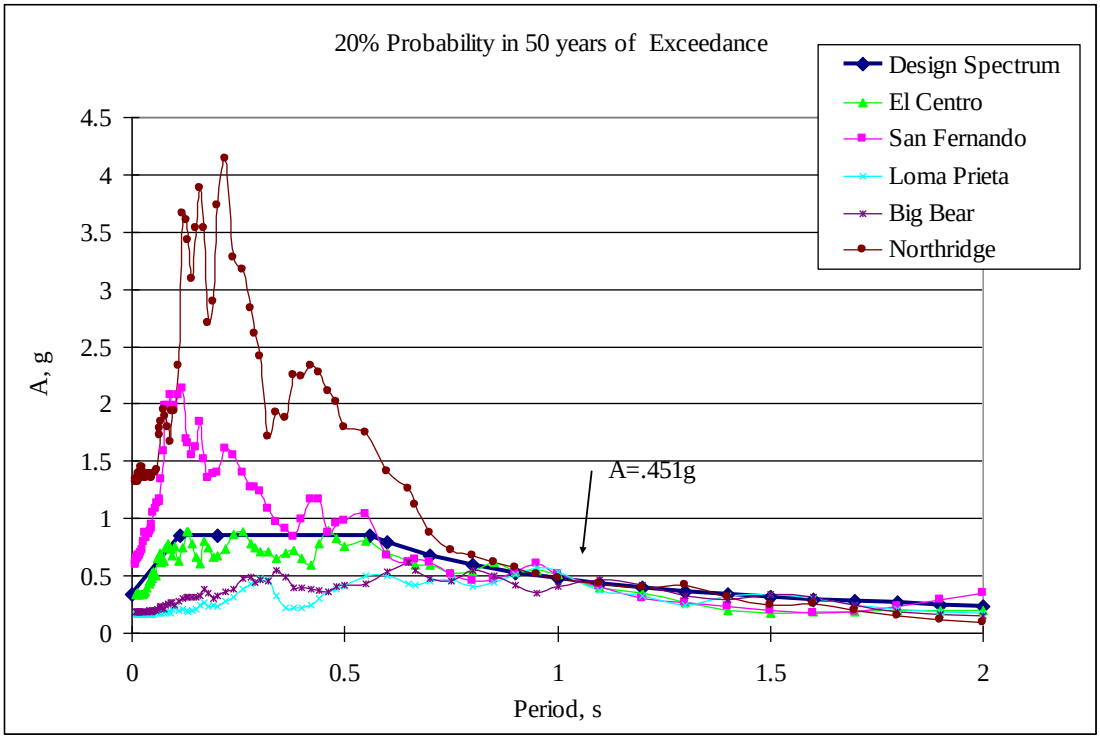

Figure 4.12 Design spectrum with different response spectra for 20%/50yrs

The scaled Northridge earthquake can be seen to have very high excitation level at low periods. It will be very likely to excite the structure in an unrealistic manner at its higher modes but was included to specifically evaluate the importance of the higher mode effects. The second period for the SAC 3-story model was 0.396s with the flexible connections. The excitation level was extremely high for this mode (unreasonably so), exceeding the design spectrum at the second period from Figure 4.11 and 4.12 by a factor of 2.5. The excitation levels for other earthquake records were either slightly over or under the design spectrum at the second period. The behaviors of the claddings were affected by higher modes, which the flexible cladding connection had a shift in mass participation to higher modes of the overall structural frame.

4.4 Analysis results and discussion for SAC 3-story model

From analysis results presented in Chapter 3, the "Hys.6" cladding connections appeared promising based on analysis using an unscaled El Centro earthquake. The identical SAC 3-story model was analyzed in OPENSEES with both rigid and "Hys.6" cladding connections and subjected to the suite of scaled time-history record with scaling factor determined by using Figures 4.11 and 4.12.

Hysteretic energy dissipation for individual member of the structure was reported. The number of structural frame members which exceeded M_y was also recorded in order to show which members in the model were dissipating significant energy (resulting in significant damage). Figure 4.13 and 4.14 show a plot of moments versus rotations for "beam 231" at node 31 and "column 111" at node 21 of the SAC 3-story model with both

rigid and Hys.6 cladding connections subjected to the El Centro earthquake with design level of 10%/50yrs. The locations of the "beam 231" and "column 111" can be found in Figure 3.4. In order to show the difference in energy dissipation between the rigid and Hys.6 flexible connection in a more clear way, the moment-rotation plots were plotted as moment-plastic-rotation plots which are shown in Figure 4.15 and 4.16. Moment-plastic-rotation plots focused on the behaviors of the connections after yielding. The plastic rotations from the moment-plastic-rotation plots were calculated per Equation 4.1:

$$R_p = R - \frac{M(R)}{k}$$

(4.1)

Where,

R_p = plastic rotation of the connection (radian);

R = rotation of the connection (radian);

M(R) = Moment as a function of connection rotation (k-ft);

k = Elastic slope of the moment-rotation plastic (k-ft/radian);

The hysteretic energy dissipated by the connection of an inelastic structural member through its inelastic behavior was represented by the areas under the moment-rotation curve or moment-plastic-rotation curve. The hysteretic energy dissipated by an inelastic structural member during the earthquake can be calculated by following Equation 4.2:

$$E = \sum_{i=1}^{t}\left(\frac{M_t + M_{t+1}}{2} \cdot (R_{t+1} - R_t)\right)$$

(4.2)

Where,

E = Hysteretic energy dissipated by the inelastic structural member (k-ft), note that the radian term was left out for conventional unit of energy;

M_t = Moment at time step t (k-ft);

M_{t+1} = Moment at next time step t+1 (k-ft);

R_t = Rotation at time step t (radian);

R_{t+1} = Rotation at next time step t+1 (radian);

The results of hysteretic energy dissipation for the SAC 3-story model with both rigid and Hys.6 cladding connections under El Centro earthquake (10%/50yrs) for all connections in the structural members is shown in Table 4.4. Different members experienced different level of inelastic behaviors or elastic behaviors which could be seen in their moment-rotation or moment-plastic-rotation plots (Figure 4.13 – 4.18).

Table 4.4 Energy dissipation for El Centro earthquake (10%/50yrs)

Column 1 (W14X257)		Elasticity	Rigid (k-ft)		Hys.6 (k-ft)	
			Node 1	Node 2	Node 1	Node 2
Element	111	Inelastic	0.00	21.10	0.00	17.17
	121	Elastic	0.00	0.00	0.00	0.00
	131	Inelastic	34.34	22.89	26.01	18.14
Column 2 (W14X311)						
Element	112	Inelastic	0.00	24.47	0.00	19.37
	122	Elastic	0.00	0.00	0.00	0.00
	132	Inelastic	45.76	33.32	34.07	24.78
Column 3 (W14X311)						
Element	113	Inelastic	0.00	25.61	0.00	20.24
	123	Elastic	0.00	0.00	0.00	0.00
	133	Inelastic	47.67	35.38	35.66	26.22
Column 4 (W14X257)						
Element	114	Inelastic	0.00	23.96	0.00	19.58
	124	Elastic	0.00	0.00	0.00	0.00
	134	Inelastic	39.04	25.46	29.99	20.20
Column 5 (W14X68)						
Element	115	Elastic	0.00	0.00	0.00	0.00
	125	Elastic	0.00	0.00	0.00	0.00
	135	Elastic	0.00	0.00	0.00	0.00
Beam 1 (W33X118)						
Element	221	Inelastic	22.65	15.15	17.47	11.28
	222	Inelastic	11.29	11.41	7.91	8.00
	223	Inelastic	16.04	24.14	11.93	18.70
Beam 2 (W30X116)						
Element	231	Inelastic	18.89	15.10	10.18	7.69
	232	Inelastic	13.13	13.75	6.29	6.70
	233	Inelastic	17.12	23.50	9.02	13.24
Beam 3 (W24X68)						
Element	241	Inelastic	5.28	4.54	1.67	1.24
	242	Inelastic	4.13	4.99	0.94	1.38
	243	Inelastic	6.63	9.63	2.24	3.82
Beam 4 (W21X44)						
Element	224	Elastic	0.00	0.00	0.00	0.00
	234	Elastic	0.00	0.00	0.00	0.00
	244	Elastic	0.00	0.00	0.00	0.00
Total energy dissipated			616.37		431.10	
▵ %			30.1			

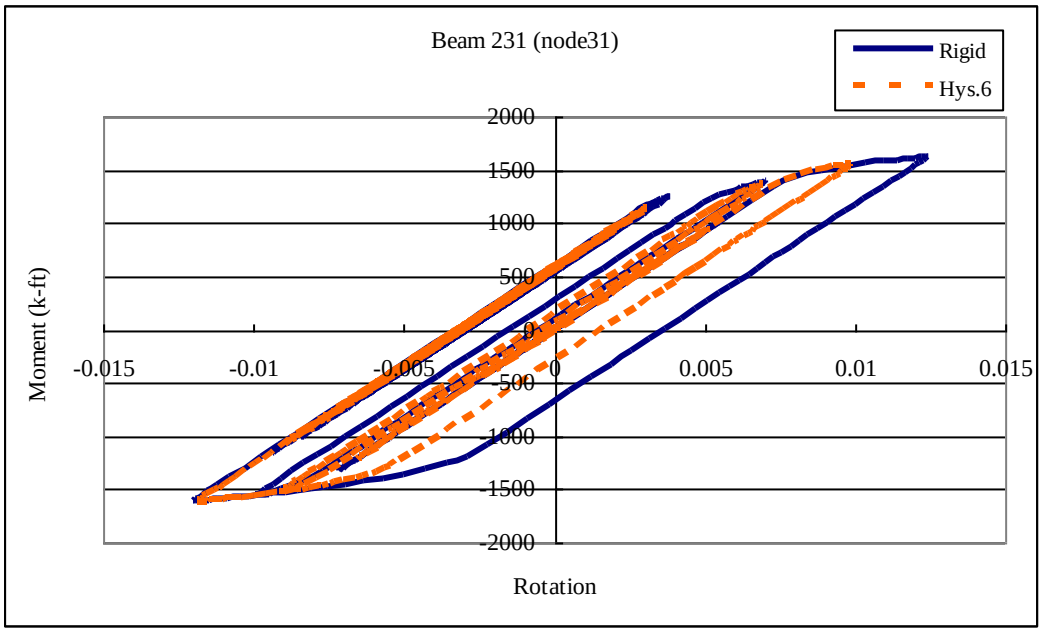

Figure 4.13 Moment-rotation plot for Beam 231 at node 31

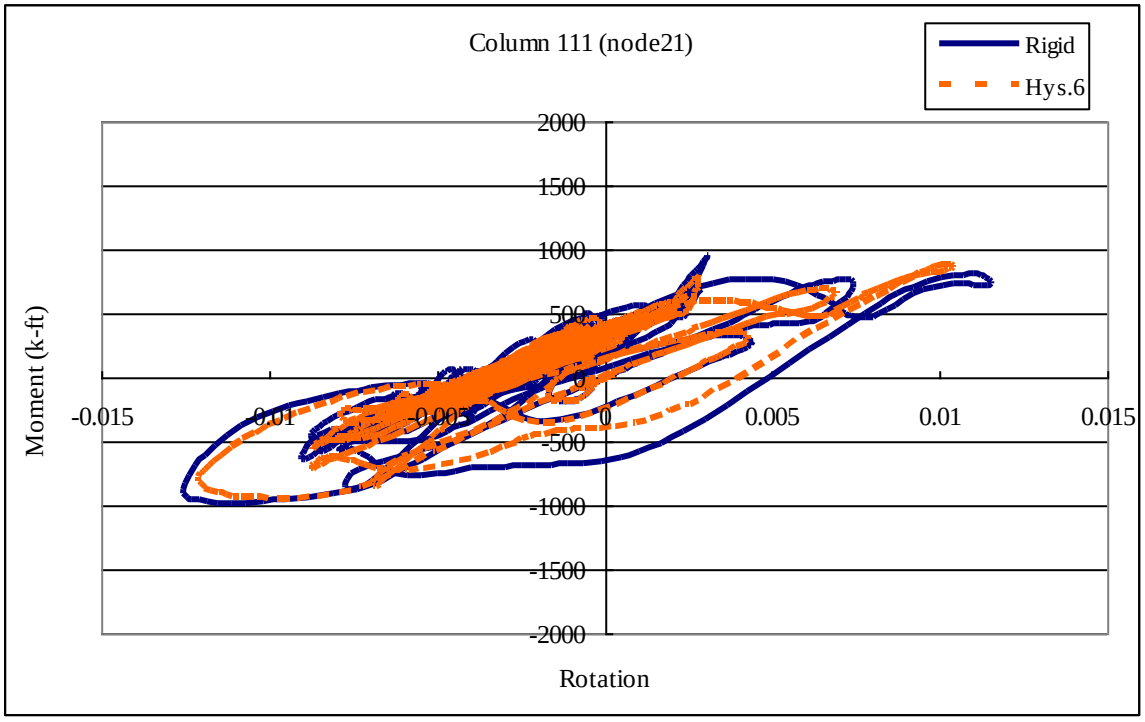

Figure 4.14 Moment-rotation plot for Column 111 at node 21

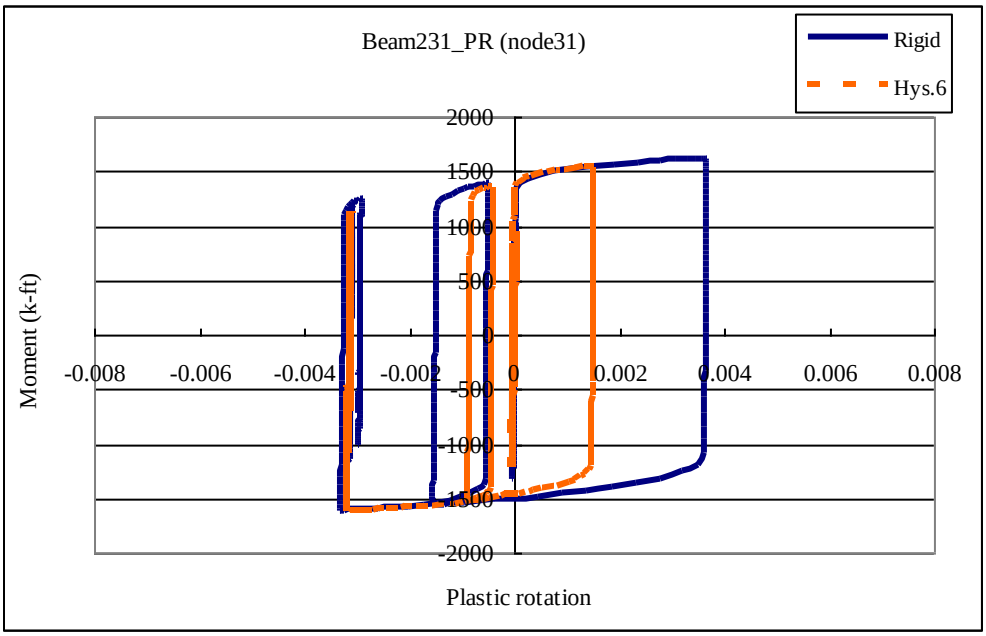

Figure 4.15 Moment-plastic-rotation plot for Beam 231 at node 31

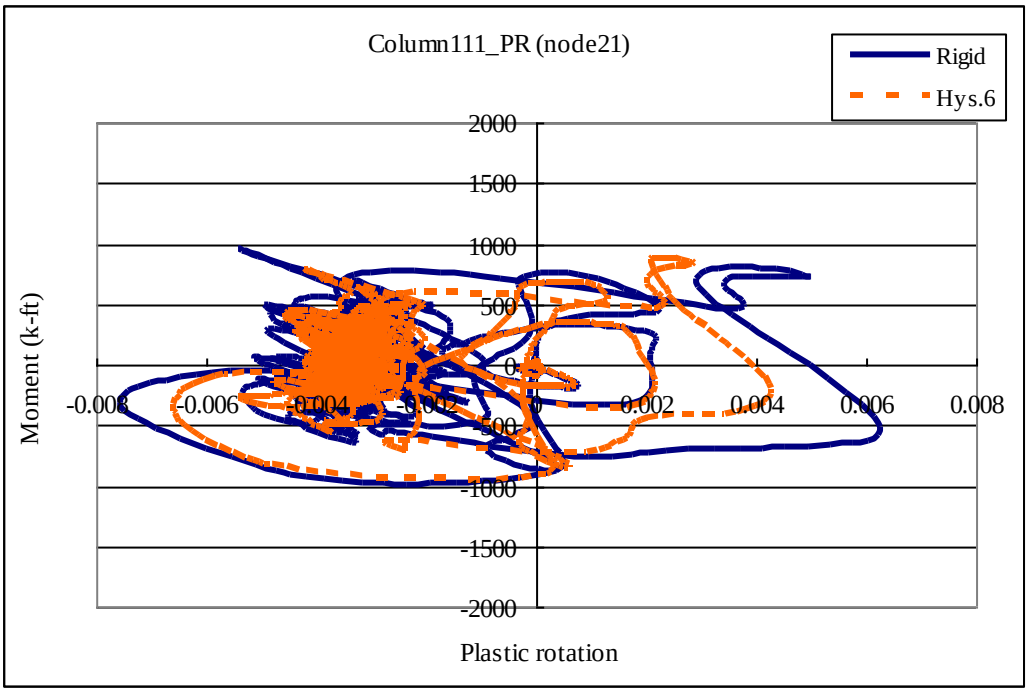

Figure 4.16 Moment-plastic-rotation plot for Column 111 at node 21

The SAC 3-story model was designed as special moment resisting frames which could sustain 0.04 radians of total rotations (Krawinkler, 2000). For the purpose of this study, more than 0.015 radians rotation will be considered as significant rotation which will undergo significant inelastic behavior. If the rotation of a connection were under 0.01 radians, it will be under the elastic range. The rotations between these limits will be considered as moderate inelastic behaviors. The moment-rotation plot in Figure 4.13 showed moderate inelastic behavior on "beam 231" at node 31, which could be seen from the extension of the rotation after yielding. There were reductions on the extent of the demand rotations on the steel frame member when "Hys.6" connections are compared to "Rigid" cases for both "column 111" and "beam 231".

Figure 4.17 showed lower inelastic demand for moment-rotation plot of "beam 241" at node 42 under the same El Centro earthquake at the same design level (10%/50yrs). When "Hys.6" cladding connections were introduced most of the inelastic behaviors were eliminated. The same "beam 241" member at node 42 was analyzed under the El Centro earthquake, but with a lower design level (20%/50yrs). The moment-rotation plots of "beam 241" at node 42 in Figure 4.18 showed almost all elastic behaviors for both "rigid" and "Hys.6" case.

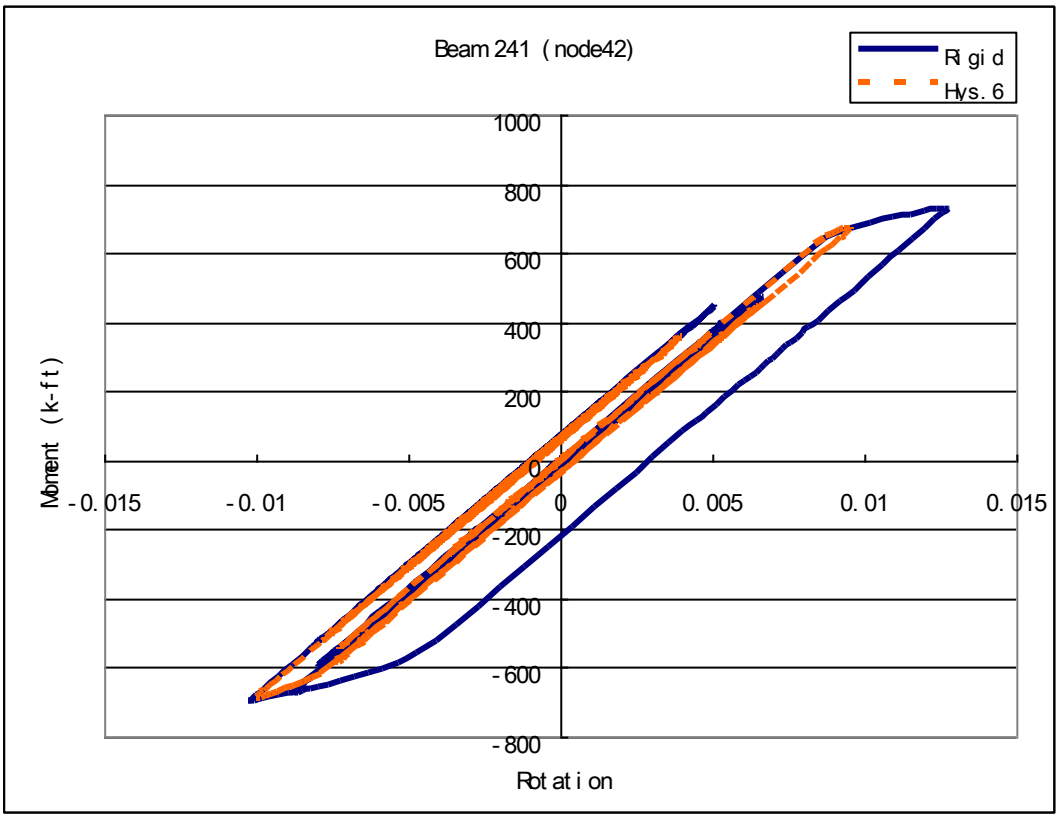

Figure 4.17 Moment-rotation plot for Beam 241 at node 42 (10%/50yrs)

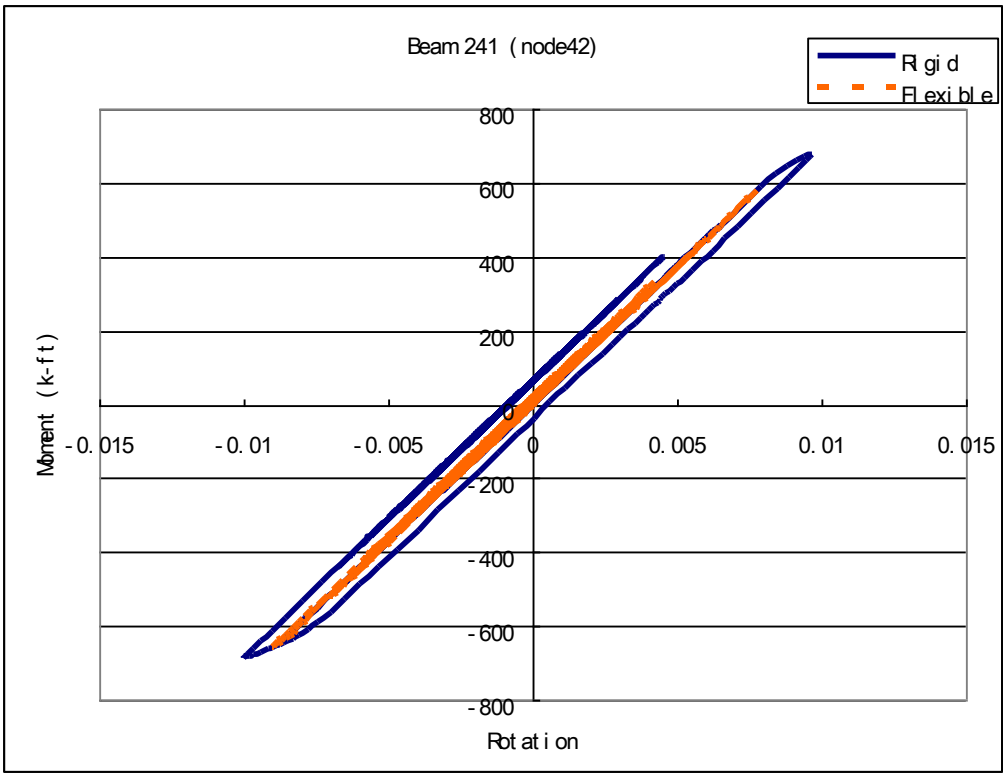

Figure 4.18 Moment-rotation plot for Beam 241 at node 42 (20%/50yrs)

In this analysis, rigid cladding connections did not contribute in energy dissipation. The total hysteretic energy dissipation during an earthquake included the hysteretic energy dissipated by the structural frame and the flexible cladding connections. Since input energy is constant for each earthquake record reduction in dissipated energy by the structural members with the flexible cladding connections (shown in Table 4.4) indicates that the differential energy was dissipating by the flexible cladding connections. From Table 4.4, the energy dissipated by the structure with the rigid cladding connections was 616.37 k-ft (835.67 kJ), but the energy dissipated by the structure with "Hys.6" flexible cladding connections was 431.10 k-ft (584.49 kJ). The difference in energy dissipation

between the two was 30.1%. Therefore, 30.1% of the hysteretic energy was dissipated by the flexible cladding connections.

With the same design level of 10%/50yrs, the hysteretic energy dissipation results for all the members in the structure with "Hys.6" and "Rigid" cladding connection subjected to different earthquake excitations were shown in Table 4.5 to 4.8. The difference in hysteretic energy dissipation by the two different types of cladding connections when subjected to the 10%/50yrs scaled San Fernando, Loma Prieta, Northridge, and Big Bear earthquake were 28.3%, 29.8%, 5.8%, and 25.9%. Note that the Northridge Earthquake scaled record was previously noted to provide unreasonably high accelerations to higher frequency mode shapes. The fact that the flexible cladding connections were not effective in this situation highlights that additional mode shapes were introduced with lower frequencies which were highly excited by this record. However, there was still a net reduction in structural frame energy dissipation.

Table 4.5 Energy dissipation for San Fernando earthquake (10%/50yrs)

Column 1 (W14X257)		Elasticity	Rigid		Hys.6	
			Node 1	Node 2	Node 1	Node 2
Element	111	Inelastic	0.00	28.41	0.00	23.30
	121	Elastic	0.00	0.00	0.00	0.00
	131	Inelastic	49.74	28.70	40.33	22.47
Column 2 (W14X311)						
Element	112	Inelastic	0.00	31.89	0.00	25.80
	122	Inelastic	0.00	44.08	0.00	29.44
	132	Inelastic	67.27	43.86	51.82	33.04
Column 3 (W14X311)						
Element	113	Inelastic	0.00	33.35	0.00	27.21
	123	Inelastic	0.00	47.50	0.00	31.65
	133	Inelastic	70.38	46.09	54.11	35.06
Column 4 (W14X257)						
Element	114	Inelastic	0.00	32.93	0.00	27.00
	124	Elastic	0.00	0.00	0.00	0.00
	134	Inelastic	58.98	29.96	45.78	23.59
Column 5 (W14X68)						
Element	115	Elastic	0.00	0.00	0.00	0.00
	125	Elastic	0.00	0.00	0.00	0.00
	135	Elastic	0.00	0.00	0.00	0.00
Beam 1 (W33X118)						
Element	221	Inelastic	24.09	15.15	17.88	11.56
	222	Inelastic	10.53	10.55	7.80	7.95
	223	Inelastic	16.31	25.50	12.56	19.46
Beam 2 (W30X116)						
Element	231	Inelastic	34.27	26.61	21.68	16.56
	232	Inelastic	22.00	23.39	13.29	14.24
	233	Inelastic	30.11	42.44	18.87	27.69
Beam 3 (W24X68)						
Element	241	Inelastic	9.87	8.22	3.41	2.74
	242	Inelastic	7.52	9.17	2.48	3.57
	243	Inelastic	12.49	17.93	5.86	9.25
Beam 4 (W21X44)						
Element	224	Elastic	0.00	0.00	0.00	0.00
	234	Elastic	0.00	0.00	0.00	0.00
	244	Elastic	0.00	0.00	0.00	0.00
Total energy dissipated			959.28		687.44	
▵ %			28.3			

Table 4.6 Energy dissipation for Loma Prieta earthquake (10%/50yrs)

Column 1 (W14X257)		Elasticity	Rigid		Hys.6	
			Node 1	Node 2	Node 1	Node 2
Element	111	Inelastic	0.00	22.03	0.00	15.78
	121	Elastic	0.00	0.00	0.00	0.00
	131	Inelastic	21.46	16.93	19.03	14.62
Column 2 (W14X311)						
Element	112	Inelastic	0.00	26.41	0.00	16.36
	122	Elastic	0.00	0.00	0.00	0.00
	132	Inelastic	33.55	21.57	24.62	17.46
Column 3 (W14X311)						
Element	113	Inelastic	0.00	27.11	0.00	16.93
	123	Elastic	0.00	0.00	0.00	0.00
	133	Inelastic	35.22	22.94	25.95	18.80
Column 4 (W14X257)						
Element	114	Inelastic	0.00	23.53	0.00	17.01
	124	Elastic	0.00	0.00	0.00	0.00
	134	Inelastic	24.72	19.27	21.85	16.85
Column 5 (W14X68)						
Element	115	Elastic	0.00	0.00	0.00	0.00
	125	Elastic	0.00	0.00	0.00	0.00
	135	Elastic	0.00	0.00	0.00	0.00
Beam 1 (W33X118)						
Element	221	Inelastic	36.93	24.34	22.28	13.70
	222	Inelastic	17.92	18.13	8.33	8.47
	223	Inelastic	25.18	38.59	14.36	23.49
Beam 2 (W30X116)						
Element	231	Inelastic	17.24	12.63	12.75	9.21
	232	Inelastic	9.46	10.05	6.71	7.19
	233	Inelastic	14.56	21.32	10.71	15.98
Beam 3 (W24X68)						
Element	241	Inelastic	0.27	0.18	0.22	0.15
	242	Inelastic	0.17	0.35	0.11	0.32
	243	Inelastic	1.26	1.82	1.33	1.99
Beam 4 (W21X44)						
Element	224	Elastic	0.00	0.00	0.00	0.00
	234	Elastic	0.00	0.00	0.00	0.00
	244	Elastic	0.00	0.00	0.00	0.00
Total energy dissipated			545.13		382.57	
▵ %			29.8			

Table 4.7 Energy dissipation for Northridge earthquake (10%/50yrs)

Column 1 (W14X257)		Elasticity	Rigid		Hys.6	
			Node 1	Node 2	Node 1	Node 2
Element	111	Inelastic	0.00	43.11	0.00	39.64
	121	Elastic	0.00	0.00	0.00	0.00
	131	Inelastic	61.32	12.58	60.86	19.03
Column 2 (W14X311)						
Element	112	Inelastic	0.00	44.56	0.00	40.76
	122	Inelastic	31.07	45.92	31.30	41.10
	132	Inelastic	76.67	27.45	72.88	35.46
Column 3 (W14X311)						
Element	113	Inelastic	0.00	49.48	0.00	44.63
	123	Inelastic	34.01	49.32	33.69	44.21
	133	Inelastic	80.23	24.04	75.84	32.87
Column 4 (W14X257)						
Element	114	Inelastic	0.00	57.97	0.00	52.18
	124	Inelastic	38.73	47.91	37.52	44.11
	134	Inelastic	71.36	0.00	68.82	7.01
Column 5 (W14X68)						
Element	115	Inelastic	0.00	22.41	0.00	20.32
	125	Inelastic	22.46	12.88	20.37	12.07
	135	Inelastic	16.02	0.00	16.02	0.00
Beam 1 (W33X118)						
Element	221	Inelastic	16.90	8.80	12.25	6.66
	222	Inelastic	4.74	4.82	2.88	2.98
	223	Inelastic	10.67	19.37	8.05	14.72
Beam 2 (W30X116)						
Element	231	Inelastic	17.31	13.47	14.29	10.72
	232	Inelastic	11.64	12.87	8.82	9.88
	233	Inelastic	16.11	24.53	12.55	20.03
Beam 3 (W24X68)						
Element	241	Inelastic	10.20	9.10	8.70	7.73
	242	Inelastic	8.23	10.97	6.93	9.64
	243	Inelastic	12.43	20.34	11.36	18.95
Beam 4 (W21X44)						
Element	224	Elastic	0.00	0.00	0.00	0.00
	234	Elastic	0.00	0.00	0.00	0.00
	244	Elastic	0.00	0.00	0.00	0.00
Total energy dissipated			1101.98		1037.82	
▵ %			5.80			

Table 4.8 Energy dissipation for Big Bear earthquake (10%/50yrs)

Column 1 (W14X257)		Elasticity	Rigid		Hys.6	
			Node 1	Node 2	Node 1	Node 2
Element	111	Inelastic	0.00	27.85	0.00	22.49
	121	Elastic	0.00	0.00	0.00	0.00
	131	Inelastic	37.77	26.62	28.75	20.99
Column 2 (W14X311)						
Element	112	Inelastic	0.00	32.97	0.00	27.31
	122	Inelastic	13.89	24.32	9.42	15.84
	132	Inelastic	53.49	35.74	41.47	28.40
Column 3 (W14X311)						
Element	113	Inelastic	0.00	34.21	0.00	28.31
	123	Inelastic	14.24	26.25	9.46	16.80
	133	Inelastic	56.07	38.20	43.30	29.90
Column 4 (W14X257)						
Element	114	Inelastic	0.00	30.65	0.00	24.81
	124	Elastic	0.00	0.00	0.00	0.00
	134	Inelastic	43.23	30.58	33.00	23.79
Column 5 (W14X68)						
Element	115	Inelastic	0.00	3.30	0.00	3.10
	125	Elastic	0.00	0.00	0.00	0.00
	135	Inelastic	5.64	1.19	5.09	1.39
Beam 1 (W33X118)						
Element	221	Inelastic	40.53	26.97	30.68	20.72
	222	Inelastic	19.79	20.05	15.92	16.13
	223	Inelastic	28.30	43.07	21.55	32.26
Beam 2 (W30X116)						
Element	231	Inelastic	23.58	17.30	14.01	10.60
	232	Inelastic	13.13	13.95	8.24	8.73
	233	Inelastic	19.92	29.36	11.72	17.00
Beam 3 (W24X68)						
Element	241	Inelastic	1.51	1.21	0.67	0.52
	242	Inelastic	1.01	1.47	0.37	0.57
	243	Inelastic	3.33	5.20	1.23	2.14
Beam 4 (W21X44)						
Element	224	Elastic	0.00	0.00	0.00	0.00
	234	Elastic	0.00	0.00	0.00	0.00
	244	Elastic	0.00	0.00	0.00	0.00
Total energy dissipated			845.88		626.71	
Δ %			25.9			

With a lower design level of 20%/50yrs, the hysteretic energy dissipation results for all the members in the structure with "Hys.6" and "Rigid" cladding connection subjected to different earthquake excitations are shown in Table 4.9 to 4.13. The total input energy input was much lower than (roughly half of, depending on the record) the 10%/50yrs design level. The difference in hysteretic energy dissipation by the two different types of cladding connections when subjected to the 20%/50yrs scaled El Centro, San Fernando, Loma Prieta, Northridge, and Big Bear earthquake were 37.0%, 41.9%, 53.6%, 4.0%, and 32.5%.

Table 4.9 Energy dissipation for El Centro earthquake (20%/50yrs)

Column 1 (W14X257)		Elasticity	Rigid		Hys.6	
			Node 1	Node 2	Node 1	Node 2
Element	111	Inelastic	0.00	21.10	0.00	17.17
	121	Elastic	0.00	0.00	0.00	0.00
	131	Inelastic	20.68	13.83	14.78	10.49
Column 2 (W14X311)						
Element	112	Inelastic	0.00	13.89	0.00	9.71
	122	Elastic	0.00	0.00	0.00	0.00
	132	Inelastic	25.45	18.56	17.85	13.64
Column 3 (W14X311)						
Element	113	Inelastic	0.00	14.65	0.00	10.35
	123	Elastic	0.00	0.00	0.00	0.00
	133	Inelastic	27.10	19.94	18.86	14.44
Column 4 (W14X257)						
Element	114	Inelastic	0.00	15.00	0.00	11.40
	124	Elastic	0.00	0.00	0.00	0.00
	134	Inelastic	24.35	15.61	17.40	11.60
Column 5 (W14X68)						
Element	115	Elastic	0.00	0.00	0.00	0.00
	125	Elastic	0.00	0.00	0.00	0.00
	135	Elastic	0.00	0.00	0.00	0.00
Beam 1 (W33X118)						
Element	221	Inelastic	31.89	7.97	22.43	4.25
	222	Inelastic	4.98	5.04	2.24	2.31
	223	Inelastic	8.61	14.24	4.73	8.67
Beam 2 (W30X116)						
Element	231	Inelastic	10.45	7.50	3.18	2.48
	232	Inelastic	5.54	6.10	1.98	2.20
	233	Inelastic	9.14	14.13	2.94	4.81
Beam 3 (W24X68)						
Element	241	Inelastic	1.73	1.30	0.23	0.13
	242	Inelastic	0.99	1.49	0.07	0.26
	243	Inelastic	2.72	4.57	0.54	1.12
Beam 4 (W21X44)						
Element	224	Elastic	0.00	0.00	0.00	0.00
	234	Elastic	0.00	0.00	0.00	0.00
	244	Elastic	0.00	0.00	0.00	0.00
Total energy dissipated			368.52		232.25	
$\triangle$ %			37.0			

Table 4.10 Energy dissipation for San Fernando earthquake (20%/50yrs)

Column 1 (W14X257)		Elasticity	Rigid		Hys.6	
			Node 1	Node 2	Node 1	Node 2
Element	111	Elastic	0.00	0.00	0.00	0.00
	121	Elastic	0.00	0.00	0.00	0.00
	131	Elastic	0.00	0.00	0.00	0.00
Column 2 (W14X311)						
Element	112	Inelastic	0.00	15.03	0.00	12.13
	122	Inelastic	0.00	20.73	0.00	9.99
	132	Inelastic	33.40	22.40	22.19	21.75
Column 3 (W14X311)						
Element	113	Inelastic	0.00	16.05	0.00	12.85
	123	Inelastic	0.00	22.93	0.00	11.11
	133	Inelastic	35.35	23.90	23.35	16.18
Column 4 (W14X257)						
Element	114	Inelastic	0.00	17.57	0.00	14.15
	124	Elastic	0.00	0.00	0.00	0.00
	134	Inelastic	33.08	15.59	22.71	10.57
Column 5 (W14X68)						
Element	115	Elastic	0.00	0.00	0.00	0.00
	125	Elastic	0.00	0.00	0.00	0.00
	135	Elastic	0.00	0.00	0.00	0.00
Beam 1 (W33X118)						
Element	221	Inelastic	8.01	4.44	5.60	3.19
	222	Inelastic	1.72	1.75	1.31	1.34
	223	Inelastic	5.13	8.95	3.50	6.15
Beam 2 (W30X116)						
Element	231	Inelastic	15.72	10.83	5.12	2.80
	232	Inelastic	7.71	8.57	1.26	1.65
	233	Inelastic	13.34	21.90	3.88	8.26
Beam 3 (W24X68)						
Element	241	Inelastic	3.31	2.59	0.25	0.20
	242	Inelastic	2.19	3.18	0.06	0.53
	243	Inelastic	5.91	9.23	1.61	3.13
Beam 4 (W21X44)						
Element	224	Elastic	0.00	0.00	0.00	0.00
	234	Elastic	0.00	0.00	0.00	0.00
	244	Elastic	0.00	0.00	0.00	0.00
Total energy dissipated			390.51		226.82	
▵ %			41.9			

Table 4.11 Energy dissipation for Loma Prieta earthquake (20%/50yrs)

Column 1 (W14X257)		Elasticity	Rigid		Hys.6	
			Node 1	Node 2	Node 1	Node 2
Element	111	Inelastic	0.00	13.36	0.00	6.48
	121	Elastic	0.00	0.00	0.00	0.00
	131	Inelastic	14.27	11.89	9.01	7.66
Column 2 (W14X311)						
Element	112	Inelastic	0.00	13.54	0.00	6.04
	122	Elastic	0.00	0.00	0.00	0.00
	132	Inelastic	18.28	13.88	10.34	9.18
Column 3 (W14X311)						
Element	113	Inelastic	0.00	14.06	0.00	6.32
	123	Elastic	0.00	0.00	0.00	0.00
	133	Inelastic	19.47	14.70	11.14	9.69
Column 4 (W14X257)						
Element	114	Inelastic	0.00	14.46	0.00	7.24
	124	Elastic	0.00	0.00	0.00	0.00
	134	Inelastic	16.66	13.47	10.82	8.77
Column 5 (W14X68)						
Element	115	Elastic	0.00	0.00	0.00	0.00
	125	Elastic	0.00	0.00	0.00	0.00
	135	Elastic	0.00	0.00	0.00	0.00
Beam 1 (W33X118)						
Element	221	Inelastic	19.63	11.72	6.75	3.40
	222	Inelastic	6.87	7.01	1.56	1.59
	223	Inelastic	12.39	20.91	3.68	7.36
Beam 2 (W30X116)						
Element	231	Inelastic	9.07	6.07	2.63	1.35
	232	Inelastic	3.86	4.28	0.52	0.73
	233	Inelastic	7.51	12.13	2.13	4.45
Beam 3 (W24X68)						
Element	241	Elastic	0.00	0.00	0.00	0.00
	242	Elastic	0.00	0.00	0.00	0.00
	243	Elastic	0.00	0.00	0.00	0.00
Beam 4 (W21X44)						
Element	224	Elastic	0.00	0.00	0.00	0.00
	234	Elastic	0.00	0.00	0.00	0.00
	244	Elastic	0.00	0.00	0.00	0.00
Total energy dissipated			299.49		138.83	
▵ %			53.6			

Table 4.12 Energy dissipation for Northridge earthquake (20%/50yrs)

Column 1 (W14X257)		Elasticity	Rigid		Hys.6	
			Node 1	Node 2	Node 1	Node 2
Element	111	Inelastic	0.00	25.52	0.00	23.03
	121	Elastic	0.00	0.00	0.00	0.00
	131	Inelastic	35.71	6.10	37.07	10.68
Column 2 (W14X311)						
Element	112	Inelastic	0.00	26.38	0.00	24.13
	122	Inelastic	23.16	24.05	23.01	22.09
	132	Inelastic	44.15	15.52	42.68	20.72
Column 3 (W14X311)						
Element	113	Inelastic	0.00	29.57	0.00	26.75
	123	Inelastic	25.30	26.11	24.81	24.04
	133	Inelastic	46.94	13.79	45.06	19.49
Column 4 (W14X257)						
Element	114	Inelastic	0.00	35.24	0.00	31.05
	124	Elastic	0.00	0.00	0.00	0.00
	134	Inelastic	42.56	0.00	42.26	2.59
Column 5 (W14X68)						
Element	115	Inelastic	0.00	14.95	0.00	13.78
	125	Elastic	0.00	0.00	0.00	0.00
	135	Inelastic	9.99	0.00	10.66	0.00
Beam 1 (W33X118)						
Element	221	Inelastic	6.06	2.63	2.26	1.18
	222	Inelastic	0.68	0.72	0.00	0.06
	223	Inelastic	3.64	7.64	1.93	3.69
Beam 2 (W30X116)						
Element	231	Inelastic	6.03	3.84	5.16	3.01
	232	Inelastic	2.43	3.08	1.54	2.20
	233	Inelastic	5.03	9.66	4.11	8.69
Beam 3 (W24X68)						
Element	241	Inelastic	3.83	3.17	3.36	2.76
	242	Inelastic	2.59	4.43	2.17	3.87
	243	Inelastic	5.65	11.03	5.41	10.65
Beam 4 (W21X44)						
Element	224	Elastic	0.00	0.00	0.00	0.00
	234	Elastic	0.00	0.00	0.00	0.00
	244	Elastic	0.00	0.00	0.00	0.00
Total energy dissipated			527.19		505.99	
▵ %			4.0			

Table 4.13 Energy dissipation for Big Bear earthquake (20%/50yrs)

Column 1 (W14X257)		Elasticity	Rigid		Hys.6	
			Node 1	Node 2	Node 1	Node 2
Element	111	Inelastic	0.00	16.80	0.00	-0.17
	121	Elastic	0.00	0.00	0.00	0.00
	131	Inelastic	20.29	15.56	16.61	13.72
Column 2 (W14X311)						
Element	112	Inelastic	0.00	18.21	0.00	13.52
	122	Elastic	0.00	0.00	0.00	0.00
	132	Inelastic	29.12	21.85	21.06	17.34
Column 3 (W14X311)						
Element	113	Inelastic	0.00	19.08	0.00	14.18
	123	Elastic	0.00	0.00	0.00	0.00
	133	Inelastic	30.74	23.11	22.34	18.26
Column 4 (W14X257)						
Element	114	Inelastic	0.00	18.60	0.00	14.55
	124	Elastic	0.00	0.00	0.00	0.00
	134	Inelastic	23.58	19.30	19.29	15.44
Column 5 (W14X68)						
Element	115	Elastic	0.00	0.00	0.00	0.00
	125	Elastic	0.00	0.00	0.00	0.00
	135	Elastic	0.00	0.00	0.00	0.00
Beam 1 (W33X118)						
Element	221	Inelastic	21.94	13.38	14.05	8.42
	222	Inelastic	8.65	8.80	5.11	5.21
	223	Inelastic	14.27	23.57	8.99	15.26
Beam 2 (W30X116)						
Element	231	Inelastic	8.91	6.96	4.86	3.42
	232	Inelastic	5.58	5.96	2.48	2.74
	233	Inelastic	7.96	11.42	4.10	6.41
Beam 3 (W24X68)						
Element	241	Inelastic	0.43	0.33	0.09	0.05
	242	Inelastic	0.24	0.40	0.05	0.15
	243	Inelastic	0.78	1.42	0.25	0.48
Beam 4 (W21X44)						
Element	224	Elastic	0.00	0.00	0.00	0.00
	234	Elastic	0.00	0.00	0.00	0.00
	244	Elastic	0.00	0.00	0.00	0.00
Total energy dissipated			397.25		268.25	
▵ %			32.5			

While energy dissipation results indicate that the flexible cladding connections can significantly reduce the demand on the structural frame, displacement issues must be addressed. Cladding displacement results are addressed in three different ways. First, there is the overall global displacement of the frame, which does not have significant repercussions under the drift limit but is provided for reference. More important is the relative displacement between the cladding and structural frame node to which it is attached, or the relative cladding to floor displacement. This is determined by the cladding connection flexibility and distortions. It is proposed that a building may be able to design around fairly significant displacements between cladding and structural frame so long as all cladding in a floor moves similarly on each wall face. This is referred to as the maximum horizontal panel to panel deformation (measured at each floor). In addition, it would be worthwhile to control the relative horizontal displacements of panels on one floor to those on the adjacent floors. This is referred to as the maximum relative panel deformation between stories. These relative displacement measurements are defined in Figure 4.19. Results for each earthquake record (design level of 10%/50yrs) are presented in Table 4.14 to 4.15. Table 4.14 shows the results for maximum frame deflection (roof deflection), maximum base shear, the number of members exceeded M_y, and the number of members exceeded M_p for SAC 3-story model with rigid cladding connection. Table 4.15 includes all the results from Table 4.14 plus maximum frame to cladding deflection, maximum horizontal panel to panel deflection, maximum relative panel deformation between stories, and percentage of hysteretic energy dissipated by the flexible cladding connections for SAC 3-story model with "Hys.6" flexible cladding connections. The

number of members exceeded M_y and M_p gave an indication of how badly the primary structure was damaged.

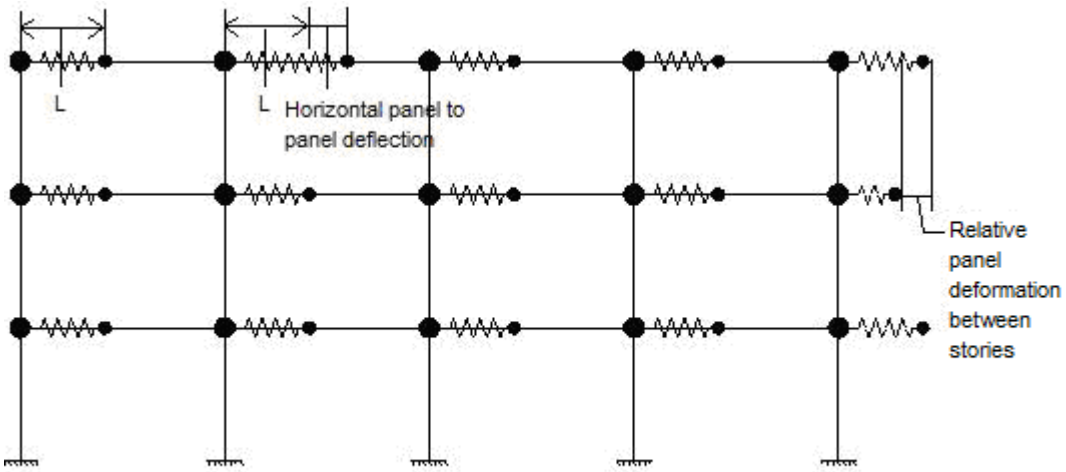

Figure 4.19 Horizontal panel to panel deflection and relative panel deformation between stories

Table 4.14 Results for SAC 3-story model with rigid connection for 10%/50yrs

Earthquakes	Rigid Connection							
	Max. Base Shear (K)	Max. frame deflection (in)	Number of members exceeded M_y			Number of members exceeded M_p		
			Columns	Beams	Total	Columns	Beams	Total
El Centro	1169.2	6.2	8	9	17	8	7	15
San Fernando	1149.4	6.5	10	9	19	4	8	12
Loma Prieta	1108	5.87	8	9	17	4	4	8
Northridge	1562.7	5.35	14	9	23	11	7	18
Big Bear	1190	6.69	12	9	21	8	6	14

Table 4.15 Results for SAC 3-story model with Hys.6 connection for 10%/50yrs

Earthq-uakes	Hys.6 Connection											Hyster-etic Energy Dissip-ated (%)
	Max. Base Shear (K)	Max. frame deflec-tion (in)	Max. frame to claddi-ng def. (in)	Max. horiz-ontal panel to panel def. (in)	Max. relativ-e panel def. btwn. stories (in)	Number of members exceeded M_y			Number of members exceeded M_p			
						Colu-mns	Bea-ms	Tot-al	Colu-mns	Bea-ms	Tot-al	
El Centro	1125.7	6.11	4.24	0.8	3.21	8	9	17	4	6	10	30.1
San Fernando	1116.7	5.77	5.72	0.71	3.97	10	9	19	4	5	9	28.3
Loma Prieta	1104.2	5.65	3.97	0.234	3.15	8	9	17	4	2	6	29.8
Northridge	1469.2	5.55	4.48	1.02	4.44	12	9	21	10	7	17	5.8
Big Bear	1176	6.56	4.14	0.45	3.97	8	9	17	8	6	14	25.9

From Table 4.14 and 4.15, there were reductions on the maximum base shear from the rigid cladding connection to the "Hys.6" flexible connection. There was a noticeable higher maximum base shear for Northridge earthquake than the others, because Northridge had significantly higher peak ground acceleration than other earthquakes (Table 4.2 and Figure 4.11). There were almost no change between the two types of cladding connections on the number of the members exceeded M_y. This was because the structure experienced great damage resulting in more than half of the members yielding. However, the number of members exceeding M_p were somewhat reduced when the "Hys.6" cladding connection was included. Members in which the plastic moment was obtained reduced from 15 to 10 members for El Centro earthquake record, 12 to 9 members for San Fernando earthquake record, and 8 to 6 members for Loma Prieta

earthquake record. In terms of hysteretic energy dissipation, the "Hys.6" flexible cladding connections dissipated from about 26 to 30% of total hysteretic energy for all the earthquake records except the Northridge earthquake record, which dissipated about 6% of the total hysteretic energy.

In terms of deflection controls, the maximum differential frame to cladding deflections were in an order of 4 to 6 in (10.16 to 15.24 cm). With a design level of 10%/50yrs, these deflection were relatively large. The maximum horizontal panel to panel deflections were under 1 in (2.54 cm) for all earthquakes except Northridge earthquake. The maximum relative panel deformation between stories was under 4 in (10.16 cm) for all earthquakes except Northridge earthquake. There were reductions in maximum structural frame deflection for all earthquakes except the Northridge earthquake.

Other relevant measures of cladding connection behaviors relate to the final condition of the connections. Final frame to cladding deflections at the end of the ground excitation provide an indication of the permanent damage sustained, while the number of cladding connections yielded in each story gives an indication of the extent of permanent damage. Slight yielding of a connection with minimal permanent offset displacements may not be significant. Results are provided for all the earthquakes with flexible cladding connections at the 10%/50yrs design level in Tables 4.16 to 4.20. There are five nodes on each story of SAC 3-story building. The final frame to cladding deflections give an indication of how badly the cladding connections were damaged after the earthquakes.

The cladding connections would be considered to remain elastic if the final frame to cladding deflections were zero; otherwise, it would be yielded.

Table 4.16 Final frame to cladding deflections for El Centro earthquake (10%/50yrs)

Story	Final frame to cladding def. (in)					Total number of cladding connections per story	number of cladding connections yielded
	node 1	node 2	node 3	node 4	node 5		
1st	0.00	0.00	0.00	-0.01	0.00	5	1
2nd	0.08	0.08	0.09	0.10	0.09	5	5
3rd	0.05	0.06	0.06	0.05	0.03	5	5

Table 4.17 Final frame to cladding deflections for San Fernando earthquake (10%/50yrs)

Story	Final frame to cladding def. (in)					Total number of cladding connections per story	number of cladding connections yielded
	node 1	node 2	node 3	node 4	node 5		
1st	0.15	0.16	0.16	0.14	0.13	5	5
2nd	0.07	0.07	0.06	0.06	0.13	5	5
3rd	0.14	0.14	0.13	0.11	0.09	5	5

Table 4.18 Final frame to cladding deflections for Loma Prieta earthquake (10%/50yrs)

Story	Final frame to cladding def. (in)					Total number of cladding connections per story	number of cladding connections yielded
	node 1	node 2	node 3	node 4	node 5		
1st	-0.16	-0.16	-0.16	-0.16	-0.16	5	5
2nd	-0.01	-0.01	-0.01	-0.01	-0.02	5	5
3rd	0.03	0.03	0.03	0.04	0.04	5	5

Table 4.19 Final frame to cladding deflections for Big Bear earthquake (10%/50yrs)

Story	Final frame to cladding def. (in)					Total number of cladding connections per story	number of cladding connections yielded
	node 1	node 2	node 3	node 4	node 5		
1st	0.13	0.13	0.13	0.14	0.15	5	5
2nd	0.08	0.08	0.08	0.09	0.16	5	5
3rd	0.09	0.09	0.09	0.11	0.15	5	5

Table 4.20 Final frame to cladding deflections for Northridge earthquake (10%/50yrs)

Story	Final frame to cladding def. (in)					Total number of cladding connections per story	number of cladding connections yielded
	node 1	node 2	node 3	node 4	node 5		
1st	-0.02	-0.02	-0.02	0.04	-0.14	5	5
2nd	-0.06	-0.06	-0.06	-0.06	-0.07	5	5
3rd	0.29	0.29	0.31	0.32	0.37	5	5

From Table 4.16 to 4.20, almost all the flexible cladding connections were yielded for all earthquakes except for El Centro earthquake. For those yielded cladding connections, the absolute final frame to cladding deflections were ranged from 0.01 to 0.37 in (.03 to .94 cm), which is fairly minimal after a major earthquake. Figure 4.20 and 4.21 shows the force-deformation response of "Hys.6" cladding connection at node 43 which is the 3rd node at the 3rd story and node 23 which is the 3rd node at the first story under El Centro earthquake with design level of 10%/50yrs. The final differential cladding deformations of the two nodes were 0.06 in (.15 cm) and 0.00 in (0.00 cm). By comparing Figure 4.20 and 4.21, the node 43 was the case which the cladding connection was yielded after the earthquake and node 23 was the case which the cladding connection remained elastic

after the earthquake. The difference could be seen from the area under the curves which indicated energy dissipation and the maximum differential connection deflection from the two plots. Cladding connection at node 43 had much energy dissipation than at node 23. The maximum differential connection deflection at node 43 was about two times at node 23.

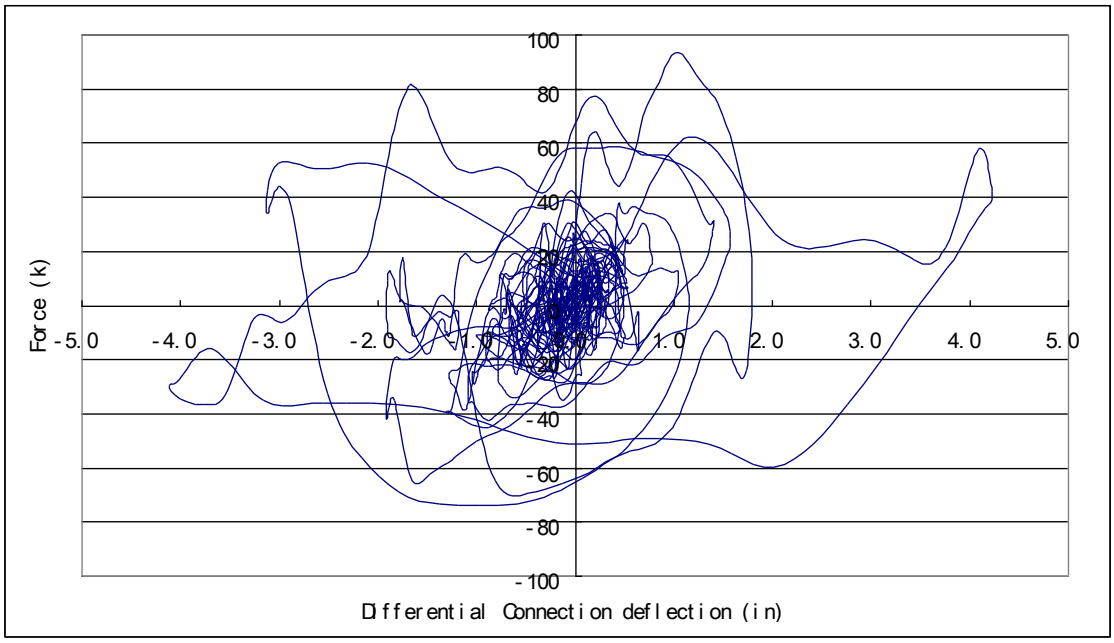

Figure 4.20 Force-deformation response of "Hys.6" cladding connection at node 43 (10%/50yrs)

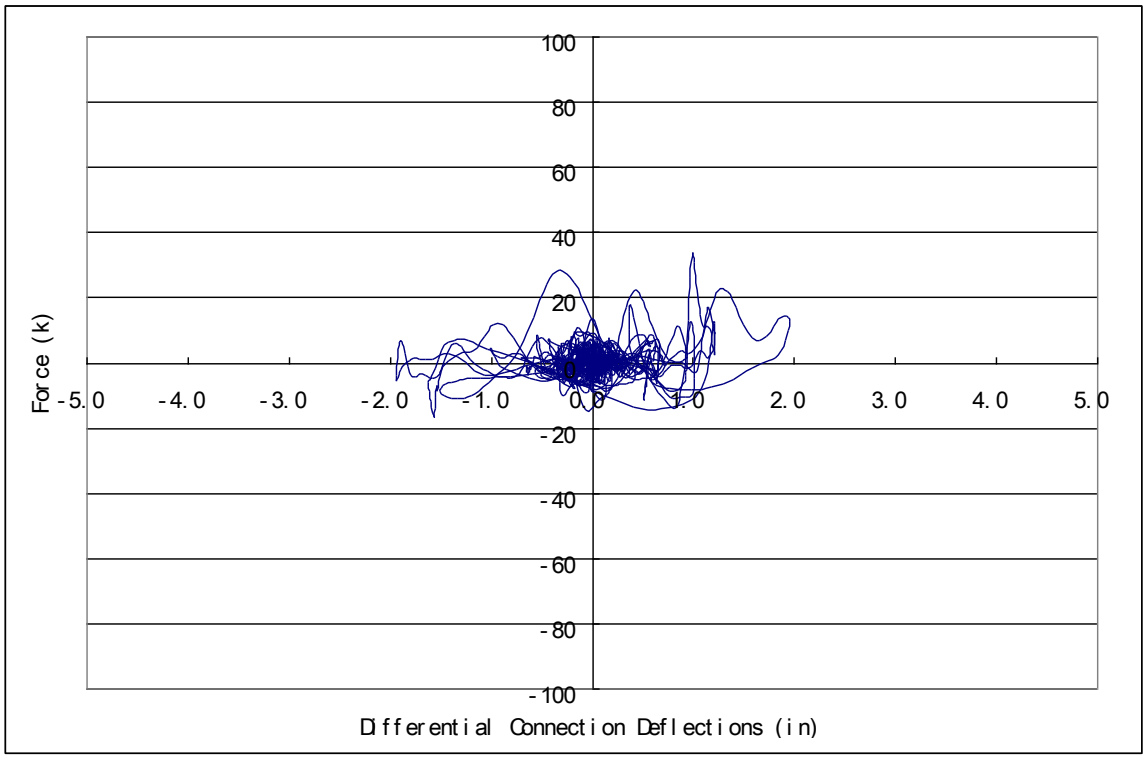

Figure 4.21 Force-deformation response of "Hys.6" cladding connection at node 23 (10%/50yrs)

In Similar results were obtained for seismic records factored to a design level of 20%/50yrs. Analysis results with different earthquake records were recorded in Table 4.21 and 4.22. Tables 4.23 to 4.27 present cladding connection final relative displacements from the structural frame and degree of cladding yielding with flexible cladding connections at the 20%/50yrs design level.

Table 4.21 Results for SAC 3-story model with rigid connection for 20%/50yrs

Earthquakes	Rigid Connection							
	Max. Base Shear (K)	Max. frame deflection (in)	Number of members exceeded M_y			Number of members exceeded M_p		
			Columns	Beams	Total	Columns	Beams	Total
El Centro	1133.1	5.9	8	9	17	4	4	8
San Fernando	1086.5	5.36	8	9	17	0	2	2
Loma Prieta	1065.6	5.45	8	6	14	4	2	6
Northridge	1487	4.59	12	9	21	10	1	11
Big Bear	1099.3	6.09	8	9	17	4	5	9

Table 4.22 Results for SAC 3-story model with Hys.6 connection for 20%/50yrs

Earthq-uakes	Hys.6 Connection											Hyster-etic Energy Dissip-ated (%)
	Max. Base Shear (K)	Max. frame deflec t-tion (in)	Max. frame to claddi -ng def. (in)	Max. horizo-ntal panel to panel def. (in)	Max. relativ e-e panel def. btwn. stories (in)	Number of members exceeded M_y			Number of members exceeded M_p			
						Colu -mns	Bea -ms	Tot -al	Colu -mns	Bea -ms	To - tal	
El Centro	1084.3	5.48	3.79	0.374	2.88	8	9	17	0	3	3	37.0
San Fernan do	991.9	4.81	4.98	0.59	3.23	4	9	13	0	0	0	41.9
Loma Prieta	1044.6	5.08	3.35	0.18	2.62	8	6	14	0	1	1	53.6
Northri dge	1370.4	4.8	4.02	1.07	5.06	11	9	20	8	0	8	4.0
Big Bear	1068.7	5.75	3.46	0.328	3.61	8	8	16	0	4	4	32.5

Again, there were no significant reductions of maximum base shear from rigid to "Hys.6" cladding connections. The number of members exceeded M_y still had no significant different between the two types of cladding connections. However, the differences in number of members exceeded M_p became more noticeable. Members in which the plastic moment was obtained reduced from 8 to 3 members for El Centro earthquake and 6 to 3 members for Loma Prieta earthquake. The "Hys.6" cladding connection dissipated from 33 to 54% of the total hysteretic energy for all earthquakes except Northridge earthquake, which only dissipated 4% of the total hysteretic energy.

From Table 4.22, the maximum differential frame to cladding deflections were in an order of 3 to 5 in (7.62 to 12.70 cm). The maximum horizontal panel to panel deflections were under 1 in (2.54 cm) for all earthquakes except for the Northridge earthquake. The maximum relative panel deformations between stories were under 4 in (10.16 cm) for all earthquakes except Northridge earthquake. There were reductions in maximum structural frame deflection for all earthquakes except for the Northridge earthquake at this design level.

Table 4.23 Final frame to cladding deflections for El Centro earthquake (20%/50yrs)

Story	Final frame to cladding def. (in)					Total number of cladding connections per story	number of cladding connections yielded
	node 1	node 2	node 3	node 4	node 5		
1st	-0.03	-0.03	-0.02	-0.03	-0.01	5	5
2nd	0.09	0.09	0.12	0.12	0.10	5	5
3rd	0.07	0.07	0.07	0.07	0.05	5	5

Table 4.24 Final frame to cladding deflections for San Fernando earthquake (20%/50yrs)

Story	Final frame to cladding def. (in)					Total number of cladding connections per story	number of cladding connections yielded
	node 1	node 2	node 3	node 4	node 5		
1st	0.11	0.11	0.12	0.12	0.11	5	5
2nd	0.07	0.08	0.07	0.08	0.13	5	5
3rd	0.08	0.08	0.07	0.05	0.05	5	5

Table 4.25 Final frame to cladding deflections for Loma Prieta earthquake (20%/50yrs)

Story	Final frame to cladding def. (in)					Total number of cladding connections per story	number of cladding connections yielded
	node 1	node 2	node 3	node 4	node 5		
1st	-0.11	-0.10	-0.11	-0.11	-0.09	5	5
2nd	0.00	0.00	-0.01	-0.01	-0.02	5	3
3rd	0.02	0.02	0.02	0.03	0.03	5	5

Table 4.26 Final frame to cladding deflections for Big Bear earthquake (20%/50yrs)

Story	Final frame to cladding def. (in)					Total number of cladding connections per story	number of cladding connections yielded
	node 1	node 2	node 3	node 4	node 5		
1st	0.14	0.14	0.14	0.15	0.16	5	5
2nd	0.12	0.12	0.12	0.15	0.20	5	5
3rd	0.08	0.08	0.08	0.10	0.13	5	5

Table 4.27 Final frame to cladding deflections for Northridge earthquake (20%/50yrs)

Story	Final frame to cladding def. (in)					Total number of cladding connections per story	number of cladding connections yielded
	node 1	node 2	node 3	node 4	node 5		
1st	-0.03	-0.03	-0.03	0.01	-0.15	5	5
2nd	-0.09	-0.09	-0.09	-0.10	-0.02	5	5
3rd	0.20	0.19	0.20	0.22	0.31	5	5

From Table 4.23 to 4.27, almost all the flexible cladding connections were yielded for all earthquakes except for Loma Prieta earthquake. For those yielded cladding connections, the absolute final frame to cladding deflections ranged from 0.01 to 0.31 in (.03 to .79 cm). The absolute final frame to cladding deflections were similar to those with the higher earthquake design level. Figure 4.22 and 4.23 shows the force-deformation response of "Hys.6" cladding connection at node 43 which is the 3rd node at the 3rd story and node 23 which is the 3rd node at the first story under El Centro earthquake with design level of 20%/50yrs. The final differential cladding deformations of the two nodes were 0.07 in (.18 cm) and -0.02 in (-0.05 cm). From Figure 4.22 and 4.23, the cladding connections of node 43 and node 23 were both yielded after the earthquake. Cladding connection at node 43 had much energy dissipation than at node 23. The maximum differential connection deflection at node 43 was about two times at node 23. By comparing Figure 4.22 and 4.23 to Figure 4.20 and 4.21, there was less energy dissipation and maximum differential connection deflection in the cladding connection with the lower design level (20%/50yrs).

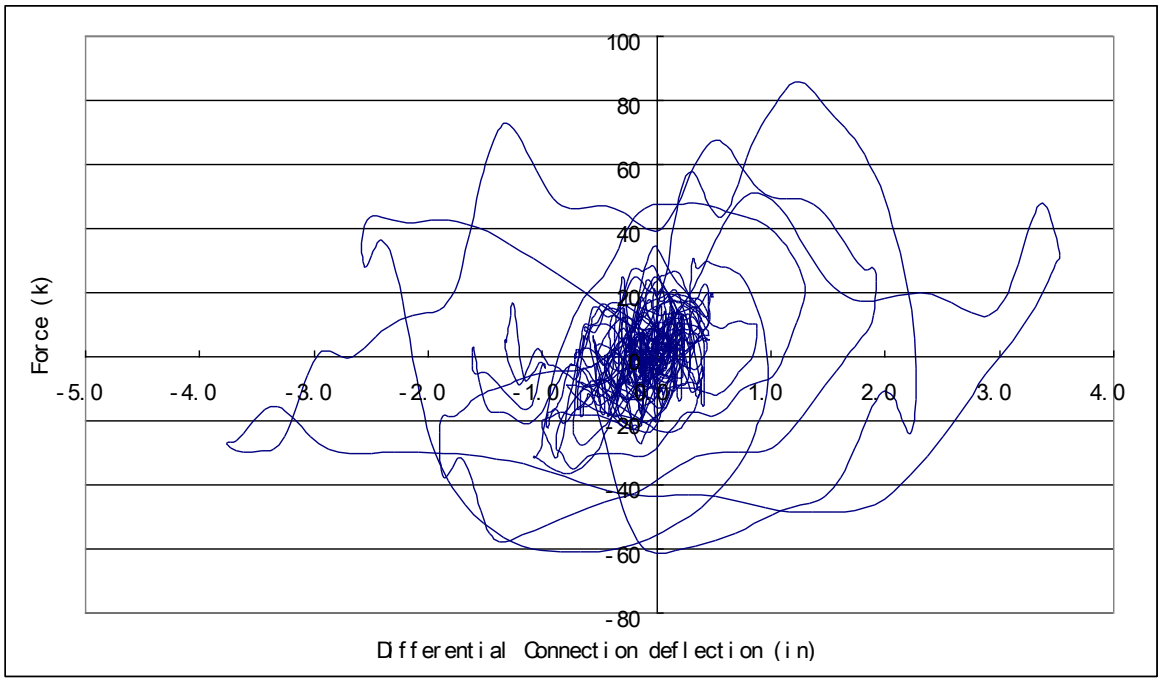

Figure 4.22 Force-deformation response of "Hys.6" cladding connection at node 43 (20%/50yrs)

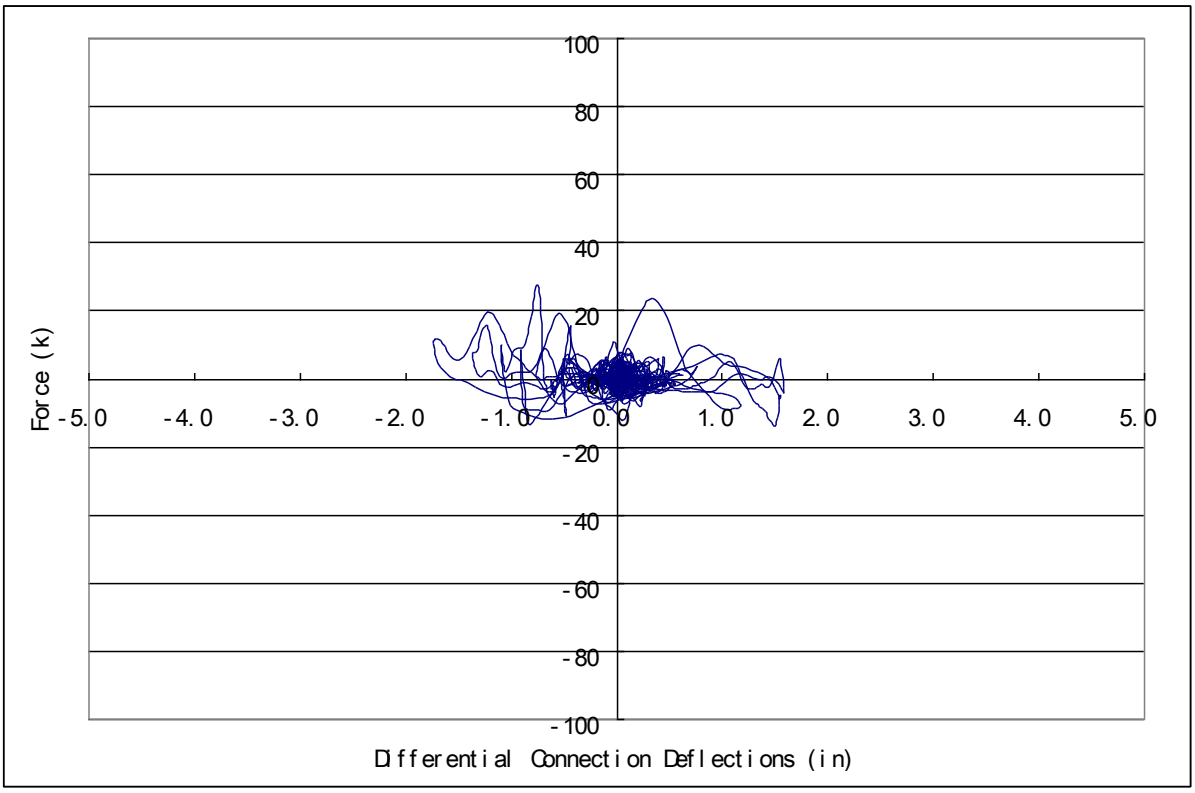

Figure 4.23 Force-deformation response of "Hys.6" cladding connection at node 23 (20%/50yrs)

The results from Table 4.14, 4.15, 4.21 and 4.22 showed Hys.6 flexible cladding connections were very effective in energy dissipation for all earthquakes except Northridge earthquake. Also, the results showed higher maximum horizontal panel to panel deflection and relative panel deformation between stories for the Northridge earthquake. The reason for the large deflection was because Northridge earthquake excited the higher modes of the SAC 3-story model by a much greater amount compared to other earthquake records, as indicated in Figures 4.11 and 4.12. Therefore, the performance of the cladding systems were greatly affected by the high excitation level at the second period of the structure for Northridge earthquake, which resulted in low

energy dissipation and excess of both horizontal panel to panel deflections and relative panel deformation between stories on the flexible cladding connections.

Final frame to cladding deflections after the earthquakes were relatively similar regardless of the scaling level of the excitations. However, from the force-deformation plots of the cladding connection, the results indicated more energy was dissipation on the cladding connection with higher design level. Again, most of the flexible cladding connections were yielded which again indicated that the energy was transferred from the structure to the flexible cladding connections.

4.5 Initial analysis results for SAC 9-story model

A partial inelastic model of SAC 9-story moment-resisting frame was built according to Ohtori's reference. The model also included "Hysteretic" springs as the flexible cladding connections which it was discussed in Chapter 3. The model consisted of both inelastic and elastic elements determined similarly to the method described for the SAC 3-story model in Chapter 3. Initial analysis with the "Hys.3" material was used as the cladding connections on the SAC-9 story model under the unscaled El Centro earthquake. This was because there was a converge problem when running the model with "Hys.6". "Hys.3" material showed better results with reduction on base shear; however, it had slightly higher maximum deflection between the frame and cladding (Table 3.8). The initial analysis results were shown in Table 4.28. A moment-rotation and a moment-plastic-rotation plots for one of connection nodes from a beam on the third story of the

SAC 9-story model with both rigid and "Hys.3" cladding connections under El Centro earthquake were shown in Figure 4.24 and 4.25.

Table 4.28 Initial analysis result for SAC 9-story model

Connection types	Rigid	Hys.3
Max. Base shear at support (k)	928.3	877.2
Max. Base shear at ground level (k)	2779	2624.4
Number of members exceeded M_y	37	20
Number of members exceeded M_p	8	0
Max. frame to cladding deflection (in.)	N/A	3.29

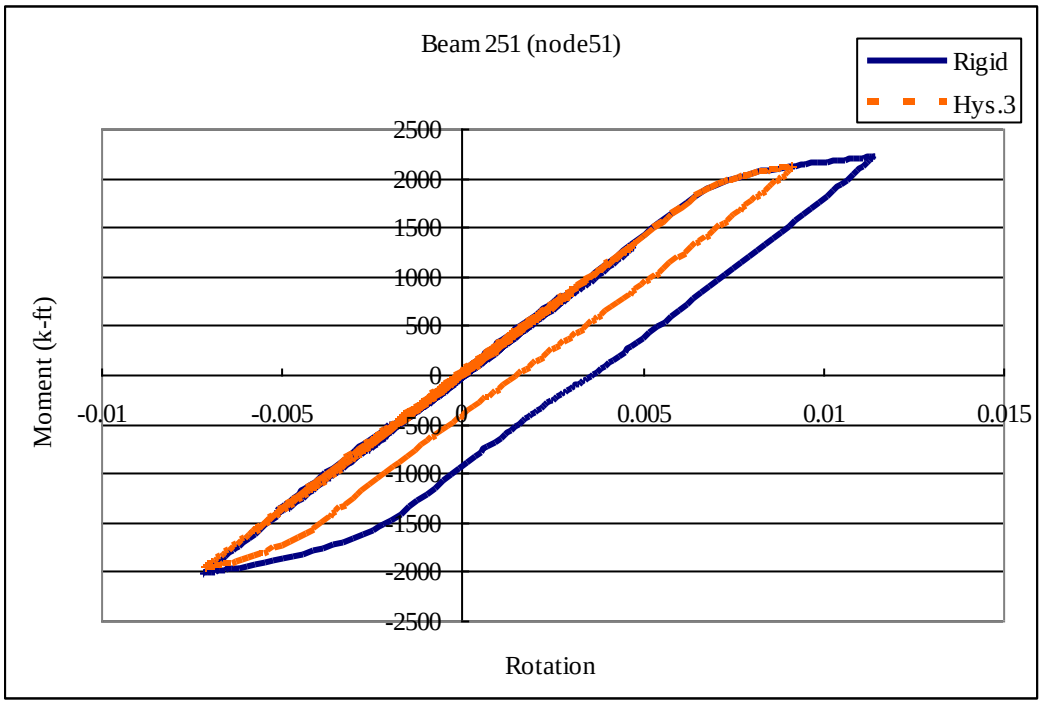

Figure 4.24 Moment-rotation plot for node51 of beam251

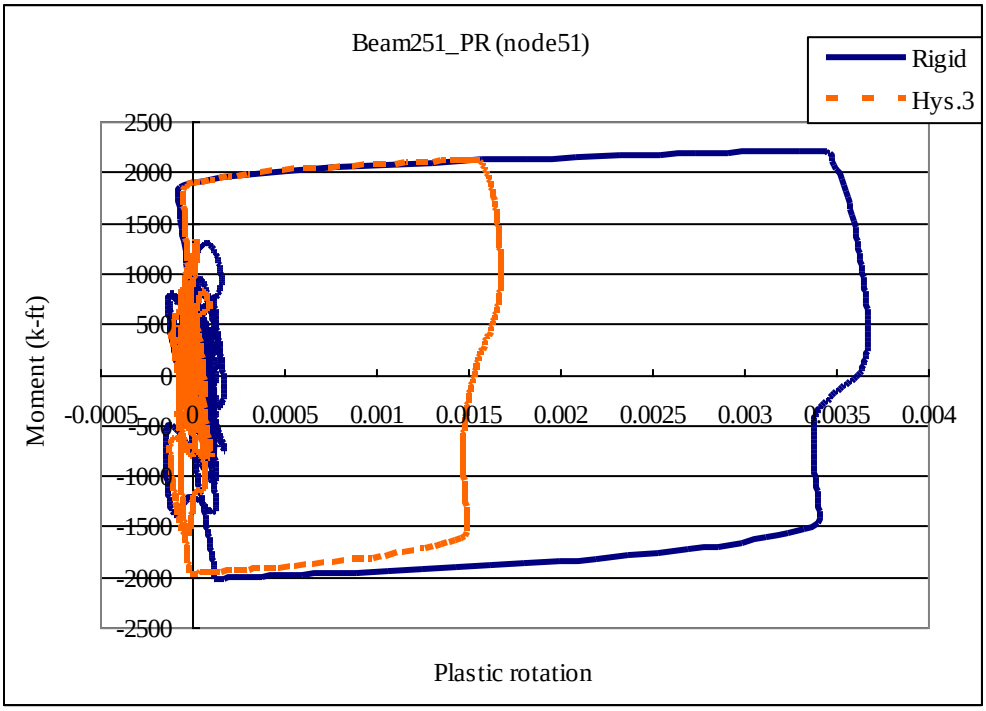

Figure 4.25 Moment-plastic-rotation plot for node51 of beam251

From Table 4.28 there were reductions on both maximum base shear at support and ground level from the rigid to "Hys.3" flexible connection. Significantly, there was a reductions on the number of members exceeding M_y and M_p, when the cladding connections were included. The maximum differential frame to cladding deflection was 3.29 in (8.36 cm). By comparing to the results with SAC 3-story model (Table 3.8), the maximum differential frame to cladding deflection with SAC 9-story model has reduction of 1.38 in (3.51 cm). This initially showed the flexible cladding connections were effective on reducing damages on the structural members.

From Figure 4.24 and 4.25, the hysteretic energy dissipated by the connection of the inelastic beam from the SAC 9-story model with rigid cladding connection was 14.35 k-ft (19.45 kJ), which was calculated by area under either the moment-rotation or moment-plastic-rotation curve using Equation 4.2. The hysteretic energy dissipated by the same connection of the inelastic beam from the SAC 9-story model with "Hys.3" flexible cladding connection was 6.46 k-ft (8.76 kJ). The difference in hysteretic energy dissipation on the connection was dissipated by flexible cladding connections. For this specific connection, about 55% of the hysteretic energy was dissipated by the flexible cladding connection. From the behaviors of this specific connection on the SAC 9-story model, the flexible cladding connection was very effective on energy dissipation under the El Centro earthquake.

4.6 Conclusions

In this chapter, two different design levels were used in the analysis of the SAC 3-story building with "Hys.6" flexible and rigid cladding connections included. A total of five earthquake records were used, representing a wide range of frequency contents. Time history records were scaled to the corresponding design level at the structural fundamental period representing 10% or 20% probablities of exceedance in 50 years. The results showed significant reductions on hysteretic energy dissipation of the structure between the rigid and "Hys.6" flexible connections under the expected earthquake excitations. Most of the yielding was reduced in the columns of the structure. The results confirmed the ability flexible cladding connections to dissipate energy. The flexible cladding connections dissipated a higher percentage of energy for the 20%/50yrs excitations rather than the 10%/50yrs design level. However, from the force-deformation plots of the flexible cladding connection, the flexible cladding connection tended to dissipate more energy at higher design level.

Preliminary analysis of the SAC 9-story model with both rigid and "Hys.3" cladding connection was also performed, subjected to the unscaled El Centro earthquake. This analysis indicated very promising results for the mid-sized structure as well, based on reductions of number of yield members, number of members exceeded M_p, and hysteretic energy dissipated of a single connection.

CHAPTER V

SUMMARY AND CONCLUSIONS

The focus of this research was to investigate the ability of flexible cladding connection on hysteretic energy dissipation through OPENSEES. Through previous researches from Nguyen and Ohtori, partial inelastic SAC 3- and 9-story models were developed which represented low- and medium-rise buildings designed for the Los Angeles, California region. The partial inelastic models have incorporated both inelastic and elastic behaviors of the structural members. The partial inelastic models had benefits on reducing the model run time in comparison of the fully inelastic models.

A set of non-linear spring materials were defined and used in modeling the flexible cladding connections on the structures. Initial analyses were conducted on the partial inelastic SAC 3-story model with the different non-linear springs as the flexible cladding connections under unscaled El Centro earthquake excitation. The results showed "Hysteretic" non-linear spring materials had better performance both in terms of reduced maximum base shear and connection deflection controls.

A series of earthquake response spectra were chosen for further analysis, which were based on including a range of predominant frequency contents. Records were scaled to the fundamental period of the SAC 3-story model. To accomplish this, two earthquake design spectra were conducted using NSHMP Hazard Map program with a zip code of 90002 which represented a relatively low seismic region in Los Angeles. The design

spectra included both 10% and 20% probability in 50 years of exceedance design levels. Depended on the each design level, all earthquake response spectra were scaled to match the excitation level at the fundamental period of the SAC 3-story model with rigid cladding connections for each design spectrum.

The partial inelastic SAC 3-story model with cladding connections included was analyzed with input excitations matching the five different earthquake records scaled to the two design levels. The results from rigid and flexible "Hys.6" cladding connection were compared. The results showed a slight reduction of base shear, maximum frame deflection, and number of members exceeding M_y. It showed more significant reductions on number of member exceeding $M_{p.}$ The number of member exceeding M_p dropped significantly from 10%/50yrs to 20%/50yrs design level. The hysteretic energy dissipated by the "Hys.6" flexible cladding connections ranged from 26 to 30% of the total hysteretic energy dissipation for the 10%/50yrs design level aside from the Northridge Earthquake which excited the higher modes at an unrealistic acceleration. The flexible cladding connections dissipated from 33 to 54% of the total hysteretic energy dissipation for the 20%/50yrs design level aside from the Northridge Earthquake which excited the higher modes at an unrealistic acceleration. The differential frame to cladding deflections and panel to panel deflections were under reasonable ranges with 20%/50yrs design level. The "Hys.6" flexible cladding connection had less ability to dissipate hysteretic energy for earthquake with high excitation level at the structural higher mode frequency, which also induced excess of connection deflections. For structure with flexible cladding connections, there were more contributions on the

response of the structure from higher modes. From the results on the SAC 3-story with flexible cladding connections, when the response spectrum from an earthquake were near the design level, the flexible cladding connections were efficient in dissipating energy during the earthquake. Most of the flexible cladding connections were yielded after the earthquakes which indicated the flexible cladding connections were dissipating hysteretic energy, though final distortions were controlled after the ground excitations. Through the force-deformation plots of the flexible cladding connection, the flexible cladding connection tended to dissipate more energy at higher design level.

The partial inelastic SAC 9-story model with "Hys.3" flexible connections was analyzed with the unscaled El Centro earthquake used as the input excitation. These results showed a significant reduction on number of yield members and members exceeded M_p from rigid to flexible cladding connections. These preliminary results indicate that the system would be effective in a mid-sized structure as well. The analysis of the SAC 9-story model could be the focus of future research.

The analysis results on the SAC 3- and 9-story models with flexible cladding connections showed distinct benefits of the flexible cladding connections and fairly large but controllable displacements of cladding. The effectiveness of the flexible cladding connections is dependent on the dynamic characteristics of the structure, material properties of the cladding connections, and characteristics of the response spectra of input excitation. If flexible connections are designed properly so that they can undergo

expected hysteretic behavior, they may prove to be very good energy absorbers during an earthquake.

REFERENCES

[1] Ohtori, Y., Christenson, R.E., Spencer, B.F., and Dyke, S. J. (2004), "Benchmark control problems for seismically excited nonlinear buildings." *Journal of Engineering Mechanics*, ASCE, 130(4), 366-385.

[2] OPENSEES Command Language Manual (2006). Open System for Earthquake Engineering Simulation - Home Page. University of California at Berkeley. 19 Jan. 2010.

[3] Brandow and Johnston Associates (1996). Consulting Structural Engineers, Los Angeles.

[4] Pinelli, J.-P., Moor, C., Crag, J., and Goodno, B. (1996), "Testing of energy dissipating cladding connections." *Earthquake engineering and structural dynamics*, 25(2), 129-147.

[5] Pinelli, J.-P., Craig, J., Goodno, B., and Hsu, C.-C. (1993), "Passive control of building response using energy dissipating cladding connections." Earthquake spectra, 9(3), 529-546.

[6] Pinelli, J.-P., Craig, J., and J., Goodno, B. (1995), "Energy-based seismic design of ductile cladding systems." Journal of structural engineering, ASCE, 121(3), 567-578.

[7] Pinelli, J.-P., Moor, C., Crag, J., and Goodno, B. (1992), "Experimental testing of ductile cladding connections for building facades." *The structural design of tall buildings*, Vol. 1, 57-92.

[8] Cohen, J. M., and Powell, G. H. (1993), "A design study of an energy-dissipation cladding system." *Earthquake engineering and structural dynamics*, 22(7), 215-228.

[9] Pinelli, J.-P., Crag, J., and Goodno, B. (1990), "Development and experimental calibration of selected dynamic models for precast cladding connections" *Proceddings of the fourth U.S. National Conference on Earthquake Engineering*, Palm Springs, California, Vol 2., 147-156.

[10] Bruneau, M., and Cohen, J. M. (1994), "Review of NBCC earthquake-resistant design requirements for cladding connectors." *Canadian journal of civil engineering*, 21(3), 455-460.

[11] Wong, K. K. F. (2008), "Seismic Energy Dissipation of inelastic structures with tuned mass dampers." *Journal of structural engineering*, ASCE, 134(2), 163-172.

[12] Chopra, A. K. (2007), "Dynamics of structures: theory and applications to earthquake engineering." 3rd ed., Prentice Hall, Upper Saddle River, New Jersey.

[13] Precast/Prestressed Concrete Institute (2007), "Architectural precast concrete manual", 3rd ed., Chicago, Illinois.

[14] Nguyen, Quan V (2009). "Seismic Energy Dissipation of Buildings Using Engineered Cladding Systems." M.S. Thesis. University of Massachusetts Amherst, 2008. Amherst: Umass Amherst.

[15] Krawinkler, Helmut (2000). "State of the Art Report on Systems Performance of Steel Moment Frames Subject to Earthquake Ground Shaking." Rep. Washington D.C.: FEMA, Print. 335C.

[16] Silva, Walt (2000). "PEER Strong Motion Database." Pacific Earthquake Engineering Research Center, Web. 6 Dec. 2009. <http://peer.berkeley.edu/smcat/index.html>.

[17] Uang, C. M., and Bertero, V. V. (1990), "Evaluation seismic energy in structures." Earthquake engineering and structural dynamics, 19(1), 77-90.